

REPORT DOCUMENTATION PAGE			Form Approved OMB No. 0704-0188	
Public reporting burden for this collection of information is estimated to average 1 hour per response, including the time for reviewing instructions, searching existing data sources, gathering and maintaining the data needed, and completing and reviewing the collection of information. Send comments regarding this burden estimate or any other aspect of this collection of information, including suggestions for reducing this burden, to Washington Headquarters Services, Directorate for Information Operations and Reports, 1215 Jefferson Davis Highway, Suite 1204, Arlington, VA 22202-4302, and to the Office of Management and Budget, Paperwork Reduction Project (0704-0188), Washington, DC 20503.				
1. AGENCY USE ONLY (Leave blank)	2. REPORT DATE 10 Sep 95	3. REPORT TYPE AND DATES COVERED		
4. TITLE AND SUBTITLE Estimation of The Convective Boundary Layer Depth Over Lake Ontario During Cold Air Outbreaks		5. FUNDING NUMBERS		
6. AUTHOR(S)  Richard Adolf Anstett				
7. PERFORMING ORGANIZATION NAME(S) AND ADDRESS(ES) AFIT Students Attending:  North Carolina State University		8. PERFORMING ORGANIZATION REPORT NUMBER  95-105		
9. SPONSORING/MONITORING AGENCY NAME(S) AND ADDRESS(ES) DEPARTMENT OF THE AIR FORCE AFIT/CI 2950 P STREET, BLDG 125 WRIGHT-PATTERSON AFB OH 45433-7765		10. SPONSORING/MONITORING AGENCY REPORT NUMBER		
11. SUPPLEMENTARY NOTES				
12a. DISTRIBUTION/AVAILABILITY STATEMENT Approved for Public Release IAW AFR 190-1 Distribution Unlimited BRIAN D. GAUTHIER, MSgt, USAF Chief of Administration		12b. DISTRIBUTION CODE		
13. ABSTRACT (Maximum 200 words)				
<div data-bbox="1049 1283 1438 1591" data-label="Image"> </div> <div data-bbox="470 1598 922 1713" data-label="Text"> <p>19951017 153</p> </div> <div data-bbox="987 1690 1386 1724" data-label="Text"> <p>DTIC QUALITY INSPECTED 8</p> </div>				
14. SUBJECT TERMS		15. NUMBER OF PAGES 86		
		16. PRICE CODE		
17. SECURITY CLASSIFICATION OF REPORT	18. SECURITY CLASSIFICATION OF THIS PAGE	19. SECURITY CLASSIFICATION OF ABSTRACT	20. LIMITATION OF ABSTRACT	

**ESTIMATION OF THE CONVECTIVE BOUNDARY LAYER DEPTH OVER  
LAKE ONTARIO DURING COLD AIR OUTBREAKS**

by

**RICHARD ADOLF ANSTETT**

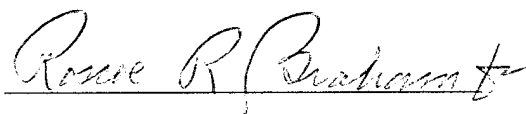
A thesis submitted to the Graduate Faculty of  
North Carolina State University  
in partial fulfillment of the  
requirements for the Degree of  
Master of Science

**MARINE, EARTH AND ATMOSPHERIC SCIENCES**


Raleigh

1995

**APPROVED BY:**

  
\_\_\_\_\_

  
\_\_\_\_\_

  
\_\_\_\_\_  
Chair of Advisory Committee

## Abstract

ANSTETT, RICHARD ADOLF. Estimation of the convective boundary layer depth over Lake Ontario During Cold Air Outbreaks. (Under the direction of Gerald F. Watson.)

The purpose of the research has been to develop and test a simple model for estimating the depth of the convective internal boundary layer (CIBL), and the height of the lifting condensation level (LCL) in the modified air over Lake Ontario. The intent is to use the hourly temporal resolution of surface observations to predict the mixed-layer depth for nowcasting and short-range forecasting purposes. These predicted CIBLs and LCLs are calculated using upwind surface and sounding data, and lake surface temperatures, and compared with downwind soundings made with mobile radiosondes. Factors such as the effects of upwind lakes, upward CIBL growth into layers of differing stability, and air mass modification over Lake Ontario are investigated.

This study was conducted using data from the Lake Ontario Winter Storms (LOWS) Project; an investigation of the mesoscale structure and physical processes involved in lake-effect snowstorms east of Lake Ontario between 5 January and 1 March 1990. The LOWS Project final technical report suggests that the convective layer depth is at least as important to forecasting lake-effect intensity as the instability. It has been shown that organized convection is inhibited by low capping inversions, even with lake surface to 850 mb temperature differences much greater than the dry adiabatic lapse rate ( $\sim 13^{\circ}\text{C}$ ).

Soundings for the LOWS Project were conducted at Egbert, Canada for upwind data, and downwind of Lake Ontario at Buffalo, NY and also with mobile radiosondes. Regular synoptic soundings are conducted at upwind locations west of Lake Huron, while Buffalo, NY is downwind of Lakes Erie and Ontario. Field forecasters could use surface observations and continuous real-time temperature and wind profiles to estimate the depth of over-lake convection with an hourly temporal resolution if upwind profiles of temperature and winds were available, or use forecast soundings from numerical models.

<input checked="checked" type="checkbox"/>	
<input type="checkbox"/>	
<input type="checkbox"/>	
Availability Codes	
Dist	Avail and/or Special
A-1	

### **Biography**

Richard A. Anstett is a weather officer in the United States Air Force.

He was born in 1962 and lived in western New York until his enlistment in the Air Force in 1980. His first assignment was at Whiteman Air Force Base, Missouri, where he met his wife-to-be, Mary Frances Werstein. While there he first served as a security policeman in an ICBM missile wing and after retraining to become a weather observer, he returned to Whiteman Air Force Base in 1984. In 1985 Staff Sergeant Anstett was reassigned to Shemya Air Force Base, Alaska as the Non-Commissioned Officer in charge of the Upper Air section, responsible for conducting upper air soundings, and the training and performance of Rawinsonde and Rocketsonde observers.

In 1986, he left the Air Force to attend college at the State University of New York at Brockport, where he earned a Bachelor of Science degree in Meteorology and Earth Science. After graduation in the spring of 1989, he successfully completed the Air Force Officer Training School and was commissioned as a Second Lieutenant in the United States Air Force in the autumn of 1989.

He was then assigned to Tinker Air Force Base, Oklahoma as a Wing Weather Officer. While there he was responsible for coordinating weather support for four flying agencies, and providing response to severe weather. He was awarded an Air Force Institute of Technology scholarship in 1993, to pursue an advanced degree in meteorology at North Carolina State University, Raleigh, North Carolina, and was promoted to the rank of Captain in September 1993. Upon completion of his masters degree, he will be assigned to the Joint Typhoon Warning Center at Nimitz Hill Naval Station, Guam where he will be a Typhoon Duty Officer.

Rick and Mary Anstett have two sons, Benjamin Richard and Nicholas Francis.

### Acknowledgements

I would like to thank Dr. Gerald Watson, Dr. Roscoe Braham, and Dr. Sethu Ramen for their advice, guidance and patience during the preparation of this thesis; the time and support they have rendered has made this document possible.

I also wish to express my gratitude to the following people and agencies who have aided my research:

- The U. S. Air Force for allowing me the opportunity to pursue this degree.
- Niagara Mohawk Power Corp for initiating and funding the LOWS project.
- Dr. Albert J. Koscielny of Kaman Sciences, Colorado Springs, Colorado. His assistance in supplying the LOWS project data was crucial to this research.
- Vann B. Gibbs, Jr. and Janet S. Wall of OL-A Environmental Technical Applications Center, USAF, Asheville, North Carolina. Their assistance in providing surface data and various facsimile charts is greatly appreciated.
- Dr. Robert J. Ballentine, State University of New York (SUNY) College at Oswego. Thanks for e-mailing the LOWS project Oswego soundings.
- Dr. Gregory P. Byrd, COMET, UCAR, Boulder, Colorado. One of the LOWS project participants, and my former instructor at the SUNY College at Brockport. Thanks for getting me involved in the snow-band soundings and studies!
- A very big thank you to Neeraja Reddy for her patience, instruction and guidance on the use of the mesoscale model.

Finally, I would like to express my most sincere thanks to my wife Mary and my sons Benjamin and Nicholas. Thanks for your love, patience and support these last two years.

## TABLE OF CONTENTS

	Page
LIST OF TABLES.....	vi
LIST OF FIGURES.....	vii
LIST OF SYMBOLS AND ABBREVIATIONS.....	x
1. INTRODUCTION.....	1
1.1 Literature Review.....	1
1.1.1 Brief Description of Lake-Effect Snowstorms.....	1
1.1.2 Physical Description of Lake Ontario and Surrounding Area.....	2
1.1.3 Controlling Physical Factors.....	4
1.1.3.1 Significant Predictors.....	8
1.2 Current Observation and Sensing Limitations.....	10
1.3 LOWS Objectives.....	11
1.4 Objectives of Present Research.....	12
1.4.1 Estimating the Over-Lake CIBL.....	12
1.4.2 Moisture Effects and LCL Estimations.....	15
1.4.3 Applications and Limitations of This Research.....	15
2. DATA AND METHODOLOGY .....	17
2.1 Data Collection.....	17
2.2 LOWS Instrumentation and Description.....	17
2.3 Methodology.....	20
2.3.1 Overwater Fetches.....	20
2.3.2 Overwater Airmass Modification.....	21
2.3.3 CIBL Invasion of Upper Layers.....	22
3. BOUNDARY LAYER CALCULATIONS .....	24
3.1 Sounding Analysis.....	24
3.2 Shoreline Windshift Estimation.....	25
3.3 Overwater Drag Coefficient.....	26
3.4 Overwater Temperatures and Windspeeds.....	27
3.5 CIBL and LCL Calculations.....	29

4. CASE STUDY .....	31
4.1 Long Fetch Case Study.....	31
4.1.1 Synoptic and Mesoscale Analysis.....	31
4.1.2 Sounding Analysis and CIBL Estimation.....	40
4.1.2.1 Sounding Analysis.....	40
4.1.2.2 CIBL Estimation.....	42
4.2 Short Fetch Case.....	45
4.2.1 Synoptic and Mesoscale Analysis.....	45
4.2.2 Sounding Analysis and CIBL Estimation.....	57
4.2.2.1 Sounding Analysis.....	57
4.2.2.2 CIBL Estimation.....	61
4.2.3 Sensitivity Tests: Short Fetch Case.....	62
5. MODEL SIMULATIONS .....	68
5.1 Model Description.....	68
5.1.1 Model Domain and Initial Conditions.....	68
5.2 Model Results.....	69
6. SUMMARY AND CONCLUSIONS.....	73
6.1 Summary.....	73
6.2 Conclusions.....	75
6.3 Future Research.....	75
7. LIST OF REFERENCES .....	76
8. APPENDIX .....	80

### List of Tables

Table 1.1.	Predictors for Lake Erie.....	9
Table 1.2.	Predictors for Lake Ontario.....	9
Table 1.3.	Predictors common to studies for both Lakes Erie and Ontario.....	9
Table 2.1.	Lake Ontario fetch as a function of wind direction.....	20
Table 2.2.	Regression equations used to estimate overwater temperature and wind values.....	22
Table 3.1.	Layer analysis for Egbert (WET) 11Z, 20 February 1990.....	25
Table 3.2.	Overwater values using a Toronto (YYZ) observation 12Z, 20 February 1990.....	28
Table 3.3.	Overwater CIBL, 20 February 1990 based on the WET 11Z sounding and the YYZ 12Z observation.....	30
Table 4.1	Model evaluations for varying input conditions.....	62



### List of Figures

Figure 1. The locations of the Great Lakes and upstream effects.....	3
Figure 2. Land regions and surface relief of the Lake Ontario area.....	5
Figure 3. Elevations of the Lake Ontario drainage basin in meters MSL.....	5
Figure 4. The Upwind effects of Lake Superior measured over Lake Michigan.....	6
Figure 5. Development of the PBL over differing surfaces in the eastern Great Lakes	6
Figure 6. Surface streamline and isotach analysis 1500 EST 4 February 1965.....	7
Figure 7.	
a) Thermally-driven land breeze.....	8
b) Dome-like development of CIBL over a warm lake.....	8
Figure 8.	
a) Shoreline frictional diffluence/confluence.....	8
b) Shoreline windspeed diffluence/confluence.....	8
Figure 9. Zeroeth-Order model for the TIBL.....	14
Figure 10. LOWS instrumentation and placement.....	19
Figure 11. Vertical cross section over Lake Michigan for 20 January 1984.....	24
Figure 12. Plot of CIBL over Lake Michigan for 20 January 1984.....	24
Figure 13. Shoreline directional windshift.....	26
Figure 14. Overwater drag coefficient.....	27
Figure 15.	
a) 500 mb analysis 0000 UTC 12 January 1990.....	33
b) 850 mb analysis 0000 UTC 12 January 1990.....	34
c) Surface analysis 0000 UTC 12 January 1990.....	35
Figure 16.	
a) 500 mb analysis 1200 UTC 12 January 1990.....	36
b) 850 mb analysis 1200 UTC 12 January 1990.....	37
c) Surface analysis 1200 UTC 12 January 1990.....	38

Figure 17. Lake Ontario lake surface temperature analysis 08 January 1990.....	39
Figure 18. Local surface analysis 1200 UTC 12 January 1990.....	40
Figure 19. Sharp Skew-T profiles for upwind and downwind locations.....	42
Figure 20. Buffalo and Oswego temperature profiles 1200 UTC 12 January 1990....	43
Figure 21. Estimated CIBL depth and LCL height, 12 January 1990.....	44
Figure 22.	
a) 500 mb analysis 0000 UTC 20 February 1990.....	47
b) 500 mb analysis 1200 UTC 20 February 1990.....	48
Figure 23.	
a) 850 mb analysis 0000 UTC 20 February 1990.....	49
b) 850 mb analysis 1200 UTC 20 February 1990.....	50
Figure 24.	
a) Surface analysis 0000 UTC 20 February 1990.....	51
b) Surface analysis 1200 UTC 20 February 1990.....	52
Figure 25.	
a) Lake Ontario Surface Temperature analysis 18 February 1990.....	53
b) Great Lakes Ice analysis 26 February 1990.....	54
Figure 26. Surface hourly observations 0600 through 1200 UTC 20 February 1984..	55
Figure 27.	
a) Surface analysis 1200 UTC 20 February 1990.....	56
b) Surface/overwater predicted data analysis 1200 UTC 20 February 1990....	56
Figure 28. Upwind and Downwind Skew-T profiles 19 and 20 February 1990.....	58
Figure 29. Theta-e sounding evolution WET 19 and 20 February 1990.....	58
Figure 30. WET 1100 UTC, BUF 1200 UTC temperature profile 20 February 1990..	59
Figure 31. Upwind and Downwind theta-e profiles 20 February 1990.....	59
Figure 32. CIBL plumes from Lake Huron, 20 February 1990.....	60
Figure 33. Estimated CIBL depth and LCL height, 20 February 1990.....	61

Figure 34. Cold air test CIBL depth and LCL height, 20 February 1990.....	64
Figure 35. Moist air test CIBL depth and LCL height, 20 February 1990.....	64
Figure 36. Longer fetch test CIBL depth and LCL height, 20 February 1990.....	65
Figure 37. Greater wind speed test CIBL depth and LCL height, 20 February 1990...	65
Figure 38. Shallow stable layer test CIBL depth and LCL height, 20 February 1990..	66
Figure 39. Observed stable layer, short fetch, optimal conditions, 20 February 1990..	66
Figure 40. Observed stable layer, long fetch, optimal conditions, 20 February 1990..	67
Figure 41. Shallow stable layer, long fetch, optimal conditions, 20 February 1990.....	67
Figure 42. Observed soundings, 12 January 1990.....	71
Figure 43. Model 3 hour over water thermal and cloud structures, 12 January 1990..	71
Figure 44. Observed soundings, 20 February 1990.....	72
Figure 45. Model 3 hour over water thermal and cloud structures, 20 February 1990.	72

# 1. INTRODUCTION

## 1.1 LITERATURE REVIEW

### 1.1.1 Brief Description of Lake-Effect Clouds and Storms

Lake-effect storms are autumn and wintertime mesoscale phenomena that occur leeward of the Great Lakes following the passage of polar or arctic air masses over the much warmer lakes. The cold, dry interiors of these air masses are usually cloud-free in most continental regimes, however the Great Lakes can initiate clouds and precipitation as the cold, stable air becomes modified over the warm lakes. Lake-effect rain and thunderstorms can develop during the months of September and October, while lake-effect snowstorms occur from October through March. Lightning-producing snow storms are infrequent, but can occur from November through December (Moore and Orville, 1990).

The cold air masses are destabilized by lake-to-air sensible and latent heat fluxes, resulting in a surface superadiabatic layer and a well-mixed convective boundary layer (CBL) below a capping subsidence inversion. The surface fluxes decrease as the season progresses, due to lake surface cooling and the reduced moisture holding capacity of colder air masses. The arctic air masses also have greater low-level stability, which limits the CBL depth. Lake-effect clouds and storms are expected when the temperature lapse between the lake surface and the 850 mb level is equal to or greater than  $13^{\circ}\text{C}$ , roughly a dry adiabatic lapse rate (Rothrock, 1969).

Byrd *et al.* (1991) addressed lake-effect storm intensity in terms of the lake-surface to 850 mb lapse rate (TL850) and the CBL depth downwind of Lake Ontario using mobile rawinsondes. Storm soundings showed a correlation between lake-effect intensity and CBL depth. Weak cases were limited by a shallow CBL (1.5 to 1.9 km AGL) with TL850 values of  $25^{\circ}\text{C}$  (nearly twice the dry adiabatic lapse rate.) Strong cases had CBL depths

ranging from 2.3 to 3.1 km, suggesting that CBL depth may be as important as the degree of instability in determining lake-effect snow intensity.

The Great Lakes offer additional complexities, such as the orientation of the large scale windflow with respect to each lake's major axis, mesoscale wind circulations driven by land-lake temperature differences, and the effects of upwind lakes. Windflow across a lake's short axis can produce multiple cloud bands, while windflow parallel to the long axis may act with land-breezes to produce an enlarged single mid-lake cloud band, or a shoreline band (Braham, 1983). Figure 1 shows that Lake Superior is upwind of Lake Michigan with northerly flow, and Lake Huron and Georgian Bay are upwind of either Lake Erie with northerly winds, or Lake Ontario with northwesterly winds.

Convection in the planetary boundary layer can erode low-level stable boundary layers and invade residual convective boundary layers from upwind lakes (Agee and Gilbert, 1989; Chang and Braham, 1991), and lift capping inversions.

#### 1.1.2 Physical Description of Lake Ontario and Surrounding area

Lake Ontario is oriented approximately east-west, with a length of 311 km, and a width of 85 km. It has an average depth of 86 meters and a maximum depth of 244 meters, with a mean surface elevation of 75 meters above mean sea level. Its depth and southeasterly location usually allows the lake to remain ice-free throughout typical winters (Eichenlaub, 1979).

The land regions and surface relief of the Lake Ontario area are shown in figure 2. The Erie-Ontario Lowland is a low plain adjacent to the lakes, gradually rising from lake level to roughly 150 m in the Lake Ontario drainage basin. The Tug Hill Plateau lies to the east of the lowland, and is separated from the Adirondack Upland by the Black River

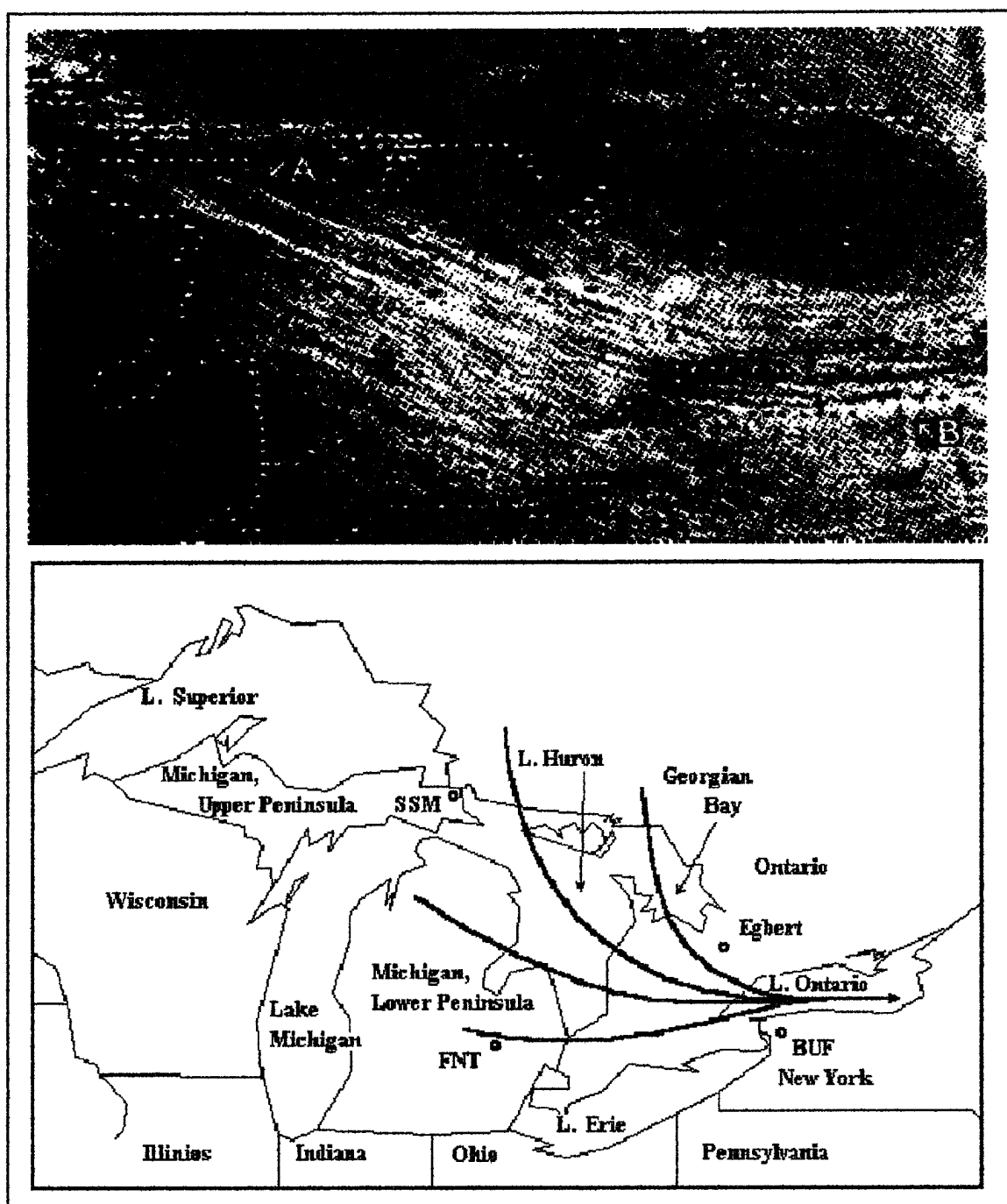


FIG. 1. The locations and orientations of the Great Lakes. Lakes Superior and Huron are typically upwind of the other lakes with northwesterly windflow. Streamlines show the upwind paths and underlying surfaces for air parcels modified by Lake Ontario. The visible satellite image (Niziol et al., 1995) shows Lake Huron snow bands crossing and being enhanced by Lake Ontario.

Valley. The plateau rises rapidly from 150 to over 450 m downwind of the long axis of Lake Ontario (fig. 3.)

### 1.1.3 Controlling Physical factors

Lake-effect snowstorms develop in response to several factors. Niziol (1987) summarized the conditions necessary for significant lake-effect snowfall east of Lakes Erie and Ontario. Strong advection of arctic air over the warm Great Lakes is required for destabilization of the lower PBL. A slow-moving or stationary 500 mb low between Hudson's Bay and Lake Ontario will direct westerly windflow parallel to the long axis of the two lakes, while upper lows moving along a more southeasterly track, with high pressure ridges over the western Great Lakes will produce windflow across the shorter axis of the lakes. Positive Vorticity Advection will enhance lake-effect snowfall by lifting or eroding any capping inversions.

Cold air masses are destabilized by sensible and latent heating from the relatively warm lakes. The resulting convection in the convective boundary layers (CBL) or convective internal boundary layers (CIBL) can erode low-level stable boundary layers (SBL), invade residual convective boundary layers (RL) from upstream lakes (Agee and Gilbert, 1989; Chang and Braham, 1991), and lift capping inversions (Lavoie, 1972; Ballentine, 1982).

Figure 1 shows Lake Huron and Georgian Bay upwind of Lakes Erie and Ontario under north windflow (Erie), to west through northwest windflow (Ontario). Synoptic windflow from 250° results in little upstream overwater fetch. Figures 4 and 5 show the effects of upwind lakes on the planetary boundary layer. Figure 5 is adapted from Stull's figure 1.7 (1988), replacing time with distance.

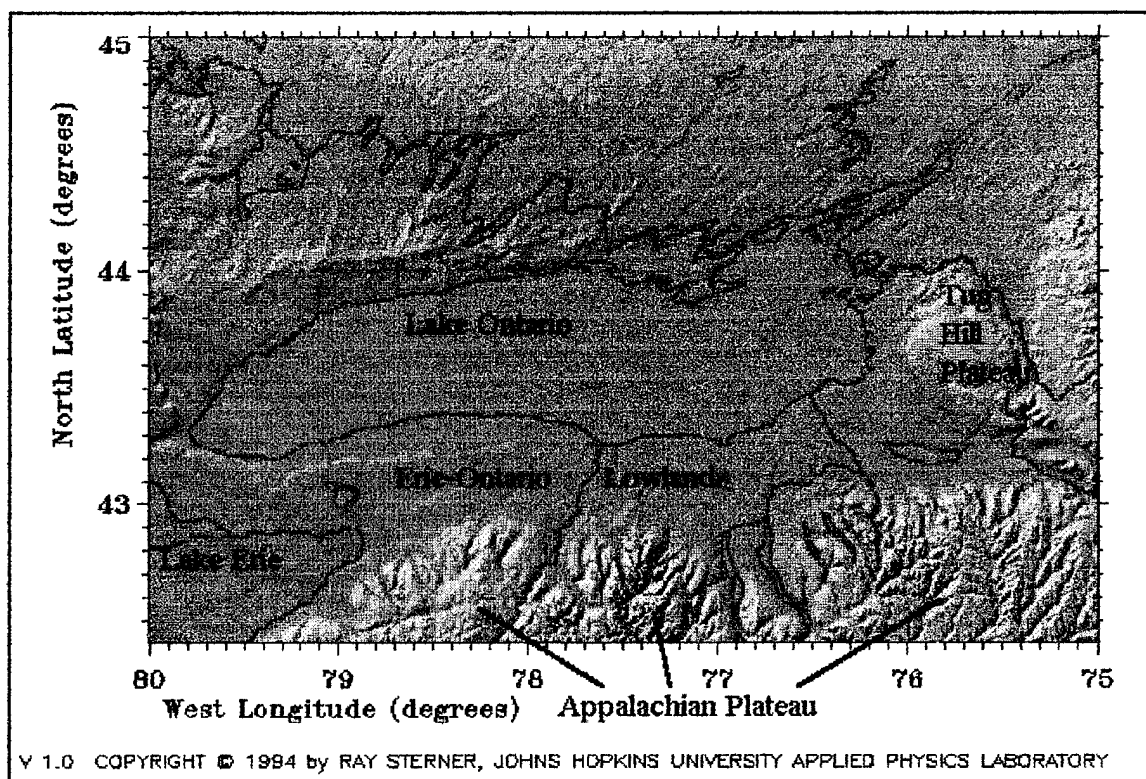


FIG. 2. Land regions and surface relief of the Lake Ontario area. Internet download from [fermi.jhuapl.edu](http://fermi.jhuapl.edu)

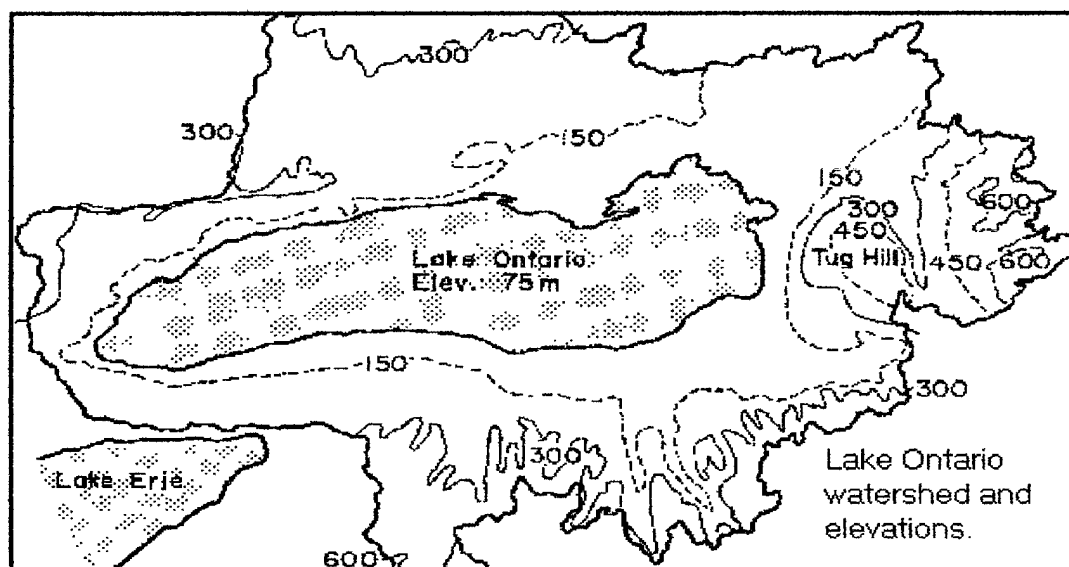


FIG. 3. Elevations of the Lake Ontario drainage basin in meters. From Holland *et al.* (1981)



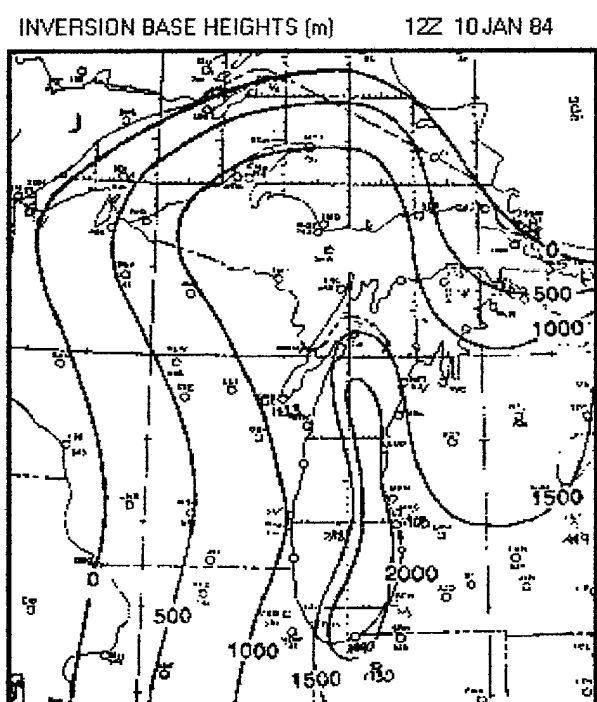


FIG. 4. The upwind effects of Lake Superior are felt over Lake Michigan as the inversion base is first acted upon over Lakes Superior and Michigan. 1200 UTC 10 January 1984. From Agee and Gilbert (1989).

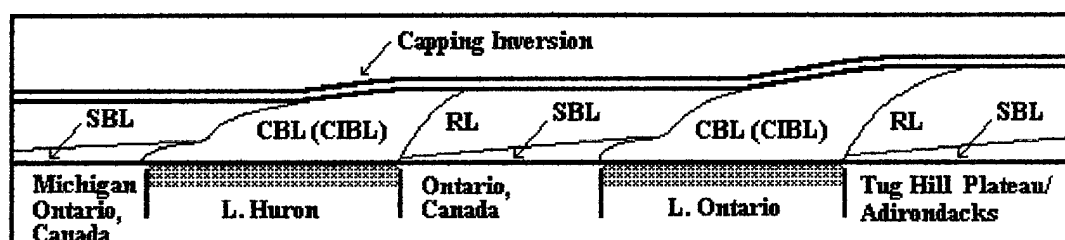


FIG. 5. Development of the PBL over differing surfaces in the eastern Great Lakes.

The sensible heat flux and lake-to-land temperature differences may initiate land breezes resulting in mid-lake convergence (Passarelli, and Braham, 1981). Peace and Sykes (1966) analyzed confluent windfields east of Lake Ontario associated with enlarged single cloud band snowstorms. Figure 6 shows a streamline and isotach analyses

associated with a lake-effect cloud band. The inflow of cold dry air from flanking shorelines may result in lower CIBL heights to either side of the over-lake convergent asymptote, while air parcels with over-land trajectories may undercut the CIBL plume at the eastern end with a SBL (Figs. 7a and 7b).

Lake-to-land frictional differences can produce convergence along the southern shores of west-east oriented lakes during periods of northwesterly windflow, since the greater friction over land will increase the cross-isobaric flow (fig. 8a). This can result in the formation of a cloudband just offshore of Lake Ontario's southern shore (Holroyd, 1971). Orographic effects can produce convergence along eastern and southern shores with westerly through northerly winds (fig. 8b), thus enhancing the snowfall on the leeward areas (Lavoie, 1972).

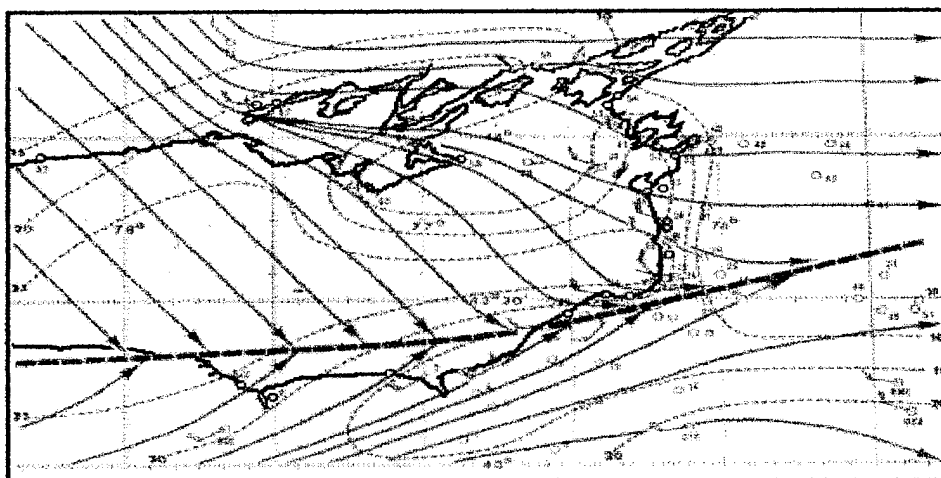


FIG. 6. A streamline and isotach (mph) analysis for 1500 EST, 4 February 1965. A confluent windfield with convergence along the southern shore (near  $43^{\circ} 20' N$ ) migrated southward from a north shore position (near  $43^{\circ} 50' N$ ) at 1200 EST 3 February 1965. From Peace and Sykes (1966).

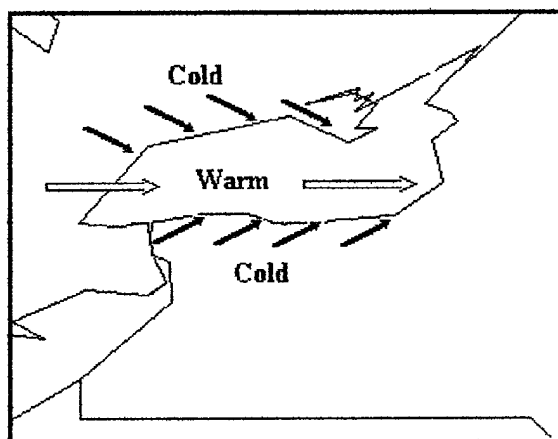


FIG. 7a. A thermally driven land-breeze wind component may be superimposed on the large-scale windflow.

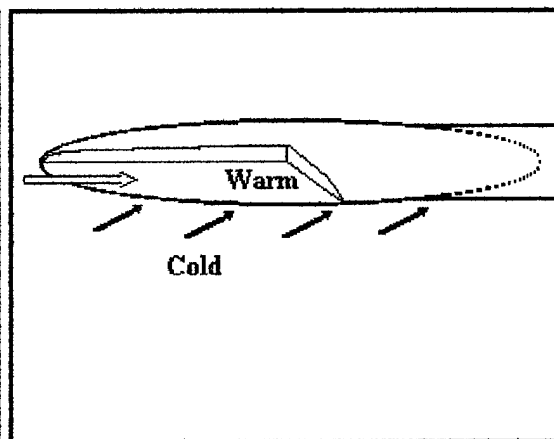


FIG. 7b. The flanking intrusion of cold, dry air may result in CIBL heights increasing from opposite shorelines to a confluent asymptote.

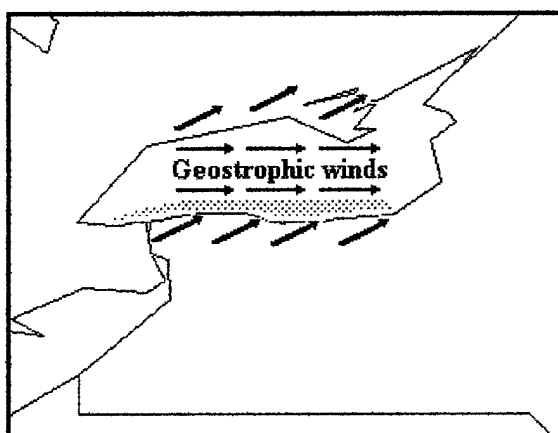


FIG. 8a. Frictional confluence along the southern shore with diffluence along the northern shore.

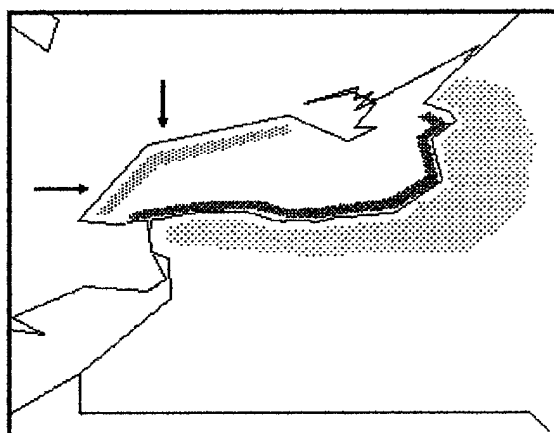


FIG. 8b. Windspeed divergence and convergence act in concert with downslope and upslope flow with westerly through northerly winds.

#### 1.1.3.1 Significant Predictors

Two studies of Lake Erie and Lake Ontario by Dewey used statistical analyses to define lake-effect storm predictors (Table 1.1) for a Lake Erie lake-effect forecast model (Dewey, 1979a), and storm predictors (Table 1.2) for Lake Ontario (Dewey, 1979b).

Some factors are used in lake-effect forecasting (Niziol, 1987), while others are not easily derived or applied. Table 1.3 is a list of predictors common to both studies.

Table 1.1. Predictors for Lake Erie (Dewey, 1979a).

- 
- 
1.  $e_s - e_a$  (vapor pressure gradient at 2.5 m over the lake)
  2. 850 mb saturation deficit
  3.  $T_w - T_u$  (water temperature - upwind land temperature)
  4. Surface wind velocity over the lake
  5. Percent ice cover on the lake
  6. Stability of the air mass (Lifted Index)
  7.  $T_w - T_{850}$  (water temperature - 850 mb temperature, or TL850)
  8. 850 mb wind speed
  9. Surface wind fetch over the lake
- 

Table 1.2. Predictors for Lake Ontario (Dewey, 1979b).

- 
- 
1.  $T_w - T_{850}$  (TL850)
  2. Surface wind fetch over the lake
  3. Percent ice cover on the lake
  4. Surface wind velocity over the lake
  5.  $e_s - e_a$  (vapor pressure gradient at 2.5 m over the lake)
  6. Wind fetch at 850 mb over the lake
  7. Relative humidity, surface to 500 mb
- 

Table 1.3. Predictors common to both studies include :

- 
- 
- $T_w - T_{850}$  (TL850)
- $e_s - e_a$
- Percent ice cover on the lake
- Surface wind velocity over the lake
- Surface wind fetch over the lake
-

The magnitude of TL850 is used as a measure of instability between the lake and the air mass. Ice cover is a limiting factor which reduces the sensible and latent heat fluxes from lake-to-air. Lake Erie may freeze over by mid-winter, while Lake Ontario rarely freezes over. Over-water fetch is determined by wind direction, with westerly winds having longer fetches and greater air mass modification than northerly winds.

Finally, the vapor pressure gradient at 2.5 m ( $e_s - e_a$ ) will be strongly affected by the moisture content of the unmodified air mass, the surface water temperature, and the fetch. It's interesting to note that both studies identify the degree of air mass saturation as significant, as either the 850 mb saturation deficit, or a measure of the surface to 500 mb relative humidity. Cloud and precipitation processes will not begin until the air mass is sufficiently moistened. Also notable is the high ranking of  $T_w - T_u$  in the Lake Erie study. The land-to-lake temperature difference is a factor in land breezes and midlake cloud bands, and may be a first-glance indicator of expected water-to-air surface heat flux magnitudes (latent and sensible).

## 1.2 CURRENT OBSERVATIONS AND SENSING LIMITATIONS

Buffalo NWS soundings may occasionally sample Lake Erie snowbands with a southwesterly ( $250^\circ$ ) windflow, or possibly Lake Ontario multiple bands with a northerly flow, but lake-effect snowstorms are not routinely sampled by conventional rawinsonde networks, which are spatially and temporally too coarse to detect the mesoscale temperature and windfield features and evolution.

Lake-effect echo tops are often too shallow to be accurately observed by NWS radars at ranges beyond 90 km (Niziol, 1987), while precipitation at and below 2 km will be below the radar beam at a range of 160 km. WSR-88D radars have increased sensitivity in reflectivity, but will still suffer the same earth-curvature drawbacks if located at or near

the current radar sites. A doppler radar located northeast of Buffalo will not be able to observe over-water surface winds, and may not detect low-level land breezes or offshore flow due to frictional differences, even at the lowest elevation angle scans. Convergent radial velocities in the WSR-88D base velocity display can indicate the location and magnitude of low-level convergence, which can be a precursor to convection.

Satellite imagery has good temporal resolution, and fair spatial resolution for visually observing the clouds associated with lake effect snows, but visible data is limited by the short duration of winter daylight, and can be complicated by ice on the lake. Infrared imagery may allow an estimation of cloud top heights over the warmer lakes, while smaller thermal contrasts between cloud tops and snow-covered land can introduce some uncertainty. Current satellite technology can help measure the lake surface temperature, but satellite derived soundings have poor vertical resolution in boundary layer temperature profiles.

### 1.3 LOWS OBJECTIVES

The Lake Ontario Winter Storms (LOWS) Project applied a mesoscale array of advanced remote sensors to monitor lake-effect snowstorms and their precursors over and downwind of Lake Ontario.

The LOWS Project was prompted and primarily sponsored by the Niagara Mohawk Power Corporation (NMPC) to evaluate improvements in the monitoring and prediction of lake-effect snowstorms and freezing rain storms in the company's service area, and as a test for providing specialized weather service to other industries and the public.

Since conventional observations and numerical models are spatially and temporally too coarse to detect or predict the mesoscale features, LOWS was also planned to field test new remote sensing technologies developed at NOAA's Wave Propagation Laboratory

(WPL) and other organizations, and to develop a better understanding of the phenomena for mesoscale modeling (Reinking *et al.*, 1991).

#### 1.4 OBJECTIVES OF PRESENT RESEARCH

This study attempts to estimate the over-lake CIBL depth ( $z_i$ ) and the height of the lifted condensation level (LCL) with a finer temporal resolution than twice-a-day upper air soundings can provide, using land-based data. The intent is use the mean observed lake surface temperature and upstream sounding data, with the hourly temporal resolution of surface observations to predict these values. The predicted values will then be compared to downwind soundings and surface observations, and model simulations.

##### 1.4.1 Estimating the Over-Lake CIBL

I have chosen Venkatram's (1977) Thermal Internal Boundary Layer (TIBL) equation to predict CIBL depths, and compare the results to soundings made with mobile and routine rawinsondes. This equation may be used to describe changes in over-lake CIBL growth as the input values vary.

Two of the several TIBL equations discussed in Stunder and Sethuraman (1985) can be briefly discussed here as background for the proposed use over water. TIBL equations were developed for air quality applications with stable onshore airflow, and were intended to be used over short distances inland. These equations were developed with the following assumptions:

1. TIBL growth is governed by quasi-steady conditions, the time of travel ( $x/u$ ) is much smaller than the time-scale governing the temperature change of the underlying surface (Venkatram, 1986).

2. The local rate of change of temperature ( $\partial\theta(x)/\partial t$ ) within the internal boundary is smaller than the temperature advection and diffusion, and can be neglected, leaving advection = diffusion:

$$U(\partial\theta(x)/\partial x) = (-1/\rho C_p)(\partial H(x,z)/\partial Z) \quad (\text{Equations (3) and (4), Gamo } et al., 1983).$$

3. The lapse rate in the mixing layer is near dry adiabatic ( $\partial\theta(x)/\partial z = 0$ ), except for a shallow superadiabatic surface layer.

4. The surface sensible heat flux ( $H_o(x)$ ) is constant with distance ( $x$ ).

5. The heat flux is mixed rapidly, and decreases linearly with height at any downwind distance, ( $\partial H(x,z)/\partial Z = \text{constant}$ ).

6. The mixed layer wind speed ( $U$ ) is vertically uniform.

In Weisman's (1976) equation:

$$z_1 = z_{i0} + [2 \times H_o / \rho C_p \beta u_m]^{1/2} \quad (1)$$

$z_{i0}$  is any pre-existing dry adiabatic (neutral) mixed layer height (m),  $x$  is the fetch (m), and  $H_o$  is the surface sensible heat flux.  $\rho$  is the air density,  $C_p$  is specific heat at constant pressure,  $u_m$  is the mean wind speed ( $\text{ms}^{-1}$ ), and  $\beta$  is the potential temperature lapse rate ( $d\theta/dz$ ).



Convective growth of the CIBL is driven by the surface heat flux. Gamo *et al.* (1983) derived a "No temperature jump" model identical to Weisman's equation, with the assumption that the surface sensible heat flux is mixed rapidly and decreases with height so that  $H_0 = 0$  at the top of the CIBL (fig. 9c.), and the CIBL lapse rate (fig. 9b.) is dry adiabatic ( $\partial\theta/\partial z = 0$ ). The height of the CIBL top ( $z_i$ ) can be obtained with the assumption that advection is balanced by diffusion in  $U\partial\theta/\partial x = -1/\rho C_p \partial H/\partial z$ , and the substitution of  $\beta dz$  for  $d\theta$ .

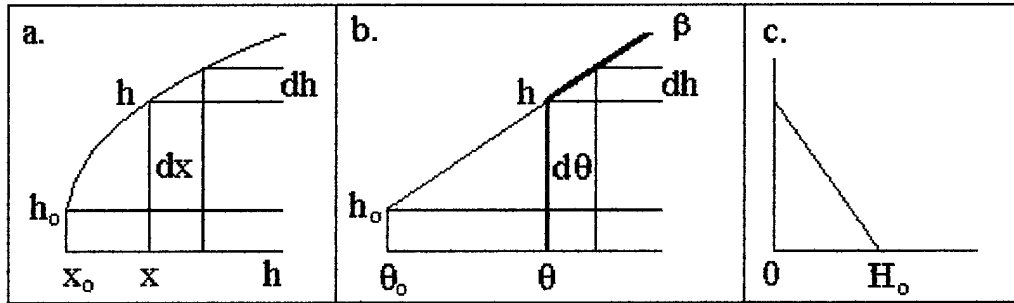


FIG. 9. A zeroth-order model for the TIBL. Figure 9a describes the idealized growth of the TIBL with increasing distance. Figure 9b shows the increase in the TIBL depth as the air column is warmed,  $\beta$  is the lapse rate of the overlying stable layer. Figure 9c represents the linear decrease of the surface sensible heat flux  $H_0$ .

Venkatram (1986) notes that direct measurements of  $H_0$  are not routinely available and can be approximated by a difference in temperature,  $\theta_{\text{warm}} - \theta_{\text{cool}}$ . Here  $\theta_{\text{warm}}$  is the temperature of the underlying warm surface (either the land surface temperature for stable onshore flow, or the water surface temperature for stable offshore flow,) and  $\theta_{\text{cool}}$  is the upwind air temperature.

Venkatram's (1977) equation is used in this study:

$$z_i = z_{i0} + (u_*/u_m) \left[ 2x |T_{\text{warm}} - T_{\text{cool}}| / |\beta|(1-2F) \right]^{1/2} \quad (2)$$

where  $F$  is an entrainment fraction ( $\sim 0.2$ ), and  $u_*$  is the friction velocity ( $\text{ms}^{-1}$ ).  $(u_*/u)$  can also be taken inside the brackets as the drag coefficient for neutral conditions,  $C_{DN}$ .

These two TIBL equations will fail if the environmental lapse rate is defined as exactly dry adiabatic (division with  $\beta = 0$ ).

Other factors must first be considered, such as:

- 1) Shoreline wind shifts/ over-water direction (affecting fetch).
- 2) Changes in land-based and estimated over-water wind speed (affecting  $C_{DN}$ ).
- 3) CIBL growth through lower layers into layers with different lapse rates ( $\beta$ ).

#### 1.4.2 Moisture Effects and LCL Estimations

The TIBL equations also do not consider moisture effects such as latent heat released by cloud droplet condensation,  $-L_v dw$ , where  $L_v$  is the latent heat of vaporization and  $dw$  is the mixing ratio change. Many studies (Lavoie, 1972; Ballentine, 1982; Hjelmfeldt, 1990, 1992) have found that dry modeling simulations underpredict the depth of the CIBL. A more accurate method would include the latent heat of condensation where the over-water CIBL exceeds the LCL height, and the released latent heat is determined. This latent heat could be applied to a modified TIBL equation.

The over-water LCL can be predicted after considering the moisture content of the unmodified air mass, (or over-land dewpoint temperature,) and the over-water air mass modification. The original moisture content determines how rapidly the modified air will become saturated while passing over the lake.

#### 1.4.3 Applications and Limitations of this Research

As a nowcasting tool, this technique is limited to air mass situations where gradual changes are expected, but is not appropriate when lapse rates and PBL structures are

expected to change rapidly, i.e. immediately behind fronts or with rapidly moving systems. It will not account for changes in upstream lapse rates between soundings, such as temperature advection, or the rise or fall of the inversion due to subsidence.

Upwind and downwind soundings of the mixed-layer are compared in this study to calculated CIBLs. Soundings which share a common origin will be selected to reduce the effect of upwind lakes. Estimated CIBLs will be compared to mixed layers observed downwind of the lake for a long fetch and a short fetch case. The CIBL will also be calculated using variations in observed input values for the following situations:

- 1) Colder air
- 2) Higher dewpoints
- 3) Different wind directions
- 4) Increasing wind speeds
- 5) Varying stable layer depths

The results of this research will show that TIBL equations can be used to estimate the depth of over-lake convective boundary layers, and predict subsequent CIBL depths based on the most recent upwind sounding and surface observations, describing changes in the CIBL depth with changing surface conditions. The greater temporal resolution of this method may aid in nowcasting the strength or absence of lake-effect snow storms.

## CHAPTER 2 DATA AND METHODOLOGY

### 2.1 DATA COLLECTION

Data were collected from 5 January 1990 through 1 March 1990, and is maintained by Kaman Sciences Corp., 1500 Garden of the Gods Rd., Colorado Springs, CO 80907.

### 2.2 LOWS INSTRUMENTATION AND DESCRIPTIONS

Figure 10 shows locations of the instruments to be described.

#### Rawinsondes

National Weather Service (NWS) and Atmospheric Environmental Science of Canada (AES) six-hour observations from Sault St. Marie, MI (SSM); Flint, MI (FNT); Egbert, CN (WET, 40 km NW of Toronto, CN); Buffalo, NY (BUF).

Mobile-sounding units from State University of New York (SUNY) colleges at Brockport (BKP) and Oswego (OSW).

#### Remote Sensing

King City, CN/AES

C-band (5-cm) Doppler Radar.

Cape Vincent, NY/Tycho Technology, Inc. (TTI)

404 MHz (75-cm) profiler

Lacona, NY/NOAA Wave Propagation Laboratory (WPL)

915 MHz (33-cm) profiler

Three-channel, passive, scanning microwave radiometer

X-band (3.2 cm) dual-polarization Doppler radar

North Rose/Pennsylvania State University (PSU)

404 MHz (75-cm) profiler

Radio Acoustic Sounding System (RASS)

Laser ceilometer

Surface Observation Arrays

United States Coast Guard (USCG) stations and light houses.

PSU/North Rose weather observations (after 00Z 02 February 1990).

SUNY Brockport and Oswego weather observations during snow events.

SUNY- Environmental Sciences and Forestry (ESF) at Syracuse, Snow Survey.

Niagara Mohawk Power Corporation (NMPC) Instrumented tower observations.  
Five towers located along/near the lake shore.

Galson Technical Services, Inc. (GTS) Volunteer snow observer network. 40 individuals with equipment to measure snowfall and liquid water equivalent. Observations every six hours and more frequent during periods of heavy snowfall. Volunteers also evaluated visibility.

GTS Weighing precipitation gauge network. Four gauges located with volunteer observers, four gauges in remote, unattended locations.

GTS Surface microbarograph network. 12 instruments collocated with volunteer observers.

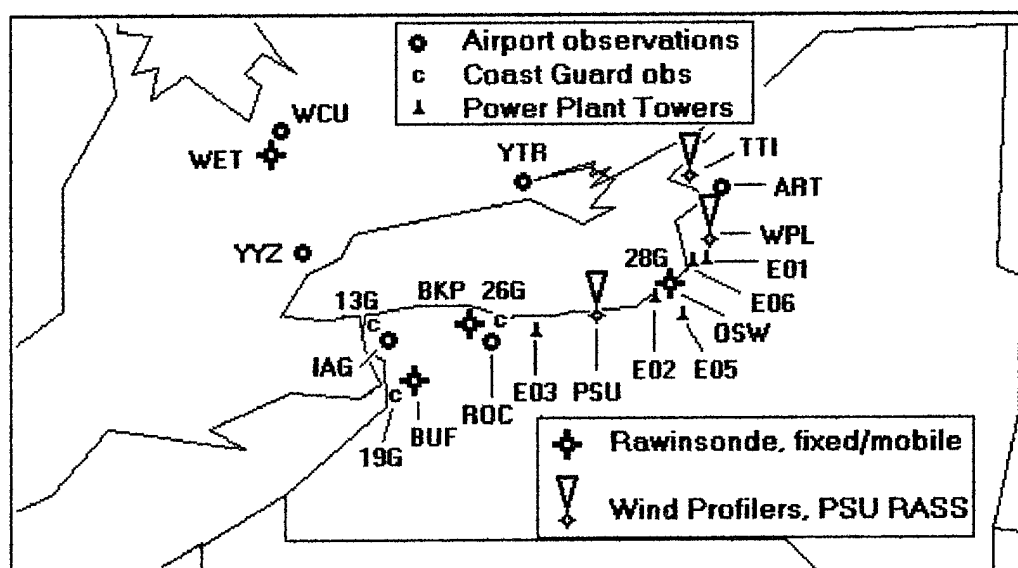


FIG. 10. Instrument placement and routine observing sites.

13G - Youngstown CGS, NY (USCG)	IAG - Niagara Falls, NY (NWS)	
19G - Buffalo CGS, NY (USCG)	OSW - Oswego, NY (SUNY)	
26G - Rochester CGS, NY (USCG)	PSU - North Rose, NY Penn. State Univ.	
28G - Oswego CGLS, NY (USCG)	ROC - Rochester, NY (NWS)	
ART - Watertown, NY (NWS)	SYR - Syracuse, NY (NWS)	
BUF - Buffalo, NY (NWS)	TTI - Cape Vencent, NY, Tycho Tech. Inc.	
BKP - Brockport, NY (SUNY)	WCU - Barre, ON (AES)	
E01 - Pulaski, NY (NMPC)	WET - Egbert, ON (AES)	
E02 - Oswego, NY (NMPC)	WPL - Lacona, NY Wave Prop. Lab.	
E03 - Ontario, NY (NMPC)	YGK - Kingston, ON (AES)	
E05 - Chaughdenoy, NY (NMPC)	YTR - Trenton, ON (AES)	
E06 - Selkirk Shores, NY (NMPC)	YYZ - Toronto, ON (AES)	

## 2.3 METHODOLOGY

Before predicting the LCL height, or utilizing equation (2) to determine the over-lake CIBL depth, we need to determine a few relevant factors, such as:

- 1) Fetch ( $x$ ) as a function land-based wind direction and shoreline wind shifts.
- 2) Over-lake air mass modification.
- 2) Changes in land-based and estimated over-water wind speed (affecting  $C_{DN}$ ).
- 3) The lapse rate ( $\beta$ ) of each layer in the lower atmosphere, since the CIBL grows upward through lower layers into layers with different stabilities.

### 2.3.1 Overwater Fetches

The growth of the CIBL is a function of the overwater distance ( $x$ ), or fetch. The hourly fetch ( $\Delta x$ ) travelled by air parcels between hourly observations is simply the windspeed in  $\text{ms}^{-1}$  converted to  $\text{km hr}^{-1}$ . Shorter fetches may also be calculated for smaller intervals of time. The growth of the CIBL over time may be described by using elapsed time commencing when the air parcel begins passage over the lake, and the parcel's modified temperature. The individual fetches and temperatures may be used in a CIBL equation to show the growth of the CIBL. The length of time necessary for an air parcel to travel from the windward shore to the leeward shore would be the total distance divided by the windspeed. The total over-lake distance is determined by the wind direction over the elongated lake (Table 2.1).

Table 2.1. Lake Ontario fetch as a function of wind direction (From Niziol, 1987).

Wind Dir ( $^{\circ}$ )	230	250	260	270	280	290	300	340	360
Total fetch (km)	110	190	240	225	180	140	130	100	085

### 2.3.2 Over-water Air Mass Modification

As discussed in section 1.4, in cases with cold air advection (CAA), subsequent air parcels would be colder, and the CIBL depth would become greater. The CIBL growth rate decreases at longer fetches as the over-lake air temperature is warmed by the lake surface, resulting in decreasing  $(T_{\text{warm}} - T_{\text{cool}})$  and  $H_0$ , which is consistent with Venkatram's (1986) assumptions. The sensible heat flux from the surface must also heat a deeper column of air at longer fetches, which implies a slower CIBL growth.

Phillips (1972) found that the maximum air temperature modification between 1 and 15 m did not exceed 55 percent of the maximum possible (the lake surface temperature) for unstable conditions, and barely reached 40 percent during extreme CAA. This is a consequence of short over-lake fetches limiting the time for air mass modification. As a result, the over water  $(T_{\text{warm}} - T_{\text{cool}})$  and  $H_0$  do not approach zero.

Phillips developed a set of regression equations relating ship-observed over-water air and dewpoint temperatures over Lake Ontario with the upwind land-based observations. The equations are based on paired observations from research ships on Lake Ontario, and upwind land-based observations. 515 observations were taken at three hourly intervals during the months of November through March from 1965 through 1969.

Table 2.2 shows a later set of equations developed from Lake Ontario data during the International Field Year of the Great Lakes (IFYGL) (Phillips and Alamazan, 1981). These equations are based on a larger sample of paired observations from research ships and buoys on the lake, and land-based observations; 6926 paired observations were taken during IFYGL in 1972/1973.

While the 1972 equations have been used in previous studies (Phillips, 1972; Dewey, 1975; Niziol, 1986), I have chosen to use these 1981 equations to estimate the over-water air and dewpoint temperatures using the upwind land-based observations.



Table 2.2. Regression equations to estimate over-water temperature and wind values.  
(Phillips and Alamazan, 1981)

Land-water Stability	Regression equations
$T_{AL} - T_W$	Over-lake air temperature (°C) at 2.5 m
$> 10.4^\circ$	$T_{AW} = 12.83 + 0.30T_{AL} + 0.56T_W - 2.77 \log \text{Time (s)}$
$> 3.4^\circ$	$T_{AW} = 7.93 + 0.29T_{AL} + 0.65T_W - 1.63 \log \text{Time (s)}$
$-3.4 \text{ to } 3.4^\circ$	$T_{AW} = 0.29 + 0.47T_{AL} + 0.52T_W$
$-10.4 \text{ to } -3.5^\circ$	$T_{AW} = 4.78 + 0.67T_{AL} + 0.42T_W + 1.12 \log \text{Time (s)}$
$< -10.4^\circ$	$T_{AW} = -9.77 + 0.60T_{AL} + 0.54T_W + 2.80 \log \text{Time (s)}$
$T_{AL} - T_W$	Over-lake dewpoint (°C) at 2.5 m
$> 10.4^\circ$	$T_{DW} = 8.07 + 0.43T_{DL} + 0.53T_W - 2.04 \log \text{Time (s)}$
$> 3.4^\circ$	$T_{DW} = 0.16 + 0.44T_{DL} + 0.55T_W$
$-3.4 \text{ to } 3.4^\circ$	$T_{DW} = -0.35 + 0.72T_{DL} + 0.31T_W$
$-10.4 \text{ to } -3.5^\circ$	$T_{DW} = 0.03 + 0.94T_{DL} + 0.11T_W + 0.02 \text{ Fetch (nmi)}$
$< -10.4^\circ$	$T_{DW} = -5.64 + 0.56T_{DL} + 0.46T_W + 0.05 \text{ Fetch (nmi)}$
$T_{AL} - T_W$	Over-lake Wind Speed (knots) at 10 m
$> 10.4^\circ$	$W_W = 3.28 + 0.32W_L + 0.00001 \text{ Time (s)} - 0.02T_{AL}$
$> 3.4^\circ$	$W_W = 2.65 + 0.49W_L + 0.00001 \text{ Time (s)} - 0.02T_{AL}$
$-3.4 \text{ to } 3.4^\circ$	$W_W = 3.55 + 0.92W_L - 0.28(T_{AL} - T_W) + 1.29 \log \text{Time (s)}$
$-10.4 \text{ to } -3.5^\circ$	$W_W = -2.50 + 1.01W_L + 1.33 \log \text{Time (s)}$
$< -10.4^\circ$	$W_W = -2.79 + 1.05W_L + 1.46 \log \text{Time (s)}$

### 2.3.3 CIBL Invasion of Upper Layers

An important consideration is the development of the CIBL upward into layers with different lapse rates. CIBL equations are usually applicable out to distances such that the CIBL remains within the initial stratification, as was pointed out in Peters and Carmichael's (1976) reply to Wiesman (1976). The height and lapse rate of each layer would have to be defined, and as the CIBL eroded upwards through each strata, the next

higher layer's lapse rate would be used in the CIBL equation until the capping inversion was finally reached and acted upon.

A sounding site upwind of a lake could observe soundings similar to Chang and Braham (1991) figure 3, where the sounding from Sheboygan, Wisconsin has a low-level mixed layer below an inversion, while above the inversion lies a neutral layer, possibly a residual layer from Lake Superior. The sounding taken at Muskegon, Michigan (Chang and Braham, 1991, Fig. 4) shows the deep neutral profile downwind of Lake Michigan, and the author's figures 5a and 7 (Figs. 11 and 12 here) also display cross sections of equivalent potential temperature and the growth of the CIBL across Lake Michigan using aircraft data. Both figures show increased CIBL growth as the low-level stable layer is breached, and the CIBL develops upward through the neutral RL to the capping inversion. Cloud and snow development may also act to increase the depth of the CIBL in addition to the invasion of less stable layers.

The sounding data and surface weather conditions observed at locations upwind and downwind of Lake Ontario will be compared to predicted values. Over-water fetch will be determined by wind direction, and will control the length of time and distance over which the air mass is modified. The Great Lakes do not have routine buoy or ship data available during the winter season, so air mass modification must be estimated using land-based observations. Regression equations offer a simple estimation of over-water values based on water surface temperature and an upwind land-based weather observation.

The temporary placement of sounding stations (Fig. 10) presents us with an opportunity to observe and investigate the effects of residual layers from upwind lakes on both the upwind boundary layer, and the subsequent CIBL development over Lake Ontario. Previous studies (Agee and Gilbert, 1989; Chang and Braham, 1991) have utilized aircraft data to define the boundary layer structure upwind, over and downwind of

Lake Michigan, measuring the convective growth of the over-lake internal boundary layer and the influence of the upwind boundary layer structure and layer stabilities.

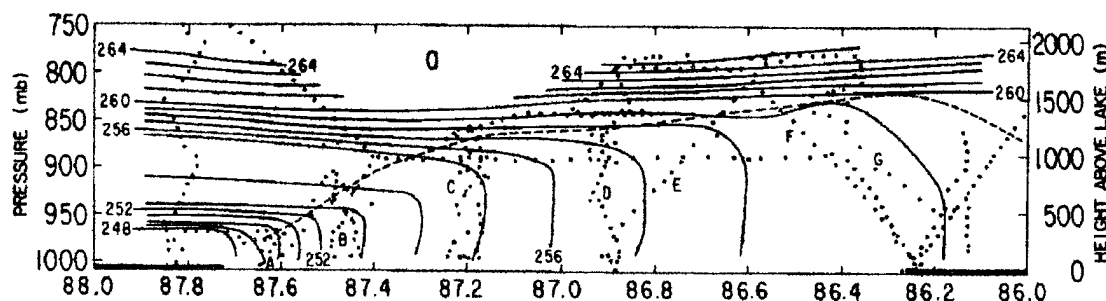


FIG. 11. Vertical cross section of equivalent potential temperature over Lake Michigan on 20 January 1984. Dotted lines indicate aircraft flight path. From Chang and Braham (1991).

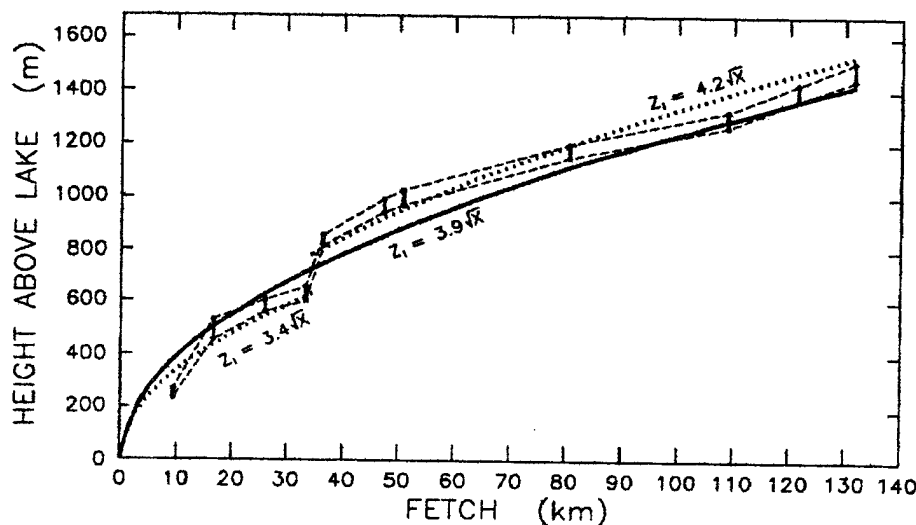


FIG. 12. Plot of the CIBL over Lake Michigan, 20 January 1984. The dotted lines are best-fitting parabolic curves for  $x < 35$  km and  $x > 35$  km, where the CIBL either penetrated the lower stable layer, or increased in growth rate with the development of clouds and precipitation, or both. From Chang and Braham (1991).

The next stage of this study is to estimate over-water air mass modification and CIBL depth using land-based data with the methods described. These estimated values will then be compared to the observed conditions downwind of Lake Ontario.

### 3. BOUNDARY LAYER CALCULATIONS

As stated in section 2.3 Methodology, some factors must be determined before the CIBL depth and LCL height are estimated. A program has been written to estimate these values as well as the CIBL depth and LCL height.

#### 3.1 SOUNDING ANALYSIS

The thickness and lapse rate of each layer of an upwind sounding must be determined for the CIBL calculations. The thickness in meters of each layer is determined using:

$$\Delta Z = R_d T_{vm} / g \ln(P_l / P_u) \quad (3)$$

where  $T_{vm}$  is the layer mean virtual temperature. The vapor pressure (mb or hPa) is calculated using equations given by Duffield and Nastrom (1983):

$$e_{sw} = 6.11 * 10^{[7.5T/(237.3 + T)]} \quad \text{for } T_d > 0 \text{ } ^\circ\text{C} \quad (4)$$

$$e_{sw} = 6.11 * 10^{[9.5T/(265.5 + T)]} \quad \text{for } T_d < 0 \text{ } ^\circ\text{C} \quad (5)$$

The resulting pressure heights are usually within six meters of the observed heights. The layer potential lapse rate is calculated using:

$$\theta = T_k (P_o / P)^{.286} \quad (6)$$

Examples are given in table 3.1.

Table 3.1. Layer analysis for Egbert (WET) 11Z, 20 February 1990.

Lyr	PPP-PPP (mb)	Base-Top heights (m)	Depth (m)	Temperatures (°C)	Lapse Rate (LR, °C/km)	Potential Temp LR
1	999-972	0-207	207	-14.3 to -15.5	-5.8/km	4.0/km
2	972-947	207-404	197	-15.5 to -15.3	+1.0/km	10.9/km
3	947-910	404-704	300	-15.3 to -16.7	-4.7/km	5.2/km
4	910-886	704-905	201	-16.7 to -16.5	+1.0/km	11.1/km
5	886-850	905-1215	310	-16.5 to -19.1	-8.4/km	1.4/km
6	850-840	1215-1303	88	-19.1 to -19.3	-2.3/km	7.9/km
7	840-786	1303-1799	496	-19.3 to -17.5	+3.6/km	14.2/km
8	786-735	1799-2300	501	-17.5 to -18.5	-2.0/km	8.4/km
9	735-716	2300-2496	196	-18.5 to -16.5	+10.2/km	21.9/km
10	716-700	2496-2666	170	-16.5 to -17.1	-3.5/km	6.9/km
11	700-688	2666-2795	129	-17.1 to -18.3	-9.3/km	0.5/km
12	688-610	2795-3691	897	-18.3 to -19.1	-8.9/km	1.0/km
13	610-500	3691-5157	1465	-19.1 to -23.7	-3.1/km	7.9/km

### 3.2 SHORELINE WINDSHIFT ESTIMATION

The windshift along the shoreline should be estimated, since over-lake fetch is a function of wind direction. Hsu (1986) presents equations developed by Schwab (1978) based on graphs given by Resio and Vincent (1977) to predict the over-water wind speed and the shoreline windshift for Lakes Erie and Ontario as a function of land-based wind speeds and air-lake temperature differences:

$$U_{\text{lake}} = U_{\text{land}}(1.2 + 1.85/U_{\text{land}})[1 - (\Delta T/|\Delta T|)(|\Delta T|/1920)^{1/3}] \quad (7)$$

$$\Delta\theta = (12.5 - 1.5\Delta T) - (0.38 - 0.03\Delta T)U_{\text{lake}} \quad (8)$$

where  $\Delta T$  is the air-lake temperature difference, and  $\Delta\theta$  is the clockwise angle between land and over-water winds. Figure 13 shows that unstable cases with light winds produce the greatest veering.

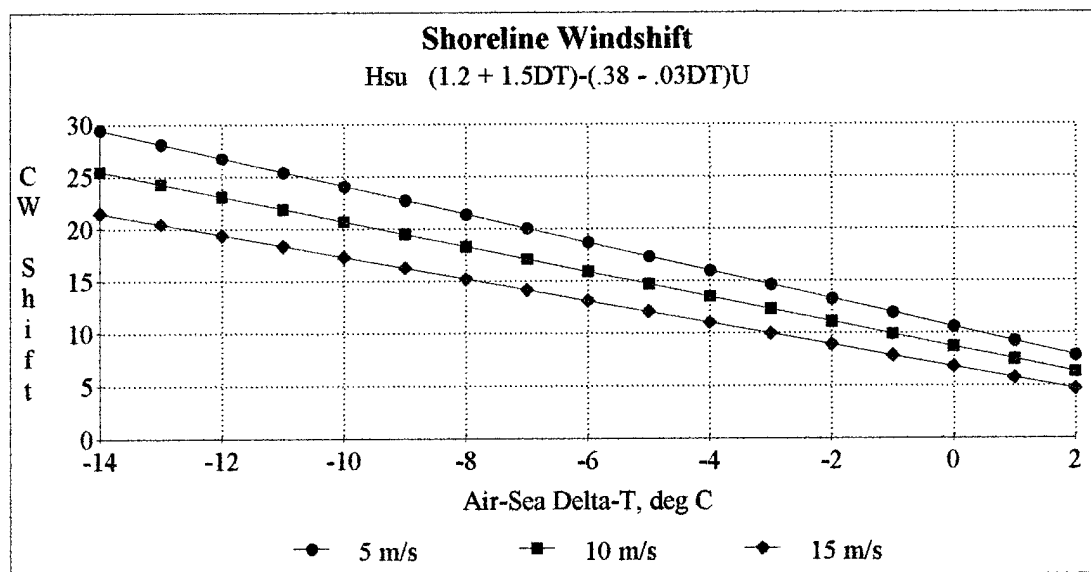


Fig. 13. Shoreline windshift as a function of the over-water windspeed and air-water temperature difference.

### 3.3 OVER-WATER DRAG COEFFICIENT

A constant drag coefficient, such as  $1.5 \times 10^{-3}$  is sometimes used for statically neutral conditions over water, or it can be obtained as a function of wind speed, using one of the equations given in Table 7-3 (Stull, 1988):

$$C_{DN} = [0.75 + 0.067U] \times 10^{-3} \quad (9)$$

where  $U$  is the 10 m mean horizontal wind magnitude. This equation yields  $C_{DN}$  values of  $1.4 \times 10^{-3}$  with a windspeed of  $10 \text{ ms}^{-1}$ , and  $1.7 \times 10^{-3}$  with a windspeed of  $15 \text{ ms}^{-1}$ . A plot of values is shown in figure 14 for a range of wind speeds.

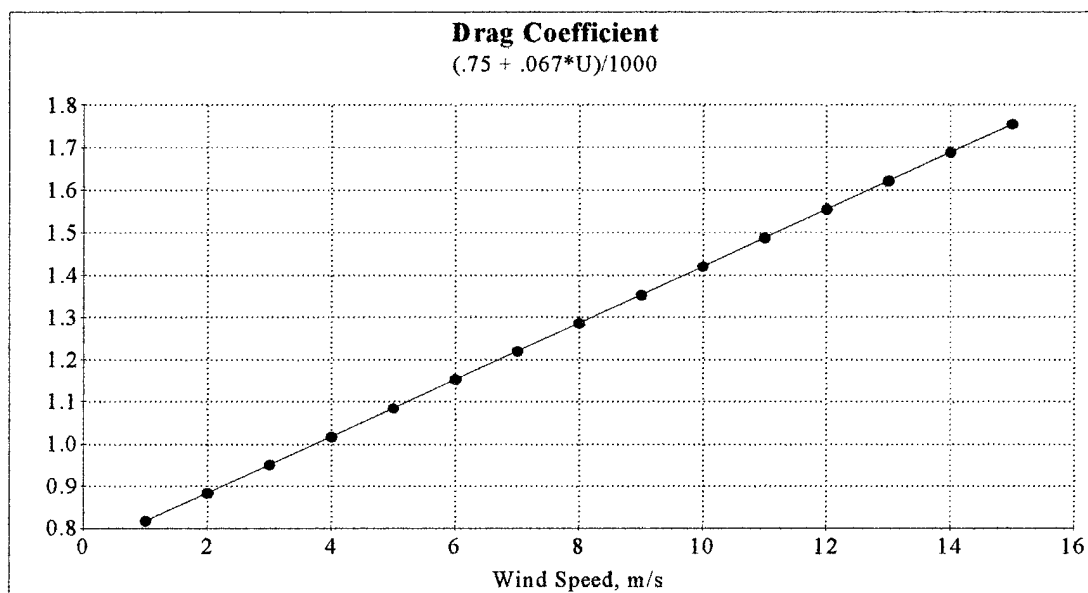


Fig. 14. Over-water drag coefficient as a function of wind speed.

### 3.4 OVER-WATER TEMPERATURES AND WIND SPEEDS

The over-water air temperatures, dewpoints and wind speeds are estimated using the equations in Table 2.2. Sensible and Latent heat fluxes can be found with:

$$hs = \rho C_p C_{DN} U (T_{aw} - T_w) \quad (10)$$

$$hq = \rho L C_{DN} U (q_{aw} - q_w) \quad (11)$$

where  $C_{DN} = C_{EN} = C_{HN}$  for statically neutral conditions (Stull, 1988).

The values are calculated every 300 seconds, with a 5-minute fetch obtained by multiplying the wind speed by elapsed time, and summed to a current total fetch (Totaldx). Table 3.2 shows the gradual increase in wind speed, and air and dewpoint temperatures, resulting in a decrease in sensible surface heat flux with increasing over-water fetch. The over-water air temperature warms more rapidly than the dewpoint temperature, with the dewpoint depression increasing from five to seven by landfall on the downwind shore.

The dewpoint temperature warming rate gradually increases with distance, a consequence of the non-linear increase of water vapor pressure as a function of temperature (figure 2.7 and figure 4.13, Wallace and Hobbs, 1977)

As noted by Phillips (1972) nearly half of the total possible temperature modification, the difference between the over-land and over-water air temperatures, takes place in the first ten minutes over water. The decrease in the warming rate is attributed to the sensible heating of air in an initially shallow mixed layer which grows progressively deeper.

Table 3.2. Over-water values using a Toronto (YYZ) observation 12Z, 20 February 1990.

YYZ 1200Z conditions: 43 BKN 7 M/-11/-16/0106/050  
Lake Temperature: 1.4 °C

Count	Totaldx	U	T	T <sub>d</sub>	q <sub>w</sub>	q <sub>aw</sub>	h <sub>s</sub>	h <sub>q</sub>
	(m)	(m/s)	(°C)	(°C)	(kg/kg)	(kg/kg)	(w/m <sup>2</sup> )	(w/m <sup>2</sup> )
1	1100	3.7	-8.7	-13.9	0.0041	0.0013	44.3	30.9
2	2267	3.9	-7.8	-13.9	0.0041	0.0013	43.8	33.2
3	3475	4.0	-7.3	-13.9	0.0041	0.0013	43.2	34.6
4	4710	4.1	-7.0	-13.8	0.0041	0.0013	42.7	35.6
5	5967	4.2	-6.7	-13.8	0.0041	0.0013	42.3	36.3
6	7242	4.3	-6.5	-13.8	0.0041	0.0013	41.9	37.0
7	8533	4.3	-6.3	-13.7	0.0041	0.0013	41.5	37.5
8	9836	4.3	-6.1	-13.7	0.0041	0.0013	41.2	37.9
9	11151	4.4	-6.0	-13.7	0.0041	0.0013	40.8	38.3
10	12476	4.4	-5.9	-13.6	0.0041	0.0013	40.5	38.6
11	13810	4.4	-5.8	-13.6	0.0041	0.0013	40.3	38.9
12	15153	4.5	-5.7	-13.5	0.0041	0.0013	40.0	39.2
13	16504	4.5	-5.6	-13.5	0.0041	0.0013	39.7	39.4
14	17862	4.5	-5.5	-13.5	0.0041	0.0013	39.5	39.6
15	19227	4.5	-5.4	-13.4	0.0041	0.0013	39.3	39.8
.								
.								
.								
76	108654	5.1	-3.4	-11.0	0.0041	0.0016	32.1	41.3
77	110179	5.1	-3.4	-11.0	0.0041	0.0016	32.0	41.2
78	111705	5.1	-3.4	-10.9	0.0041	0.0016	32.0	41.2
79	113232	5.1	-3.4	-10.9	0.0041	0.0016	31.9	41.2
80	114760	5.1	-3.3	-10.9	0.0041	0.0016	31.8	41.1
81	116290	5.1	-3.3	-10.8	0.0041	0.0016	31.8	41.1



### 3.5 CIBL AND LCL CALCULATIONS

The over-water CIBL depth is found with Venkatram's equation. The program will use the current layer lapse rate until the upward growth requires the application of the next higher layer lapse rate. The LCL temperature, pressure and height are obtained using Duffield and Nastrom's (1983) equations:

$$T_{LCL} = T_d - (0.212 + 0.001571T_d - 0.000436T_o)(T_d - T_o) + 273.16 \quad (12)$$

where the dewpoint and air temperatures ( $T_d$  and  $T_o$  respectively) are in °C, and

$$P_{LCL} = P_o(T_{LCL}/T_o)^{3.5} \quad (13)$$

$$Z_{LCL} = (RT_m/g)\ln(P_o/P_{LCL}) \quad (14)$$

where the temperatures are in °K. Table 3.3 lists the described values.

The CIBL grows with increasing fetch, sometimes slower when eroding a layer of greater stability, and more rapidly with less stable layers. The predicted LCL depends upon the regression equations for over-water air temperature and dewpoint. The predicted LCL rises over the lake as the equations predict the air will warm faster than it picks up moisture, eventually the LCL lowers before landfall, as the rate of warming decreases.

In some cases the LCL will be lower than the CIBL depth, and clouds may form. In other cases the LCL may remain above the maximum depth of the CIBL. This may be due to a shallow CIBL forming over a short fetch, or great stability limiting the CIBL growth, or an extremely dry air mass. The depth of the predicted CIBL and the anticipated cloud may be used to estimate the intensity of lake-effect convection or the non-existence of significant snowfall.

Table 3.3. Over-water CIBL, 20 February 1990 based on the WET 11Z sounding and the YYZ 12Z observation.

Count	Totaldx	Z <sub>id</sub>	Tz <sub>id</sub>	Pz <sub>id</sub>	T <sub>lcl</sub>	P <sub>lcl</sub>	Z <sub>lcl</sub>
	(m)	(m)	°K	(mb)	°K	(mb)	(m)
1	1100	64	263.9	1024	258.2	950	642
2	2267	92	264.4	1021	258.1	938	741
3	3475	115	264.7	1018	258.0	931	797
4	4710	134	264.9	1015	258.0	926	836
5	5967	151	265.0	1013	258.0	923	865
6	7242	167	265.0	1011	258.0	920	887
7	8533	182	265.1	1009	258.0	918	906
8	9836	195	265.1	1007	258.0	916	922
9	11151	208	265.1	1006	258.0	915	935
10	12476	251	264.8	1000	258.0	913	946
11	13810	269	264.8	998	258.1	912	956
12	15153	283	264.7	996	258.1	911	964
13	16504	295	264.7	994	258.1	910	972
14	17862	305	264.7	993	258.1	910	978
15	19227	315	264.7	992	258.2	909	984
.							
.							
.							
76	108654	1386	256.2	862	260.6	916	932
77	110179	1396	256.1	861	260.7	916	929
78	111705	1405	256.0	860	260.7	917	926
79	113232	1413	255.9	859	260.8	917	923
80	114760	1421	255.9	858	260.8	917	920
81	116290	1428	255.8	857	260.9	918	917

The predicted CIBL depths and LCL heights will be checked against downwind soundings and surface observations in the next chapter.

## 4. CASE STUDIES

### 4.1 LONG-FETCH CASE STUDY

The LOWS project attempted to observe the heavy lake-effect snow-producing storms associated with westerly winds and long fetches. Unfortunately, the project was hindered by a warm spell, and had fewer than normal long-fetch events (Reinking *et al.*, 1991). The first and best observed event was on 12 January 1990.

#### 4.1.1 Synoptic and Mesoscale Analysis

The 12 January 1990 storm developed under almost ideal conditions. At 0000 UTC, a 500 mb low was moving eastward between James Bay and the Great Lakes, establishing a west-southwest flow over the long axis of Lake Ontario. The weather system was nearly vertically stacked with minimal directional shear, and with lower atmospheric cold air advection to the south of the low. (Figs. 15a, 15b.)

The front moved from eastern New York at 0000 UTC to off the east coast by 1200 UTC, with west-southwesterly wind flow over the eastern Great Lakes throughout the period (Figs. 15c and 16c.) Both the 850 mb windflow and surface isobar pattern (Figs. 15b and 15c) pass over alternating land and lake surfaces, suggesting that the air arriving over Lake Ontario may have been modified by Lakes Huron, Michigan and Superior. This pre-conditioning by the upstream lakes may help to warm and moisten the post-frontal air mass, and lift the capping inversion.

The 850 mb temperature at Buffalo decreased from  $-7^{\circ}\text{C}$  at 0000 UTC to  $-11^{\circ}\text{C}$  at 1200 UTC, increasing the TL850 lapse rate to the range of  $-12$  to  $-15$  based on the lake surface temperature analysis from 8 January 1990 (Fig. 17.) The TL850 instability together with the long over-lake fetch and minimal directional shear produced four successive single snowbands.

By 1200 UTC, the system had continued moving eastward. The wind flows at the 500 mb, 850 mb and surface levels crossed over Lake Huron and Ontario Province before crossing over Lake Ontario (Fig. 16.) Cold air advection was still expected at 850 mb, and the TL850 instability would increase accordingly, but the over-lake westerly wind flow veered as the low moved east, bringing northwesterly wind flow across shorter over-lake fetches.

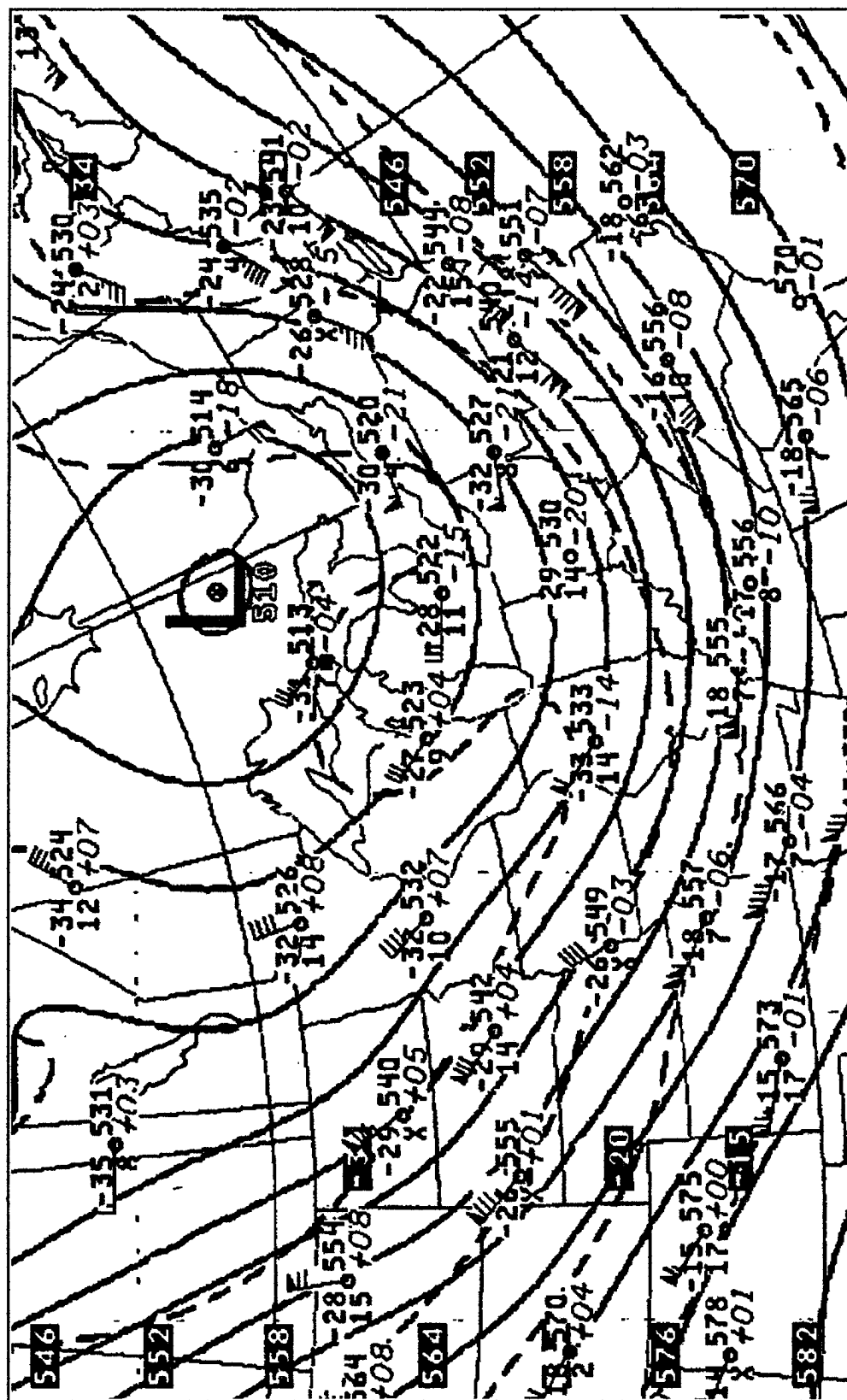


Fig. 15a. 500 mb analysis 0000 UTC 12 January 1990. A closed low moves eastward between the Great Lakes and James Bay.

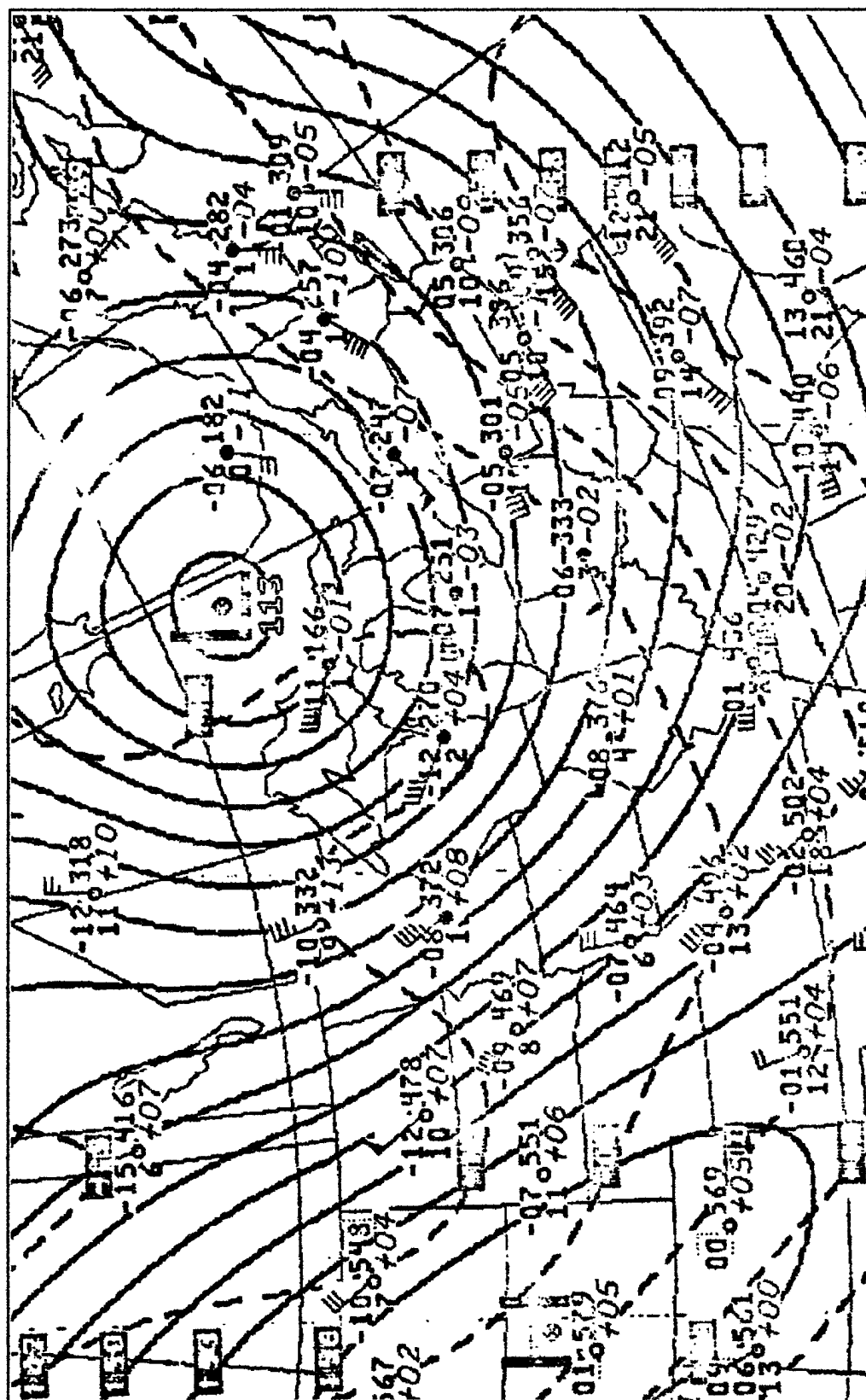


Fig. 15b. 850 mb analysis 0000 UTC 12 January 1990. An 850 mb low between the Great Lakes and James Bay is accompanied by cold air advection over the western and central lakes. Wind flow is along Lake Ontario, with upstream flow over the alternating land and lake surfaces.

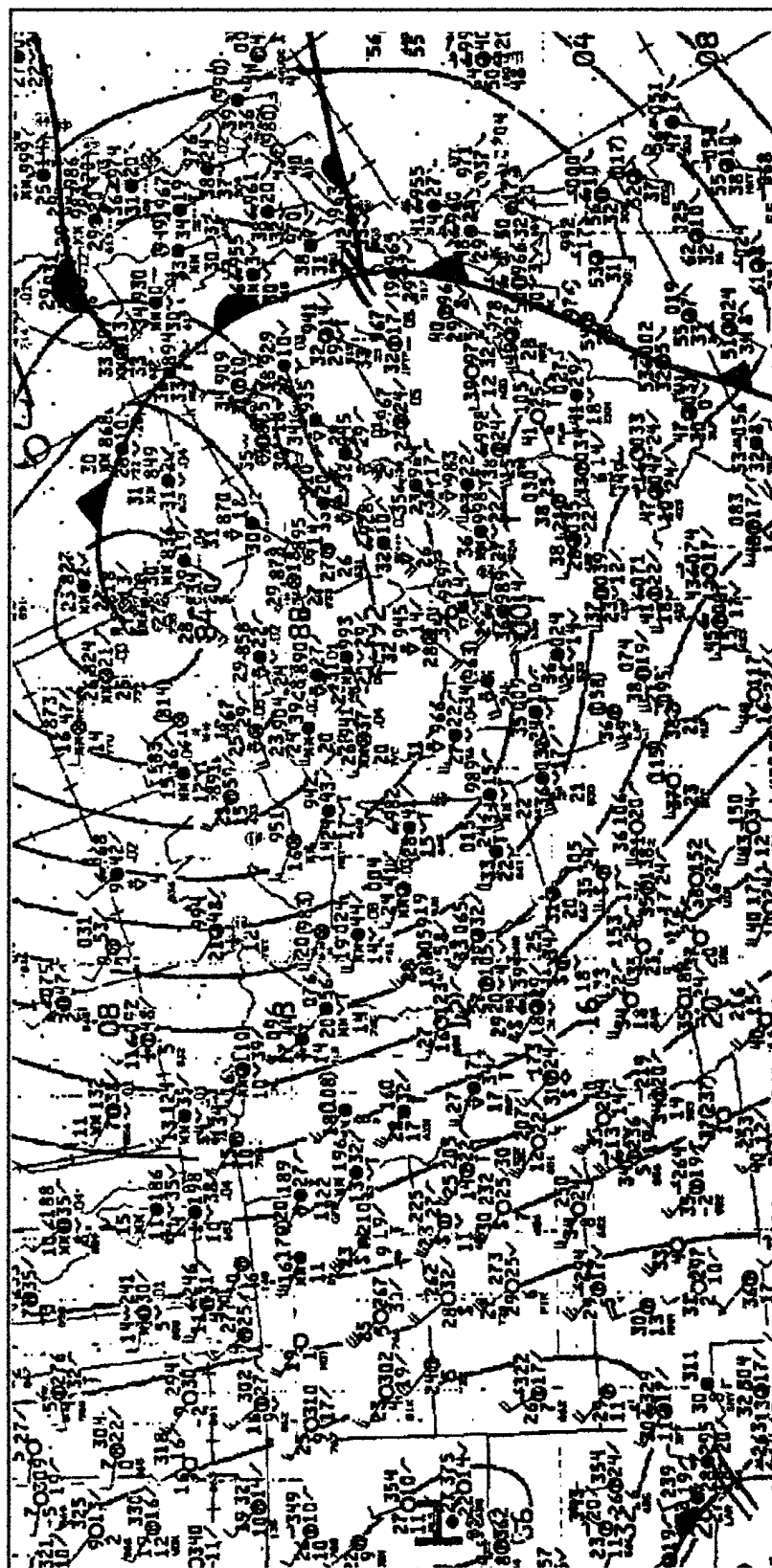


Fig. 15c. Surface analysis 0000 UTC 12 January 1990. The surface low is south of James Bay, and the occluded front is past Lake Ontario and is located in eastern New York. The post-frontal winds are southwesterly from the surface low to the east shore of Lake Michigan, with surface temperatures near or at freezing around Lake Ontario.

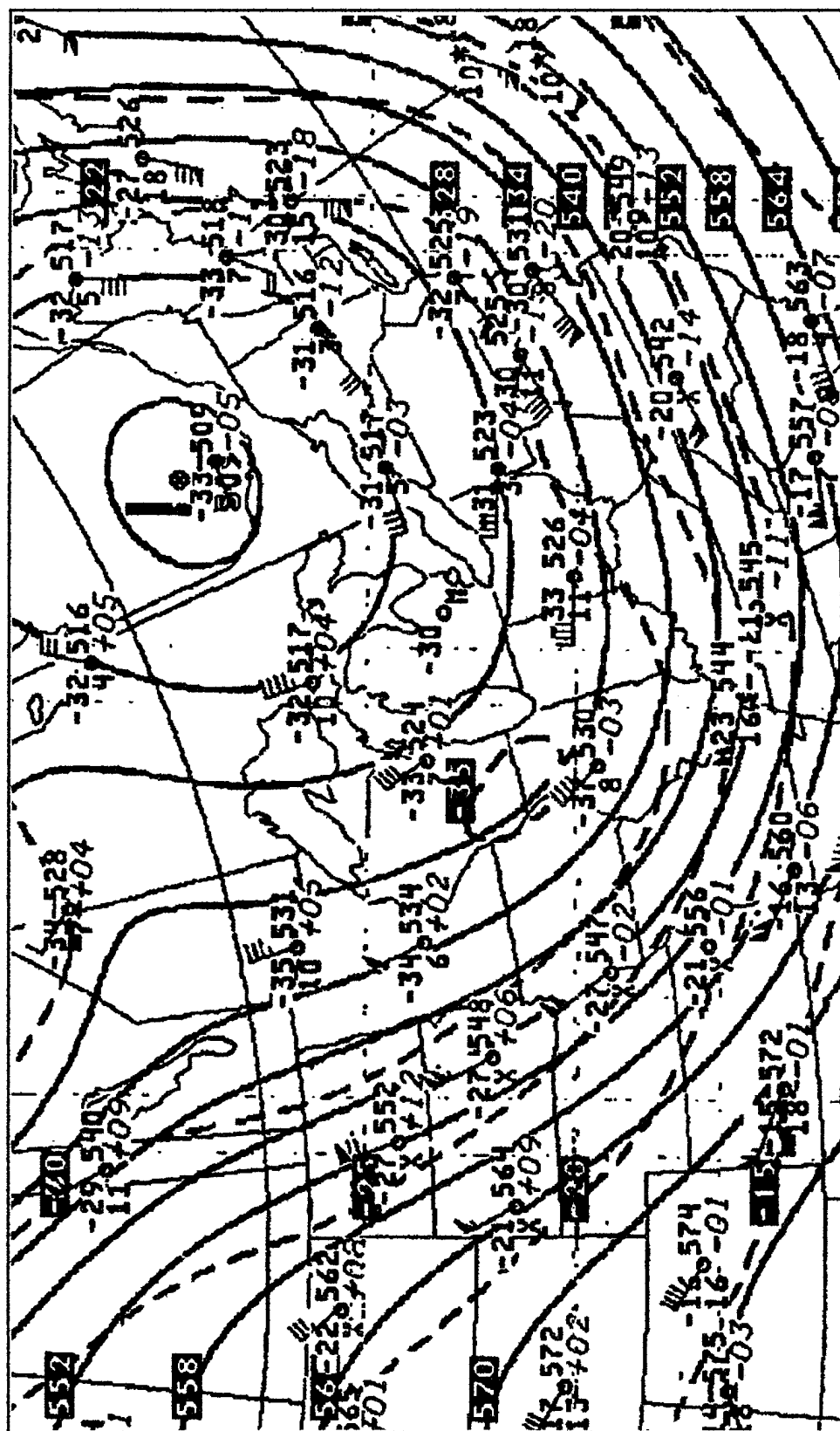


Fig. 16a. 500 mb analysis 1200 UTC 12 January 1990. The closed low has moved northeast of the Great Lakes and the upper wind flow is along the long axis of Lakes Huron and Ontario.



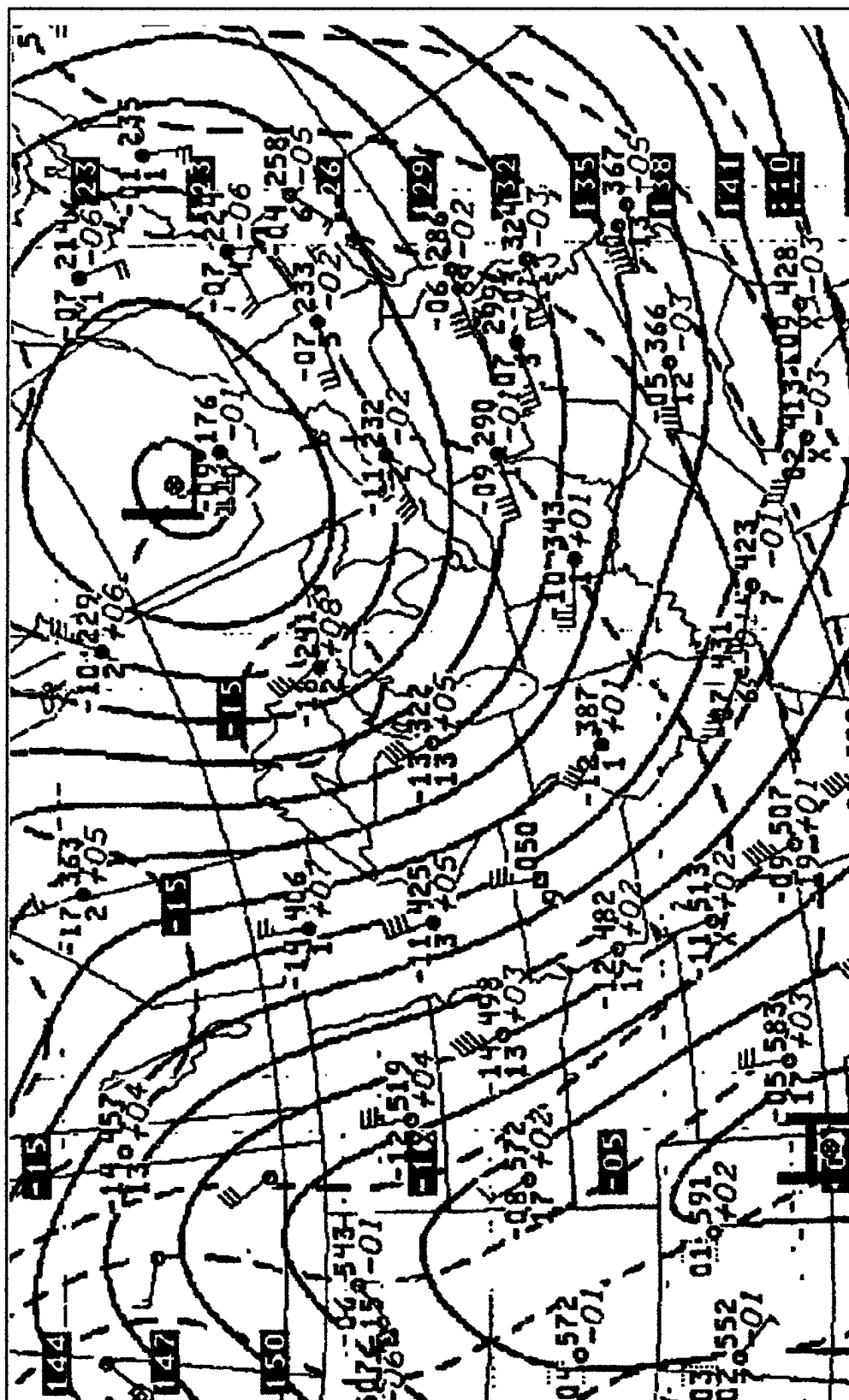


Fig. 16b. 850 mb analysis 1200 UTC 12 January 1990. The low moves eastward with cold air invading the eastern Great Lakes. Wind flow is along Lakes Huron and Ontario, with Huron upstream of Ontario.

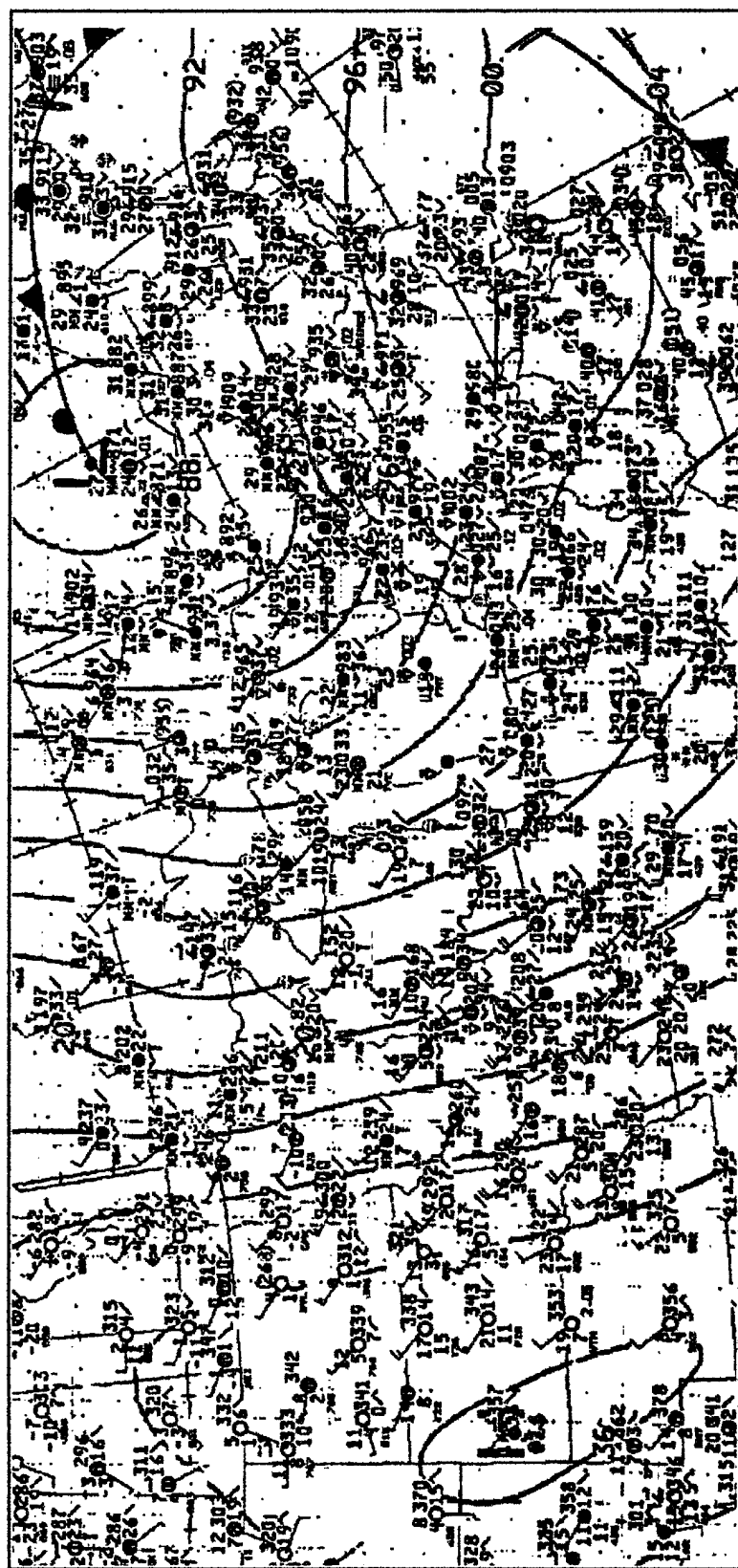


Fig. 16c. Surface analysis 1200 UTC 12 January 1990. The surface low has moved eastward, and the front is off of the east coast. A post-frontal trough is suggested by a distinct wind-shift line through the Ontario peninsula and central lower Michigan.

Lake Ontario is ice-free during typical winters due to its easterly location and depth, while the northeastern third of shallower Lake Erie is ice-covered at this time. Figure 17 is the lake surface temperature for Lake Ontario for the week of 8 January 1990. The area of  $+4^{\circ}\text{C}$  water over the southern half of the lake suggests the most likely location for greater instability and convection.

The isotherm analysis in figure 18 shows the impact of Lake Erie's ice-cover, while Lake Ontario is ice-free and able to warm the air mass. The temperature gradients north and south of the lake don't appear to be sufficient to set up a land breeze circulation, since the warmest predicted over-water air temperatures are only  $-0.9^{\circ}\text{C}$  and the nearby land areas have air temperatures ranging from  $-1$  to  $-3^{\circ}\text{C}$ .

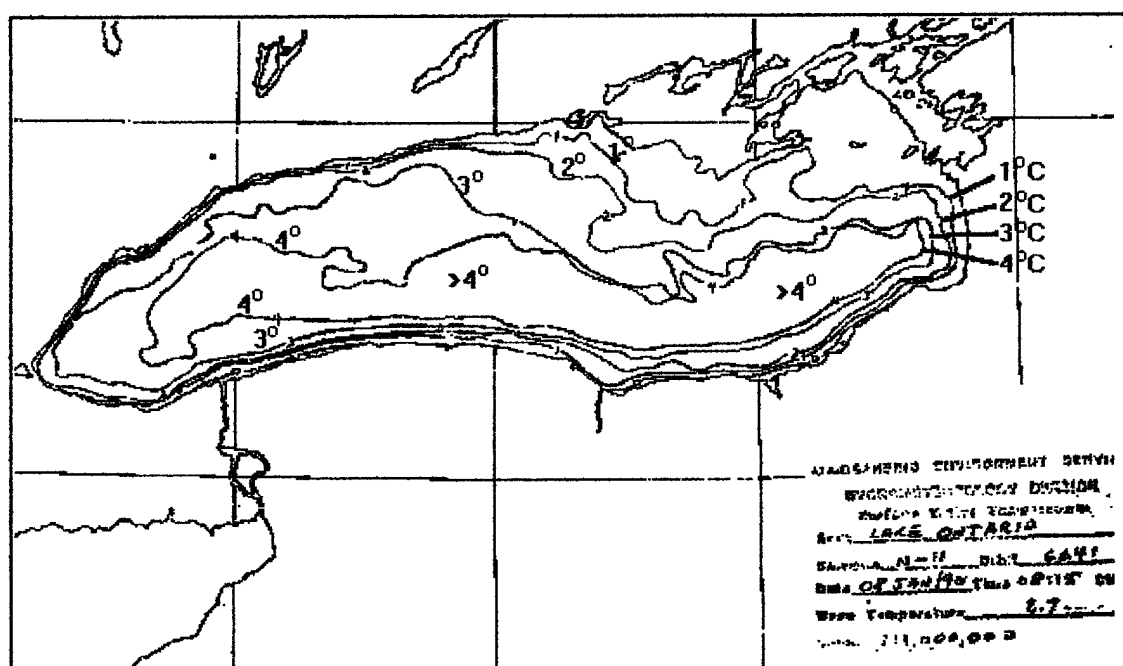


Fig. 17. Lake Ontario lake surface temperature analysis for the week of 8 January 1990.



and west-southwesterly over lakes Erie and Ontario, Buffalo had an over-land upstream wind flow, so both Egbert (WET) and Buffalo (BUF) soundings are considered upwind soundings for this case.

While subsidence is a major factor in lowering the capping inversion, the affect of upstream lakes on air mass modification may also help to explain the differences between the Buffalo and Egbert soundings in figures 19c and 19d. The lower atmosphere can become modified by passage over upstream lakes and land surfaces, and at 0000 UTC (Fig. 15b) both Egbert and Buffalo are downwind of Lake Huron (and partially Lake Erie for Buffalo.) By 1200 UTC (Fig. 16b) Buffalo is downwind of Lake Huron at 850 mb, while Egbert is downwind of Georgian Bay. The southern half of the bay was ice-free at this time, but the over-water fetch was less than that over Lake Huron.

A comparison of the Buffalo and Oswego (OSW) 1200 UTC temperature profiles in figures 19d, 19e and 20 reveal a neutral layer from surface to about 500 m, with a less-than-neutral lapse rate in the mixed-layer. The OSW lapse rate is closer to moist adiabatic with a temperature profile one to two degrees warmer than that over BUF. OSW also had a CIBL roughly 300 m higher than BUF, and a cloud layer from 500 to 2100 m. These differences reflect the exchange of heat and moisture as the air column moved across the lake. The latent heat released from condensation may also act to increase the CIBL depth.

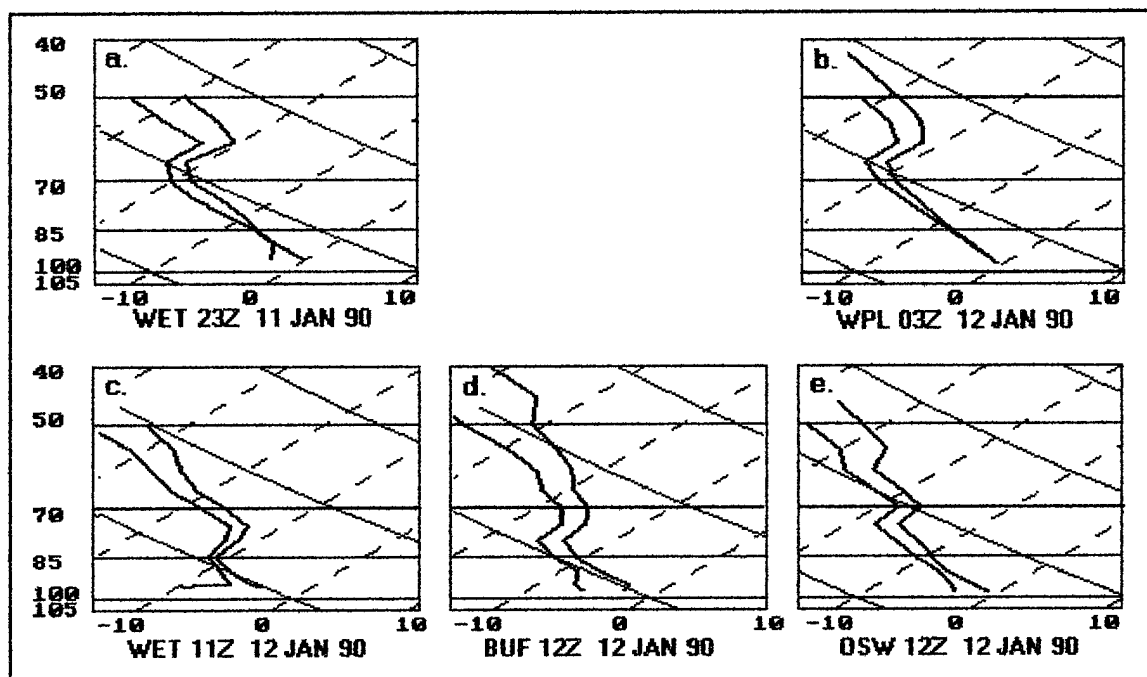


Fig. 19. Skew-T profiles for upwind (WET, BUF) and downwind (WPL, OSW) locations.

#### 4.1.2.2 CIBL Estimation

The Buffalo sounding was selected as the upwind profile, since the west-southwesterly upstream wind flow was over land rather than over Lakes Erie or Ontario, and Toronto (YYZ) was selected for the input surface observation. The input values were as follows:

```
72528 TTA 62121 72528 99968 03130 26017 00545 // // //
85232 10916 26534 70706 16319 28040 50517 31350 28042 40672
415// 28546 30862 517// 28034 25981 495// 27049 20128 477//
27565 15319 481// 27061 10583 533// 28675 88321 517// 29038
77124 27569 40706 51515 10164 00013 10194 26530 27039
```

```
72528 TTBB 6212/ 72528 00968 03130 11964 02350 22924 05716
33767 15722 44747 14116 55609 22926 66595 22326 77500 31350
88464 33350 99449 34558 11411 39757 22321 517// 33171 469//
44104 537// 55100 533// 31313 110// 1103/
```

Mean lake surface temperature: 2.5 ° C

YYZ temperature, dewpoint, winds and altimeter setting:

-4° C, -8° C, 260 at 12 knots, 29.30 inches Hg.

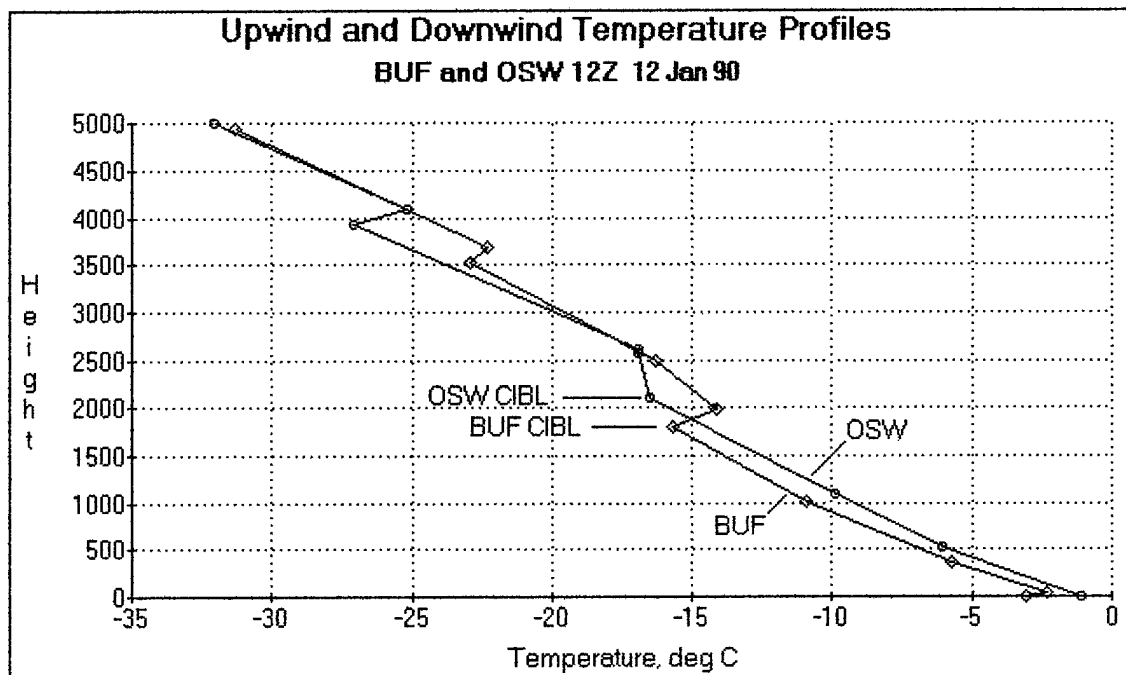


Fig. 20. Upwind and downwind temperature profiles, Buffalo (BUF) and Oswego (OSW) 1200 UTC 12 January 1990. The apparent top of the cloud-filled CIBL is approximately 1800 m AGL at BUF and 2100 m AGL at OSW.

The final result was an underestimated CIBL depth of 1800 m (Fig. 21), which was 300 m lower than observed at Oswego (Fig. 20.) The error is possibly due to applying equation (2), which is based on dry adiabatic growth, to a cloud-filled layer.

$$z_1 = z_{i0} + (u_* / u_m) [2x | T_{\text{warm}} - T_{\text{cool}} | / |\beta| (1 - 2F)]^{1/2} \quad (2)$$

Equation (2) predicts the dry adiabatic growth of a CIBL through a moist adiabatic layer which is already freely convective, resulting in an underestimated depth for the cloud-filled convective boundary layer. A better approach may be to develop a cloudy CIBL equation incorporating the release of latent heat of condensation into CIBL growth.

The program predicts an over-lake LCL (Fig. 21) at 520 m (1700 feet) above lake level (ALL). The observed ceilings were 1600' at Watertown (field elevation 79' ALL)

and 1300' at Fort Drum (400' ALL) in figure 18. The predicted LCL rises with distance in the first 40 km over water, as Phillips' equations allow the surface layer temperature to warm faster than the dewpoint over shorter fetches. The LCL lowers beyond 40 km as the dewpoint increases more rapidly than the temperature at longer fetches. The LCLs are calculated with formulae (12), (13) and (14), given in chapter 3.

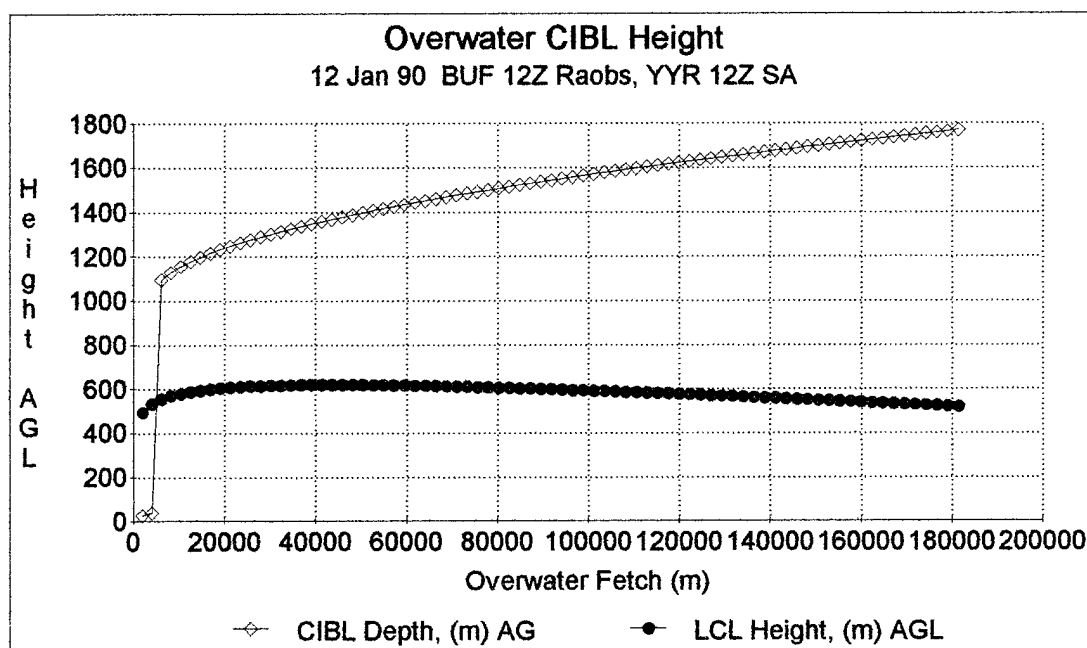


Fig. 21. Estimated over-water CIBL depth and LCL height for 12 January 90.



## 4.2 SHORT-FETCH CASE STUDY

A lake-effect event on 20 February 1990 demonstrates how much of an impact upstream lakes have on air mass modification.

### 4.2.1 Synoptic and Mesoscale Analysis

The 0000 UTC 20 February 1990 500 mb chart (Fig. 22a) shows a low east of James Bay, moving eastward. The windflow is northwesterly over the Great Lakes with a polar jet of 100 knots observed over Buffalo. The low has moved to eastern Quebec by 1200 UTC (Fig. 22b) while an approaching high pressure ridge and decreasing pressure gradient allow winds to diminish slightly over the Great Lakes. There is also some cold air advection and slight veering at 850 mb as the ridge advances between 0000 and 1200 UTC, with warm air advection to the west (Figs. 23a, 23b). The 850 mb heights at Buffalo have risen from 1441 to 1501 m during this time and temperatures have decreased from -15 to -19°.

The surface winds were generally from 270 through 300° in the eastern Great Lakes at 0000 UTC (Fig. 24a), but by 1200 UTC had veered to the north over Lakes Huron, Erie and Ontario as a high pressure area builds into the area (Fig. 24b.) The vertical shear increased with time as winds back between surface and 850 mb, and also between 850 to 500 mb by 1200 UTC.

Lake Ontario's surface temperature averages 1.4 °C with a small area of +3 °C in the eastern part of the lake (Fig. 25a). Lake Ontario remained mostly ice-free on this date, while Lakes Huron and Erie were partially ice covered, and the Georgian Bay was mostly (70-90%) ice covered (Fig. 25b). While we don't know Lake Huron's surface temperature, a conservative estimate of 0 °C would still yield a TL850 lapse rate of 18 to 19 °C,

enough to produce clouds and some isolated lake-effect snow showers in the west-northwesterly windflow between 0000 and 1200 UTC.

The winds had veered enough around Lake Huron by 1200 UTC to bring relatively unmodified air down the eastern shore of Georgian Bay and over Lake Ontario. Figure 26 shows the wind veering and sky clearing at Barre (CWCU) with decreasing temperatures and dewpoints from 0600 through 1200 UTC, while Toronto (CYYR) and Buffalo (KBUF) experience windshifts from 1000 through 1200 UTC. Barre is the closest surface reporting station to Egbert. Buffalo's snow showers also stop by 1200 UTC, possibly a result of Huron's lake-effect clouds and snow showers veering towards the south with the wind flow.

A surface data plot (Fig. 27a) shows the invasion of colder air east of Lake Huron with warmer air downwind of Lake Ontario. The isotherm analysis in figure 27b uses the predicted over water values to show the warming due to sensible heating from the lake. The observed temperatures of  $-6^{\circ}\text{C}$  at Niagara Falls, Rochester, and Oswego are quite close to the final predicted values of  $-5^{\circ}\text{C}$  just off of the southern shore. The over water values were predicted using the unstable category of equations from table 2.2.



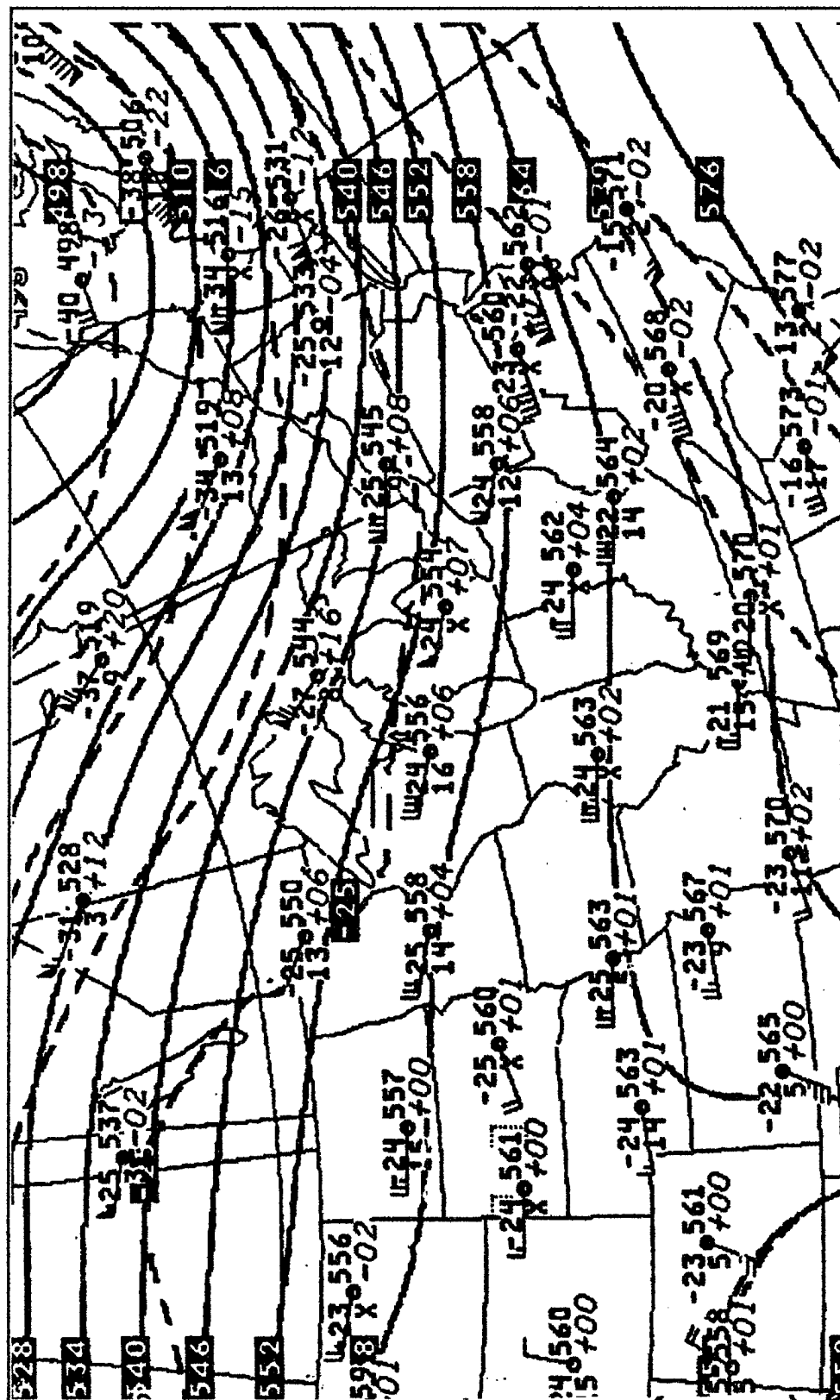


Fig. 22b. 500 mb analysis 1200 UTC 20 February 1990. The low has moved into eastern Quebec.

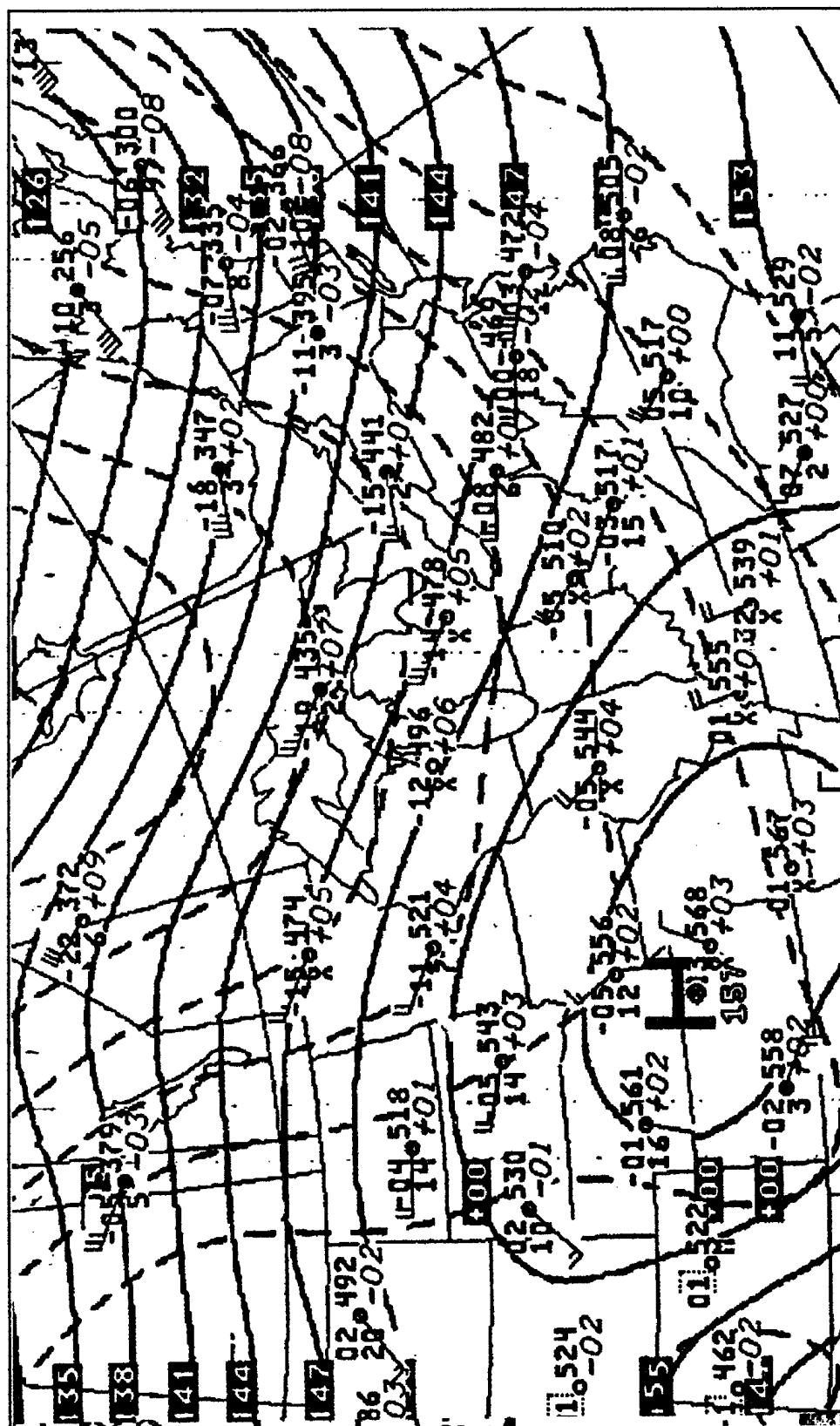


Fig. 23a. 850 mb analysis 0000 UTC 20 February 1990. Strong cold air advection over the eastern Great Lakes becomes neutral in the central and western regions.

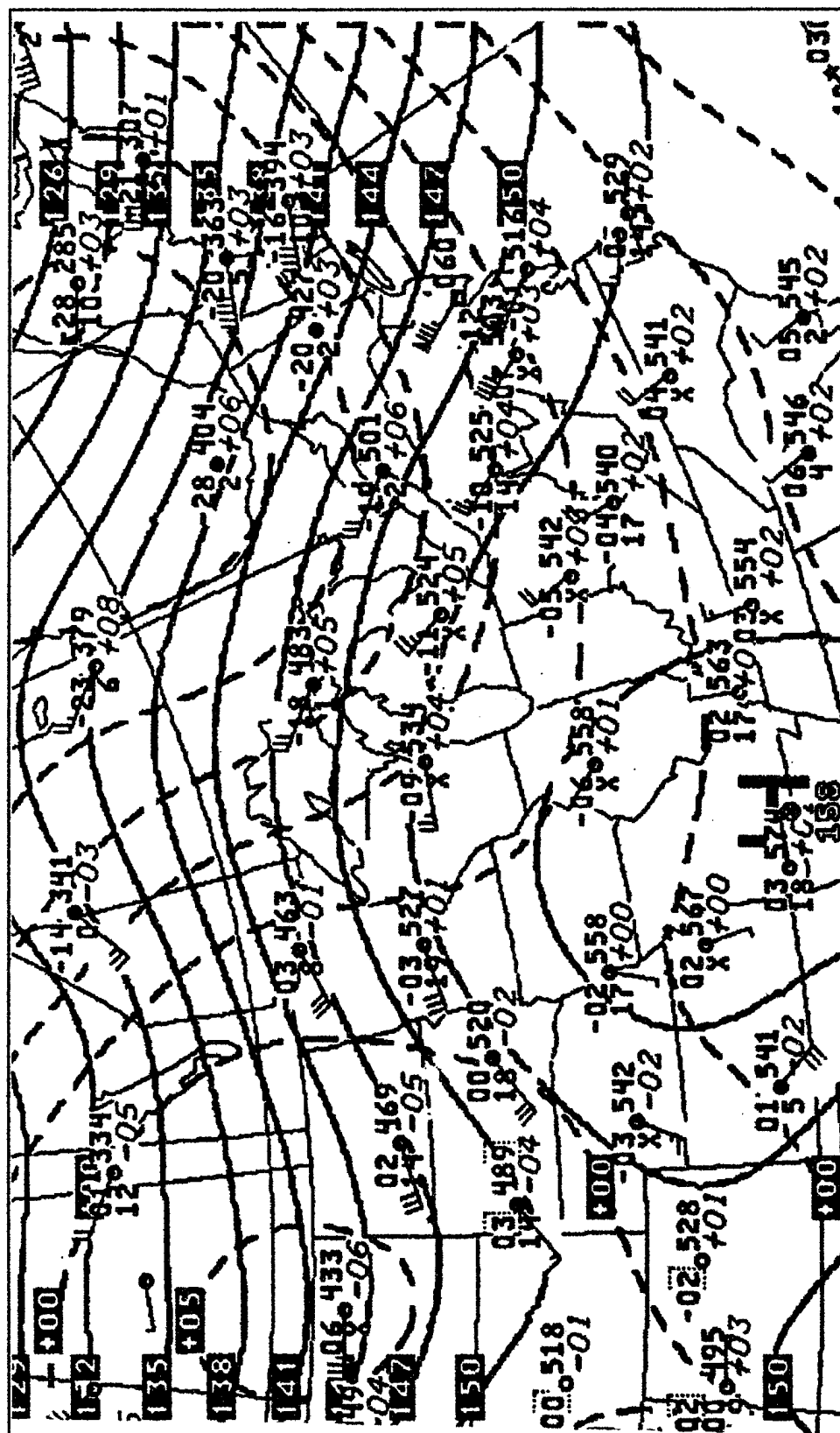


Fig. 23b. 850 mb analysis 1200 UTC 20 February 1990. Cold air advection ends over the eastern Great Lakes with warm air advection now over the western lakes. Winds over Buffalo have veered slightly since 0000 UTC.

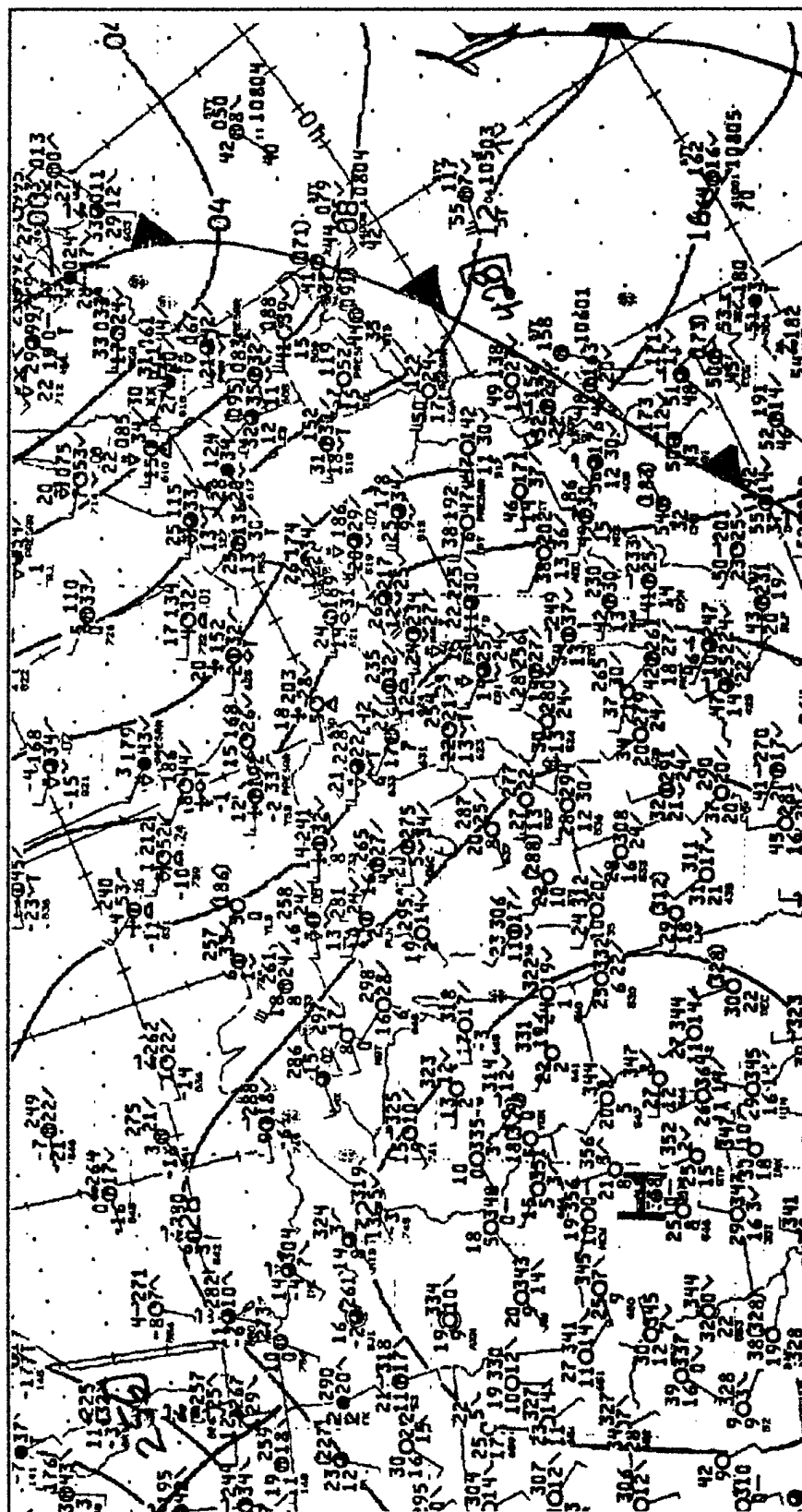


Fig. 24a. Surface analysis 0000 UTC 20 February 1990. The front has moved off the east coast with westerly post-frontal winds over the Great Lakes.

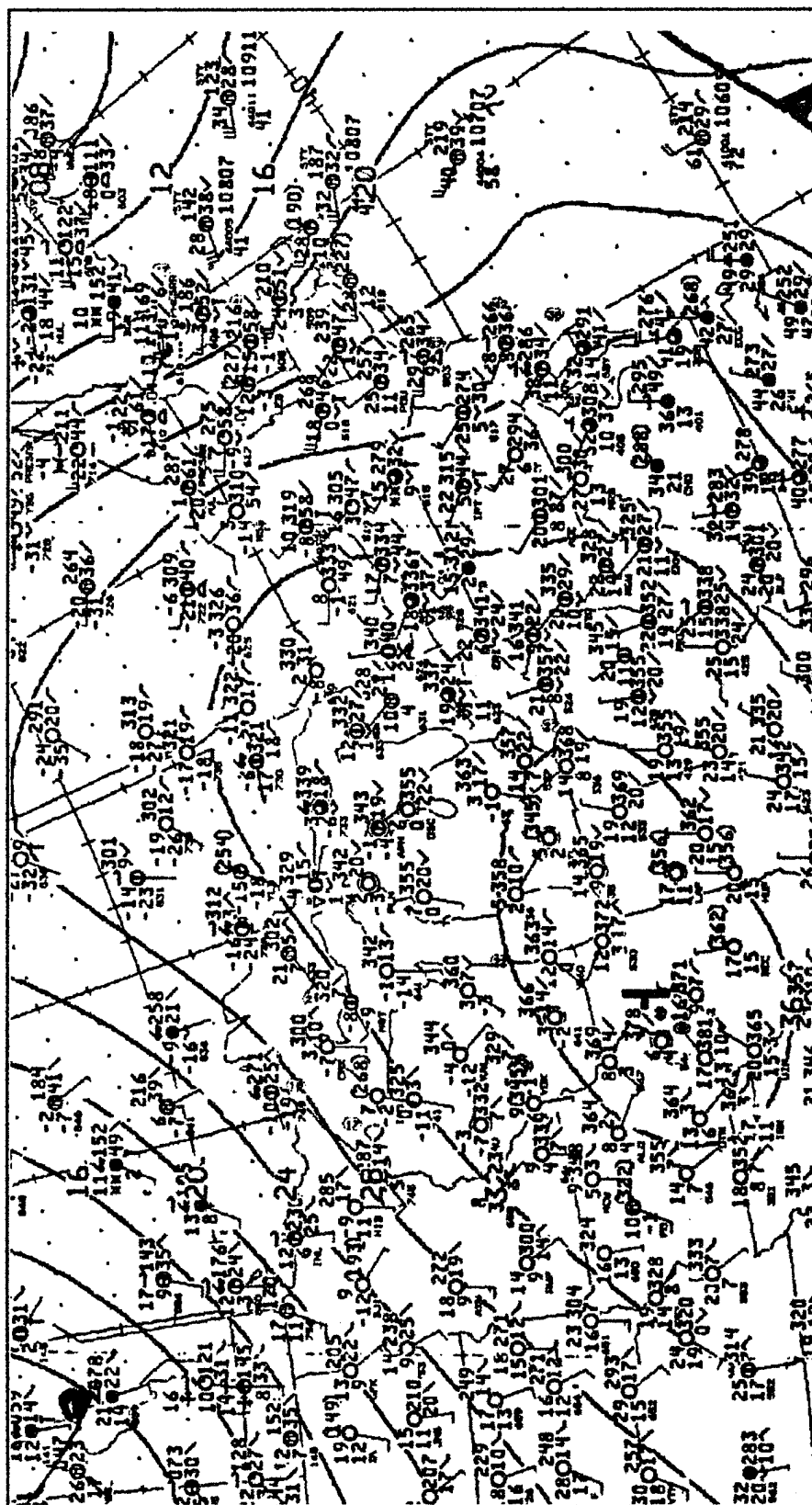


Fig. 24b. Surface analysis 1200 UTC 20 February 1990. The ridge builds into the area, shifting the winds from the north in the eastern Great Lakes.



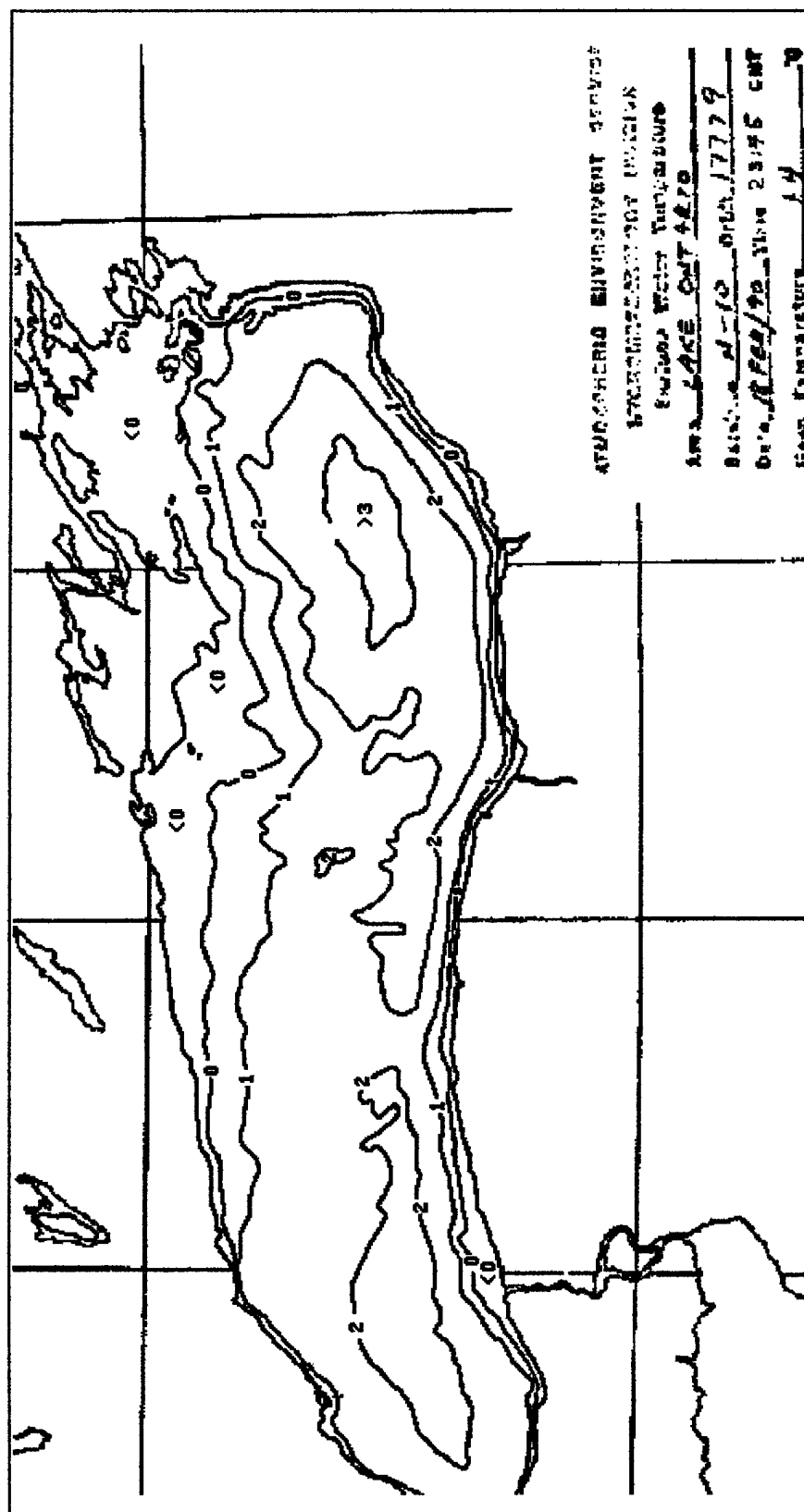


Fig. 25a. Lake Ontario surface temperature analysis, 18 February 1990.

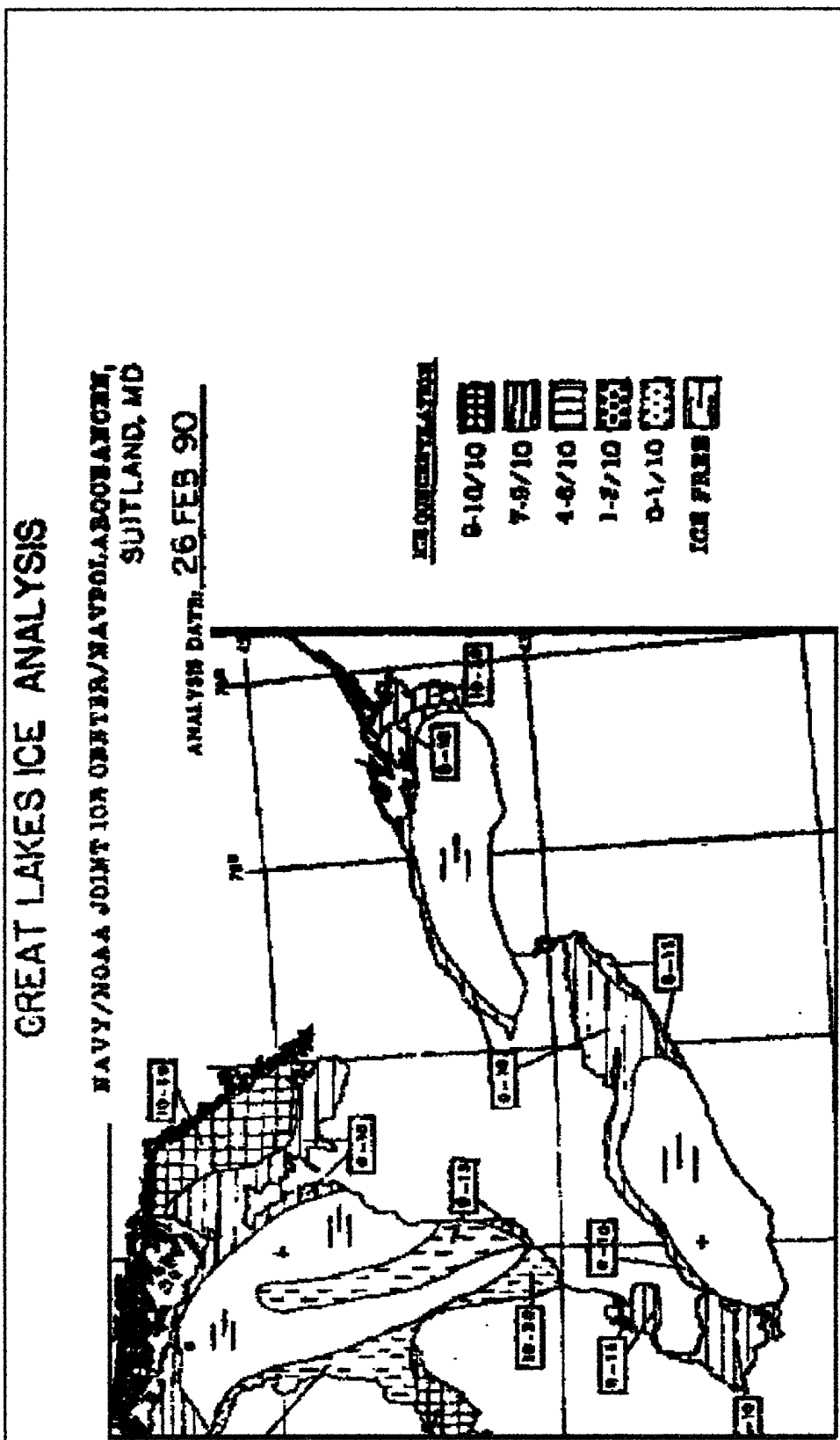


Fig. 25b. Great Lakes ice analysis 26 February 1990.

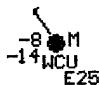
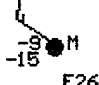
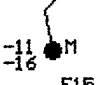
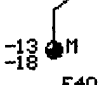
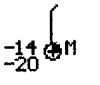
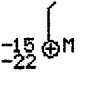
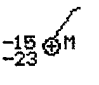
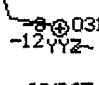
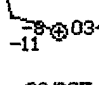
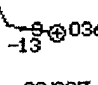
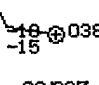
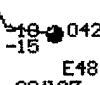
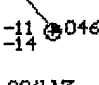
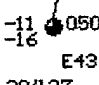
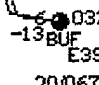
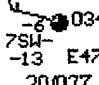
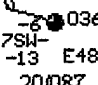
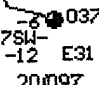
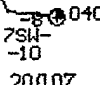
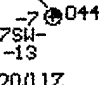
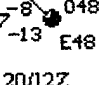
CWCU	 -9 M -14 WCU E25 20/06Z	 -9 M -15 E26 20/07Z	 -11 M -16 E15 20/08Z	 -13 M -18 E40 20/09Z	 -14 M -20 E40 20/10Z	 -15 M -22 E40 20/11Z	 -15 M -23 E40 20/12Z
CYYZ	 -8 031 -12 CYYZ E31 20/06Z	 -9 034 -11 E34 20/07Z	 -9 036 -13 E36 20/08Z	 -10 038 -15 E38 20/09Z	 -10 042 -15 E48 20/10Z	 -11 046 -14 E46 20/11Z	 -11 050 -16 E43 20/12Z
KBUF	 -6 032 -13 BUF E39 20/06Z	 -6 034 -13 7SW E47 20/07Z	 -6 036 -13 7SW E48 20/08Z	 -6 037 -12 7SW E31 20/09Z	 -8 040 -10 7SW E40 20/10Z	 -7 044 -13 7SW E44 20/11Z	 -8 048 -13 7SW E48 20/12Z

Fig. 26. Surface hourly observations 0600 through 1200 UTC 20 February 1990. Winds at Barre (see Fig. 10) gradually veer northerly through northeasterly with decreasing temperature, dewpoint and cloud cover.

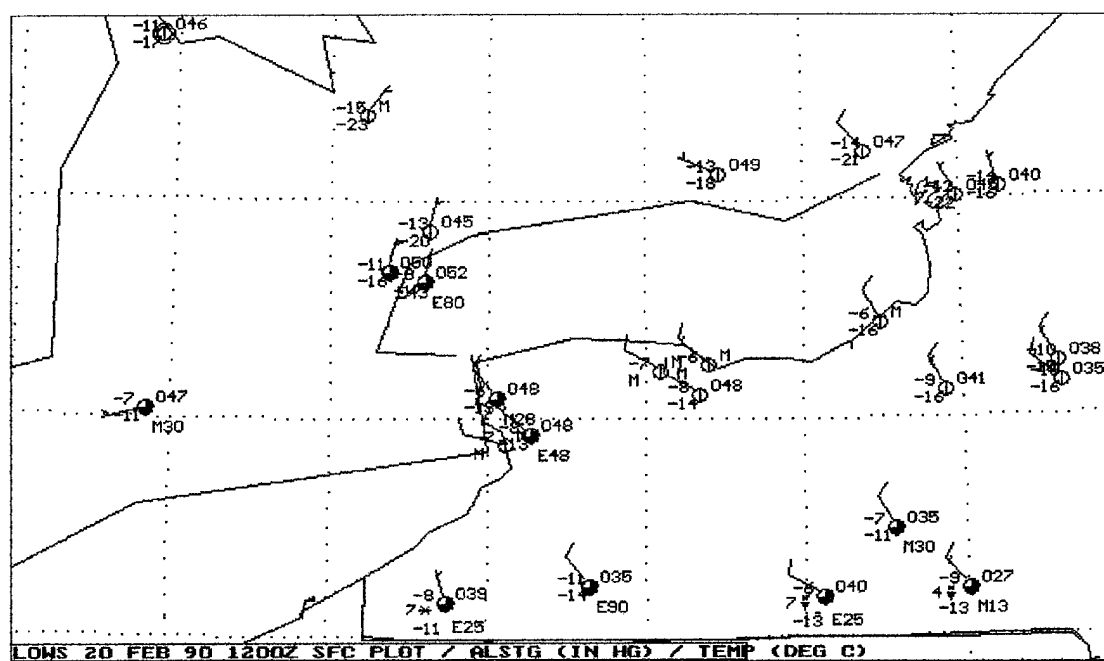


Fig. 27a. Surface analysis 1200 UTC 20 February 1990. Colder surface temperatures north of the lake warm approximately seven degrees as measured at southern shore stations.

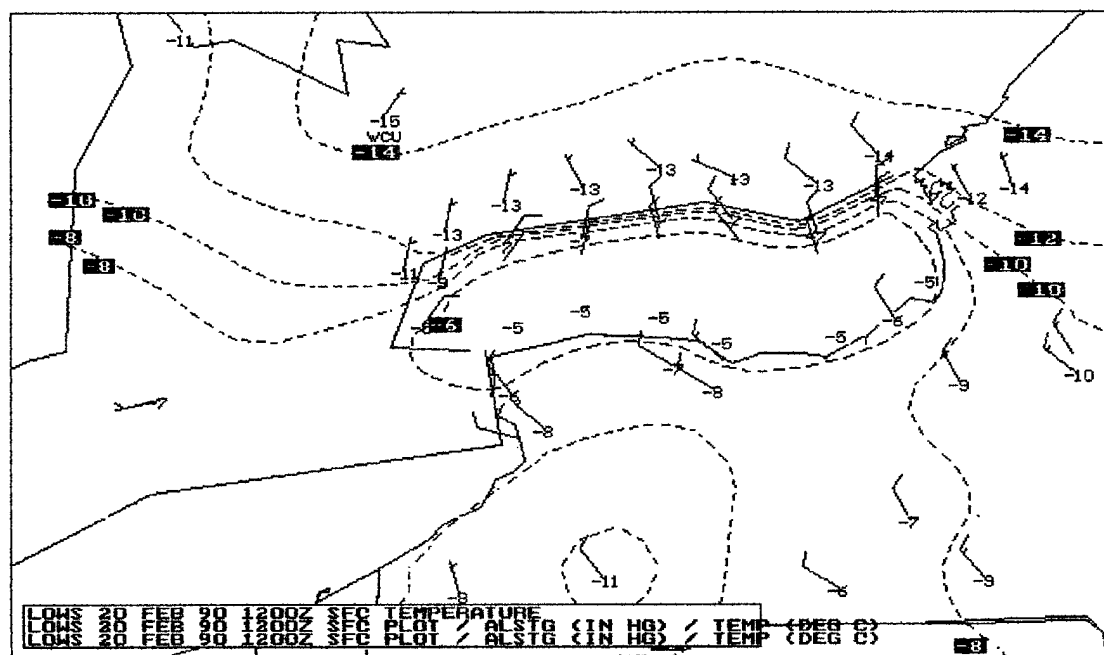


Fig. 27b. Surface analysis 1200 UTC 20 February 1990. Over water predicted values, along with the Toronto Island airport observation show the surface layer modification. Cold, dry airflow from the northeast has replaced the modified air previously observed at WET/WCU.

## 4.2.2 Sounding Analysis and CIBL Estimation

### 4.2.2.1 Sounding Analysis

The Egbert 1700 UTC 19 February 1990 sounding shows a well-mixed near-neutral boundary layer below a  $-21^{\circ}\text{C}$  isothermal layer (Fig. 28a). Egbert undergoes strong cold air advection in both the mixed-layer and in a layer from 750 mb through 550 mb by 2300 UTC 19 February (Fig. 28b). The sounding at Buffalo (Fig. 28c) also exhibits a near-neutral boundary layer below an isothermal layer of approximately  $-21^{\circ}\text{C}$ , at 0000 UTC. Both stations were downwind of Lake Huron at this time with a west-northwesterly windflow, while Buffalo is again downwind of Lake Ontario.

A shallow stable layer is observed at Egbert by 0500 UTC (Fig. 28d), due to colder air undercutting the Lake Huron CIBL. Figure 29 depicts the Egbert boundary layer evolution in terms of theta-e profiles. By 1200 UTC, the northerly low-level flow now puts Egbert upwind and Buffalo downwind of Lake Ontario (Figs. 28e, 28f). Both boundary layers are significantly colder, while subsidence has warmed the isothermal layers to about  $-18^{\circ}\text{C}$ . The stable layer observed at Egbert is eroded during passage over the lake and becomes a neutral mixed-layer over Buffalo.

The similarity of the Egbert and Buffalo soundings suggests that the former is upstream of the latter (Figs. 30 and 32). However soundings at Oswego, to the east (Figs. 28g, 28h) indicate that this 1200 UTC boundary layer had a far more stable upstream environment, away from the modifying influence of the Great Lakes (Figs. 32 and 33). The shallow mixed-layer observed over Oswego at 1200 UTC prevented cloud formation over central and eastern Lake Ontario, while clouds developed in the deeper mixed-layer over the western end of the lake, and were observed at Niagara Falls (Fig. 27a.)

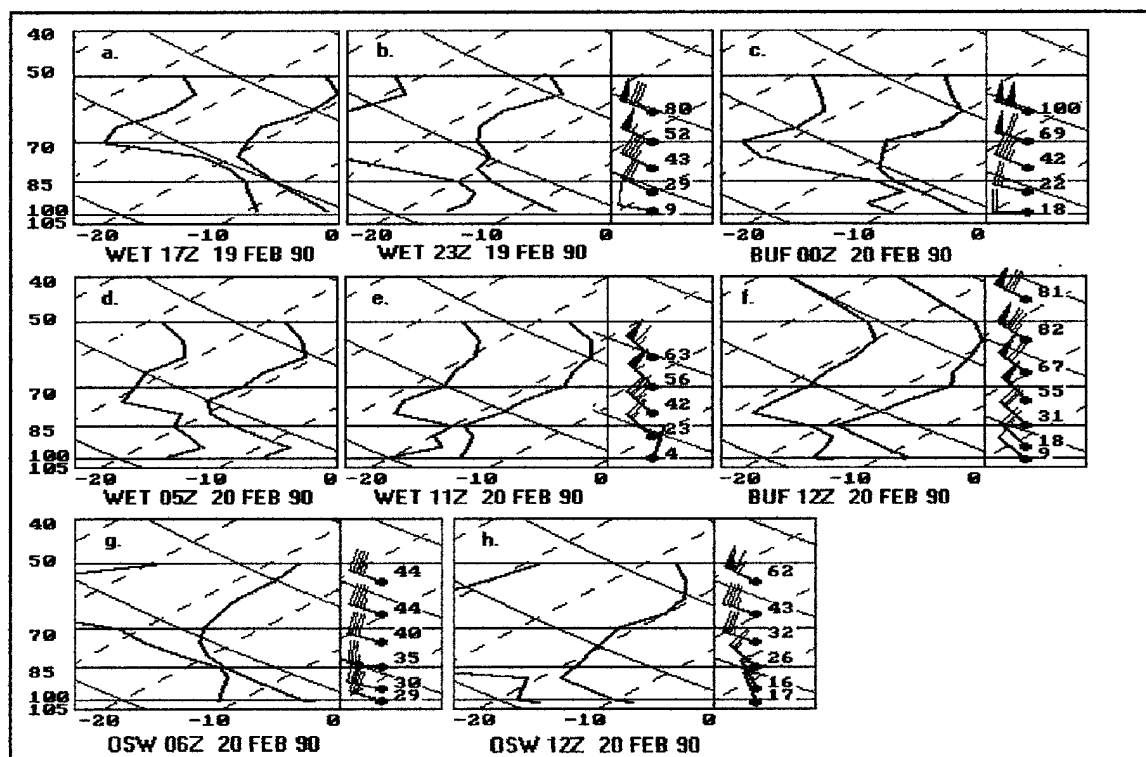


Fig. 28. Upwind and downwind location Sharp Skew-T profiles, 19 and 20 February 1990 .

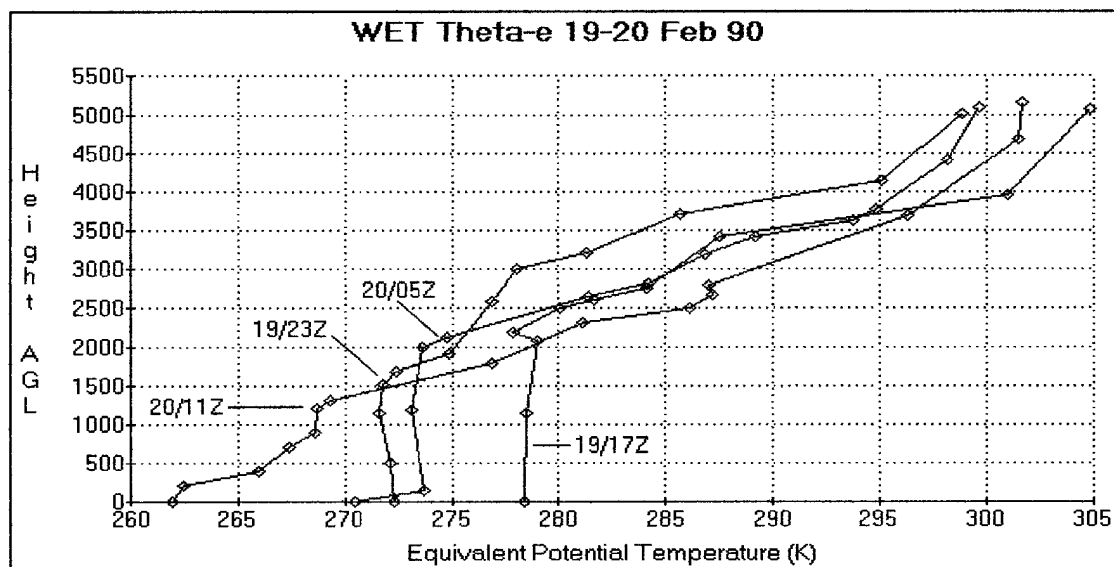


Fig. 29. Theta-e profile evolution at WET 19 through 20 February 1990. The 19/2300 UTC sounding is statically unstable, but by 20/0500 UTC a stable surface layer develops below a deep residual layer. A much deeper stable layer has formed by 20/1100 UTC, due to an invasion of unmodified air from east of Georgian Bay.

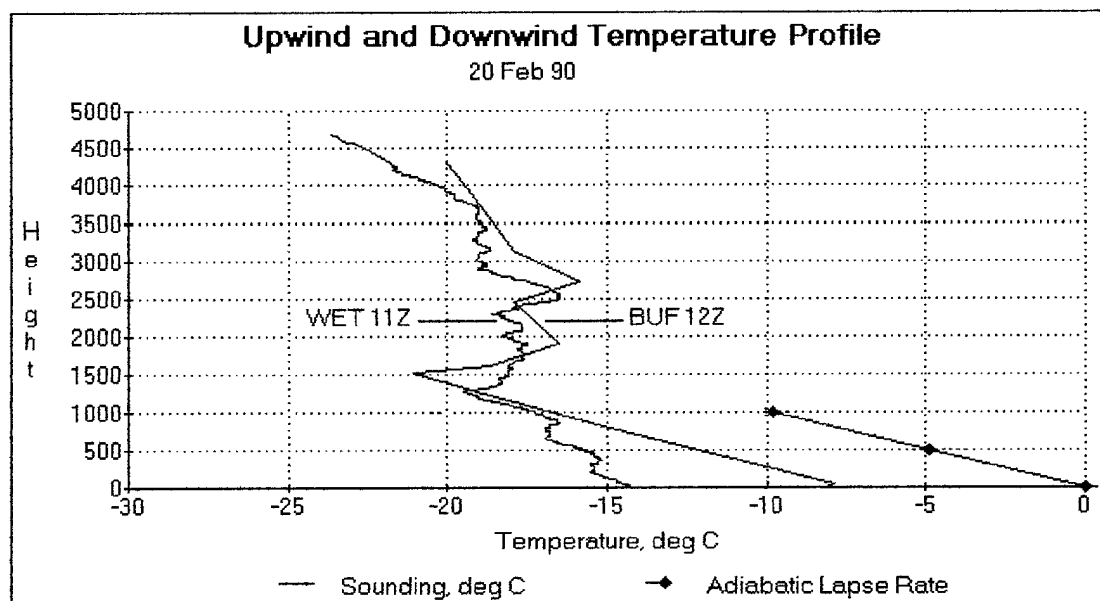


Fig. 30. Upwind and downwind profiles: WET 11 UTC, BUF 1200 UTC 20 February 1990. The BUF mixed-layer is neutral due to heating during passage over the lake, and is compared to a dry adiabatic lapse rate from 0 to -9.8 C over a kilometer depth.

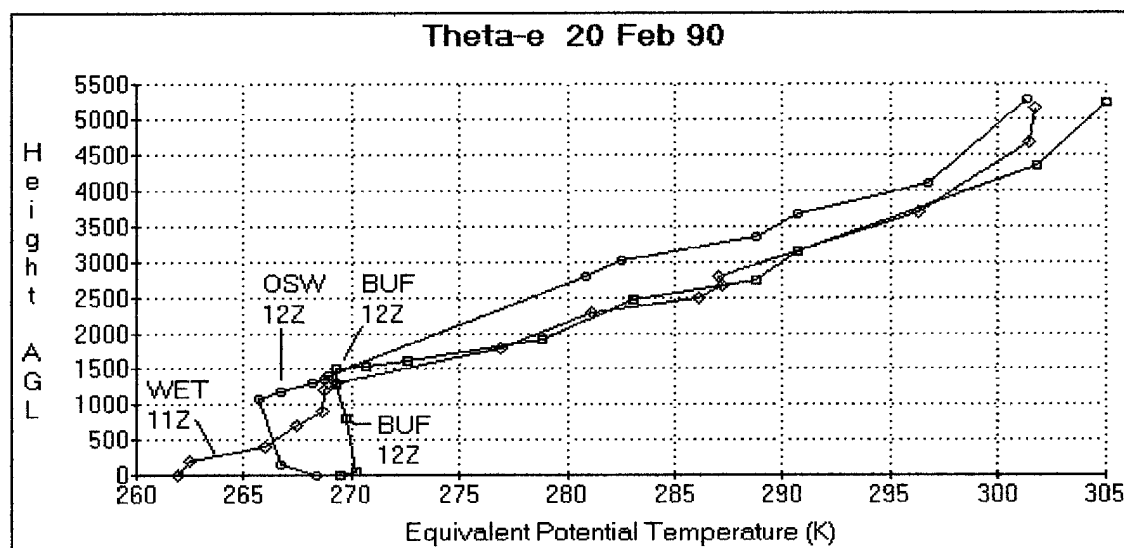


Fig. 31. Upwind and downwind theta-e profiles 20 February 1990. The free atmosphere profile above 1500 m appears to be identical for WET and BUF soundings. The OSW mixed layer is not as deep the BUF mixed layer, due to greater stability east of WET, a shorter over-water fetch, or both.

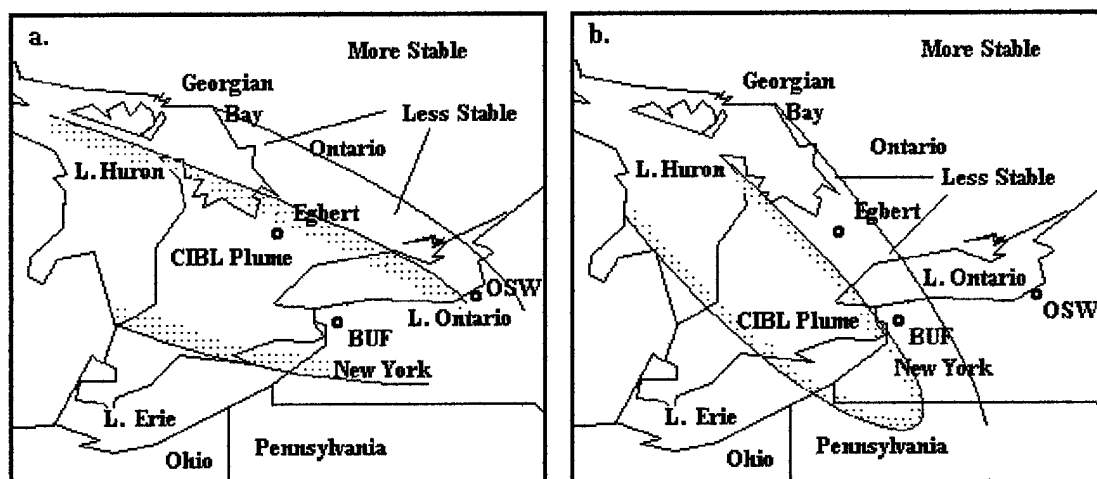


Fig. 32. A proposed explanation for the 20 February 1990 sounding structures in figure 28. The OSW mixed layer decreases from 20/0600 to 20/1200 UTC with veering winds, possibly due to greater stability east of WET. WET and BUF soundings also experience changes in depth with veering winds from 20/0000 to 20/1200 UTC, and have similar structures above 1500 m.



#### 4.2.2.2 CIBL Estimation

An estimation of the Lake Ontario CIBL was calculated using equation (2), the WET 1100 UTC sounding, the YTR (Trenton) 1200 UTC surface observation, and an average lake surface temperature of 1.4 °C. The predicted CIBL depth of 1488 m (Fig. 33) is quite close to the observed downwind mixed-layer depth of 1500 m at Buffalo (Fig. 31.) The final LCL was estimated to be 902 m (2959 feet), while Niagara Falls reported a ceiling of 2800 feet. The clouds observed at Niagara Falls could have formed over Lake Ontario, however they could also be a remnant of any lake-effect cloud cover from Lake Huron.

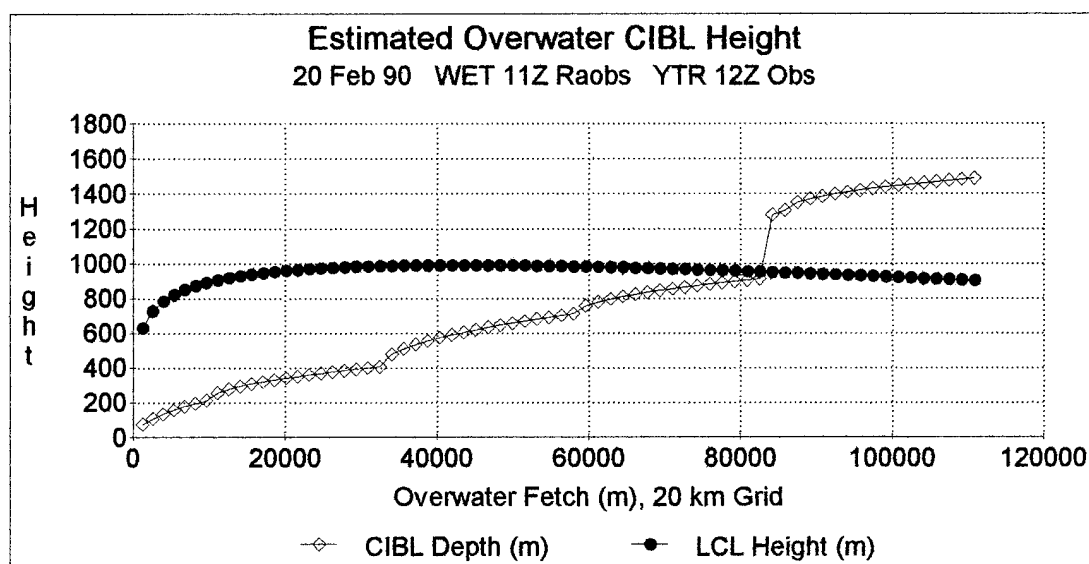


Fig. 33. Estimated CIBL depth and LCL height, 20 February 1990. Clouds are expected when the predicted CIBL exceeds the LCL height after a neutral layer is invaded. The CIBL depth is 1488 m with an LCL height of 902 m, and the lower stable layer is eroded at a fetch of 84 km.

The predicted CIBL depth curve in figure 33 demonstrates the growth through layers of differing stability. Each strata depicted in the 20/11Z profile of figure 29 has a corresponding line segment in the CIBL. The lower stable layer is finally exceeded

at a fetch of 84 km, coincidentally where the CIBL depth crosses the LCL and clouds are predicted.

#### 4.2.3 Sensitivity Tests: Short Fetch Case.

Several simulations were performed to check the effect of each input value on the predicted CIBL. Data from the 20 February 1990 case were used as the baseline for comparison. Temperatures, dewpoints, wind direction and speed, and stability were changed. The results are summarized in Table 4.1 and graphically depicted in figures 34 through 41. The control case is in figure 33 above.

Table 4.1. Model evaluations for varying input conditions.

Upwind Input Values T/Td/DDFF	CIBL Depth (m)	LCL Height (m)	Stable Break (km)	Clouds Begin (km)	Total Fetch (km)	See Figure	
<u>-13/-18/0106</u>	1488	902	84	84	110	33	Control
<b>-18/-23/0106</b>	1555	895	62	62	100	34	
-13/- <b>15</b> /0106	1488	698	84	62	110	35	
-13/-18/ <b>24</b> 06	1743	698	84	84	228	36	
-13/-18/01 <b>20</b>	1606	777	60	53	110	37	
-13/-18/0106 <b>&amp;</b>	1609	902	45	45	110	38	
-13/-15/0120 <b>*</b>	1689	824	49	49	110	39	
-13/-15/2420 <b>*#</b>	2458	339	49	35	228	40	
-13/-15/2420 <b>*&amp;</b>	2970	339	24	29	228	41	

T: Air temperature, Td: Dewpoint, DDFF: Wind direction, and speed in knots

\*: Water temperature = +6 °C, #: Original stable layer, &: 200 m stable layer.

Boldface values indicate deviations from the observed values in figure 33.

Combinations of some or all of these changes result in deeper than observed mixed layers, and lower LCLs. From the table and the figures, we can see the following:

- The greatest single impact was due to the change in wind direction. This controls the fetch, which determines how long the air parcels remain over the lake and undergo modification.
- Decreasing the depth of the upstream stable layer to 200 m allows the CIBL to erode the stable layer much earlier, and grow to a greater height.
- Increased wind speed is also an important influence on CIBL growth. The greater windspeeds allow less time over water and reduce air mass modification, so the increase in CIBL depth poses a small problem unless we can argue that the greater windspeeds increase the drag coefficient in equation (2).
- Decreasing the air temperature by five degrees (or increasing the water temperature by the same amount) does increase the CIBL depth by about 45 m.

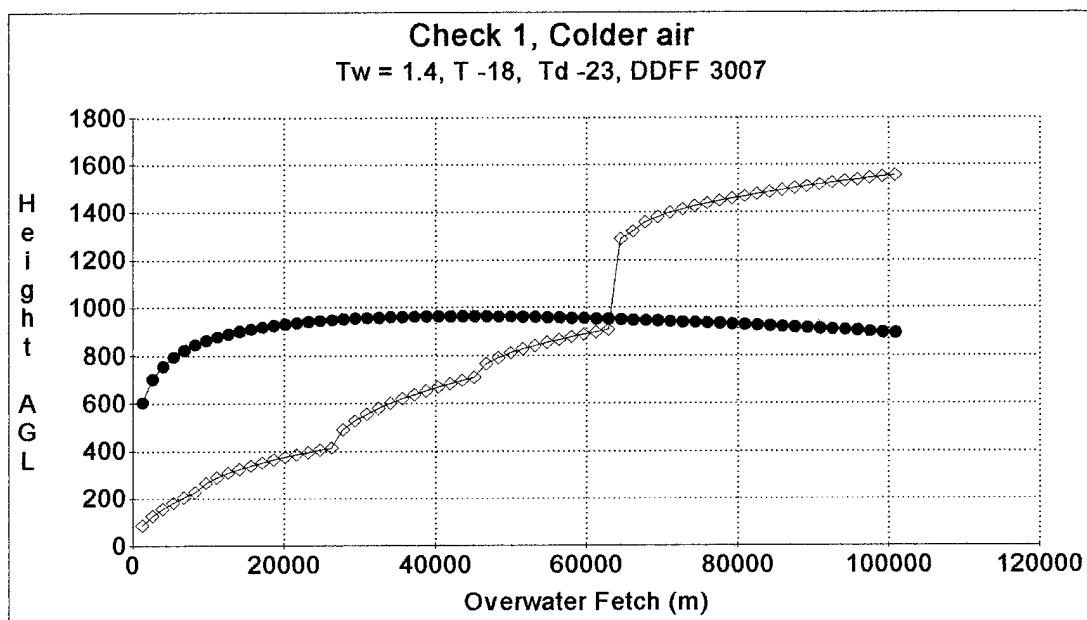


Fig. 34. Cold air test. The temperature and dewpoint are lowered by five degrees, resulting in an increase in CIBL depth from 1488 m to 1555 m, and a decrease of the LCL from 902 m to 895 m.

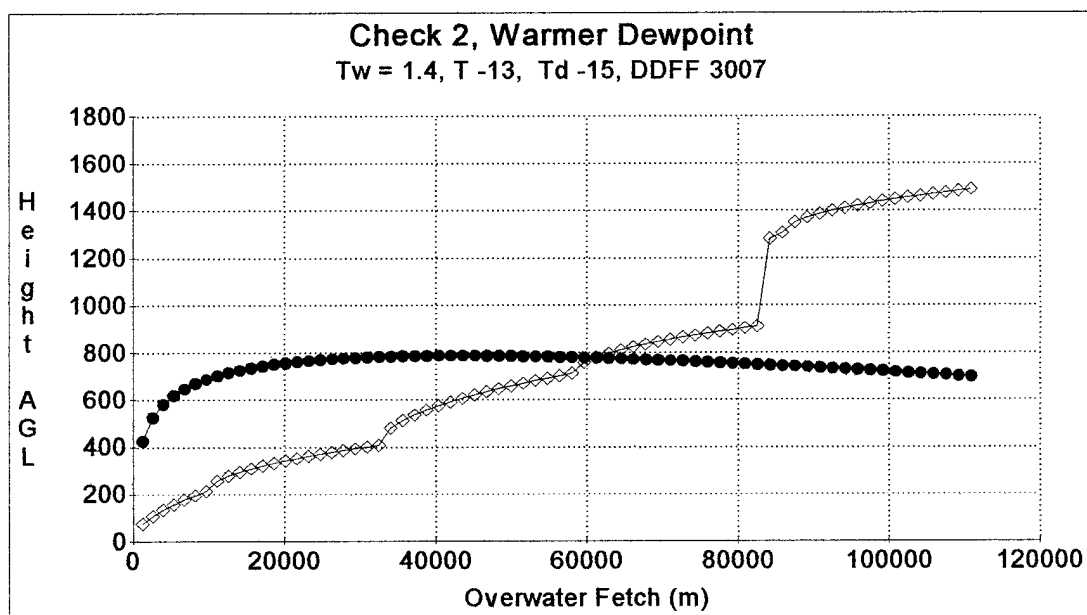


Fig. 35. Moist air test. The observed dewpoint depression is decreased to two degrees, resulting in a decrease of the LCL height from 902 m to 698 m. LCL is lower than CIBL at 62 km.

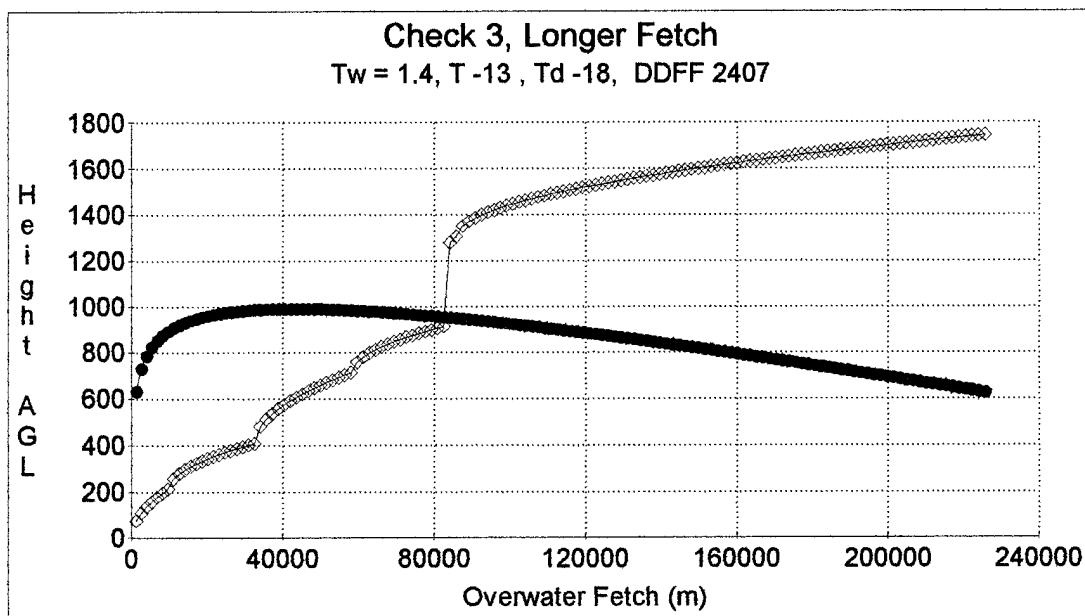


Fig. 36. Long Fetch test. The wind direction is from 240, resulting in an increase in over-water fetch. The wind veers to 270 at the shoreline, with a fetch of 225 km. The CIBL depth increases from 1488 m to 1743 m, and the LCL decreases in height from 902 m to 625 m.

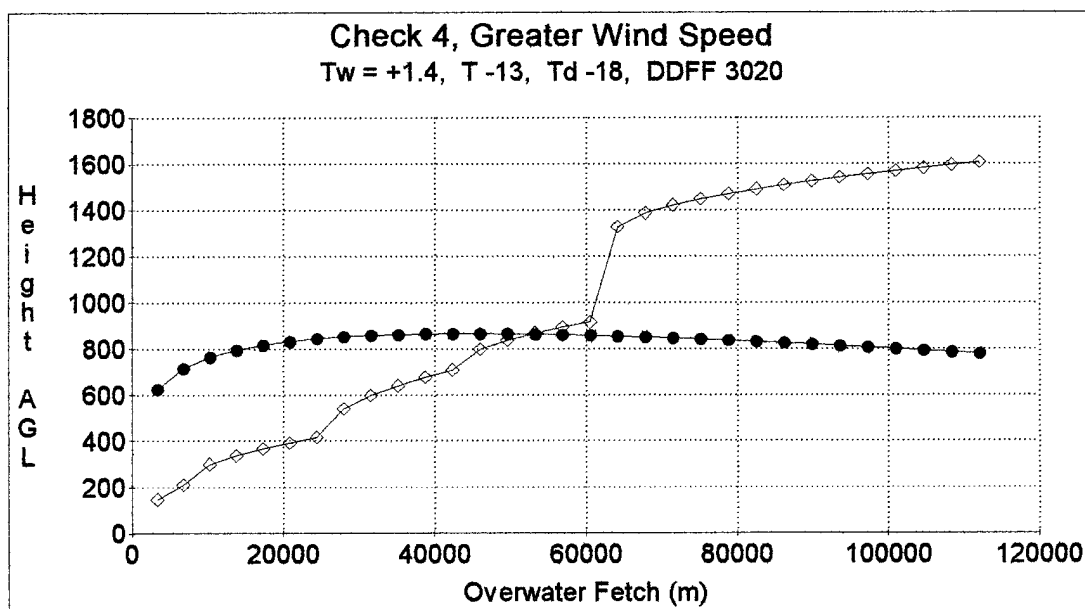


Fig. 37. Greater Wind speed test. The observed wind speed is increased to 20 knots, resulting in an increase in CIBL depth from 1488 m to 1606 m, and a decrease of the LCL height from 902 m to 777 m. The lower stable layer is eroded at a fetch of 60 km.

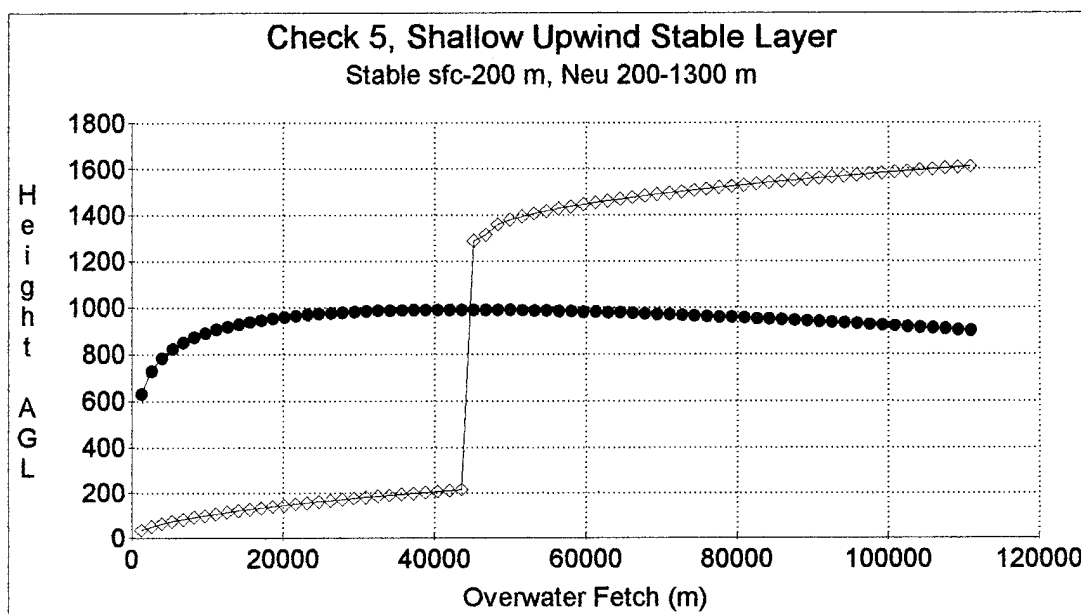


Fig. 38. Shallow stable layer test. When the surface stable layer is decreased to 200 m, the lower stable layer is eroded at 45 km. The final CIBL depth is 1609 m, and the LCL height is 902 m.

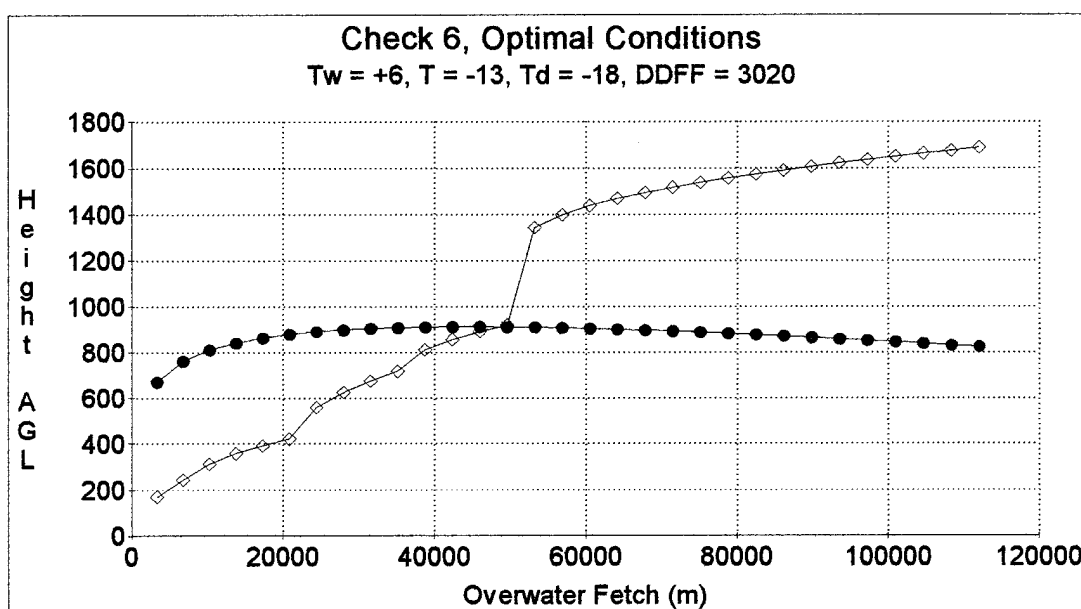


Fig. 39. Observed stable layer, optimal surface input test. Resultant is an increase in CIBL depth from 1488 m to 1689 m, and a decrease of the LCL height from 902 m to 824 m. The lower stable layer is eroded at a fetch of 49 km, where the LCL becomes lower than the CIBL.

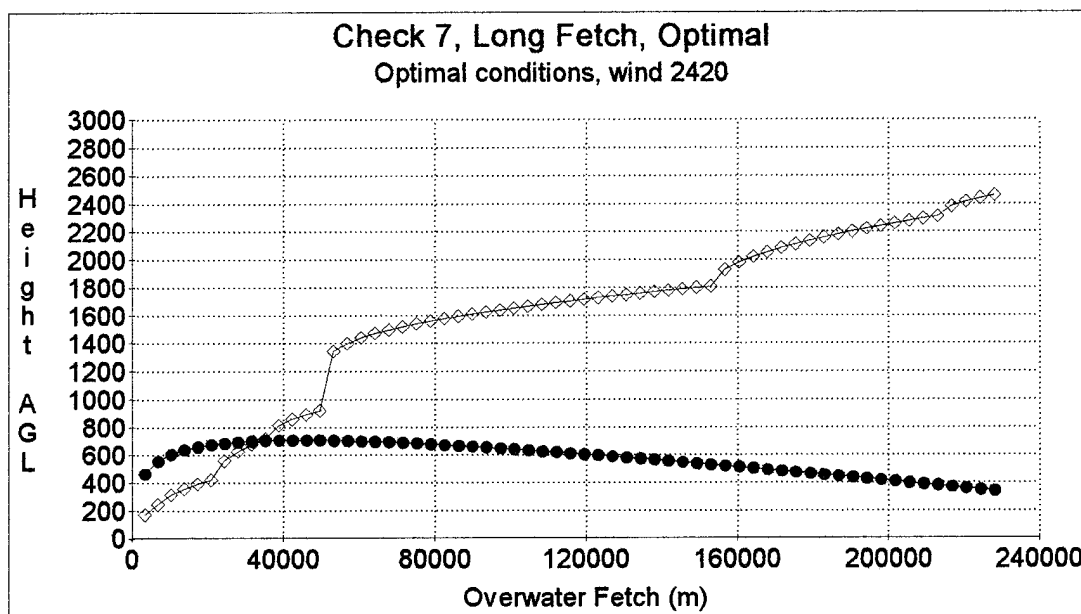


Fig. 40. Observed stable layer, short fetch, optimal surface input test. Resultant is an increase in CIBL depth from 1488 m to 2458 m, and a decrease of the LCL height from 902 m to 339 m. The lower stable layer is eroded at a fetch of 49 km, and the LCL becomes lower than the CIBL at 35 km.

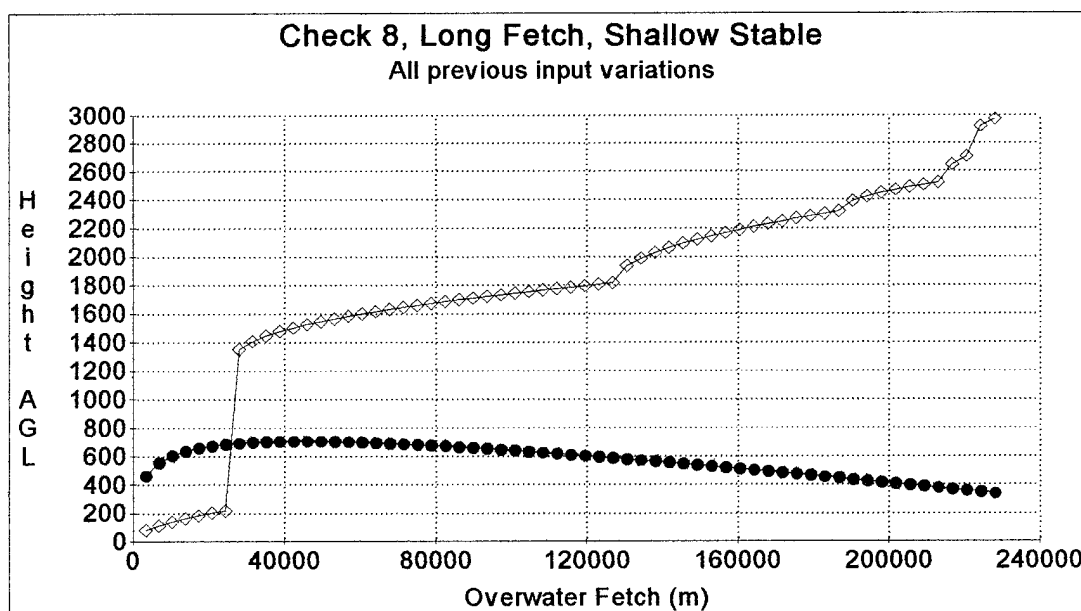


Fig. 41. Shallow stable layer optimal conditions test. Input with previous modifications and the shallow surface layer. The CIBL depth increases from 1488 m to 2970 m, and the LCL height decreases from 902 m to 339 m.

## 5. MODEL SIMULATIONS

While there was no aircraft data available from the LOWS project, a comparison has been made between the results of the empirical methods described in chapter 4 and a numerical PBL model, to check the over water characteristics and evolution of the CIBL and of cloud development. The results suggest that the empirical methods cannot account for the latent heat release by condensation in the convective boundary layer growth. The empirical model underpredicted the cloud-filled CIBL in the long-fetch case. Both models predict similar mixed-layer depths in cases with little or no cloud cover.

### 5.1 MODEL DESCRIPTION

The mesoscale numerical used in this study is a modified version of that developed and applied by Huang and Raman (1991). The model is 3-dimensional, but allows for 2-dimensional simulations. The model is hydrostatic and anelastic in a terrain-following coordinate system, in which sigma is defined by  $\sigma = (z - E)/(H - E)$ .  $H$  is the model maximum height,  $E$  is the terrain height, and  $z$  is the current level. The model treats the PBL in two parts; a surface layer, and a transitional layer. Surface layer turbulent transport is described using similarity stability functions given by Businger *et al.* (1971). Prognostic turbulent kinetic energy (TKE) and dissipation ( $\epsilon$ ) equations are used in the transitional layer. A detailed description of the model and model equations has been given by Huang (1990).

#### 5.1.1 Model Domain and Initial Conditions

The model domain is oriented north-south from 42° N to 45° N for the northerly flow case, and east-west for the westerly flow case, from 81° W to 75° W. A 10 km horizontal grid interval is employed. This provides 33 grid points in the north-south study; and 40



grid points in the east-west study. The lake is defined as a 260 km long body of water with a width of 77 km. The model has 20 vertical layers: 0, 50, 100, 150, 200, 250, 300, 400, 500, 600, 800, 1000, 1500, 2000, 2500, 3000, 3500, 4000, 4500, 5000 m. A time step of 120 s was chosen. The roughness length ( $z_0$ ) over the lake is given by Charnock's relationship:

$$z_0 = 0.018 u_*^2 / g \quad (15)$$

while assigning a roughness length  $z_0 = 1$  cm to the land surface.

Since the focus of this study is on the surface forcing from the lake, a flat terrain model is appropriate to avoid orographically driven processes. The initial wind profile is uniform in speed and direction with a no-slip condition imposed at the surface. Values for potential temperature and relative humidity are evaluated from an observed upstream sounding.

## 5.2 MODEL RESULTS

The observed soundings and model simulation for the long-fetch case of 12 January 1990 is shown in figures 42 and 43. The lake surface extends from grid points 12 through 39. The theta-e cross section (Fig. 43b) shows a superadiabatic surface layer from the lake surface to 300 meters, and a mixed layer with near-constant theta-e from 300 to 2300 meters, compared to the downwind observed mixed-layer depth of 2100 meters at Oswego (Figs. 20 and 42). The depth of the superadiabatic layer is possibly a result of the 50 m vertical resolution in the surface layer of the model domain, or a plotting program artifact.

The empirical program predicted 1800 m (Fig. 21.) The numerical model predicted a cloud-filled mixed-layer over the lake (Fig. 43d), and the empirical program predicted an LCL below the CIBL over a short over-water distance (Fig. 21).

The observed soundings and simulation for the short-fetch case of 20 February 1990 are shown in figures 44 and 45. The lake surface for the north-south domain extends from grid points 15 through 22. The model again predicts a superadiabatic surface layer from the lake surface to 300 meters, and a complex mixed layer (Fig. 45b). The numerical model CIBL breaks through the low-level inversion near grid point 21, just prior to landfall on the southern shore, similar to the empirical method CIBL (Fig. 33). The mixed-layer above the lake at the downwind shore extends from 300 to 1500 meters, with a minimum theta-e of 262 °K at 1500 m. This compares well to the observed downwind mixed-layer depth of 1500 meters at Buffalo (Figs. 30 and 31.) The model predicts a cloud layer from 300 to 800 meters, extending over the entire lake (Fig 45d). The empirical model also predicted a mixed-layer depth of 1500 meters, but with clouds developing after an 84 km over water fetch (Fig. 33.)

The numerical model appeared to overpredict the mixed-layer depth in the long-fetch case by 200 meters, while the empirical model underpredicted the mixed-layer depth by 300 meters. Both models predicted cloud cover over the entire lake. The numerical and empirical models predicted accurate mixed-layer depths for the short-fetch case, but differed in the rapidity of over water cloud development.

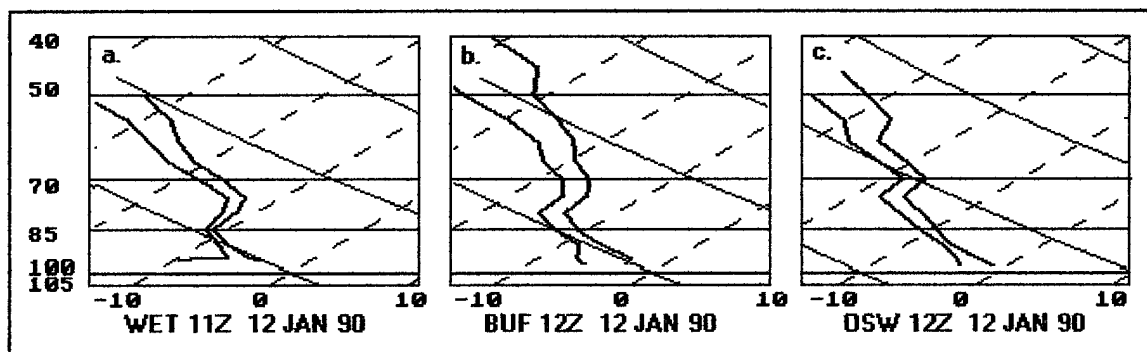


Fig. 42. Observed soundings for 12 January 1990.

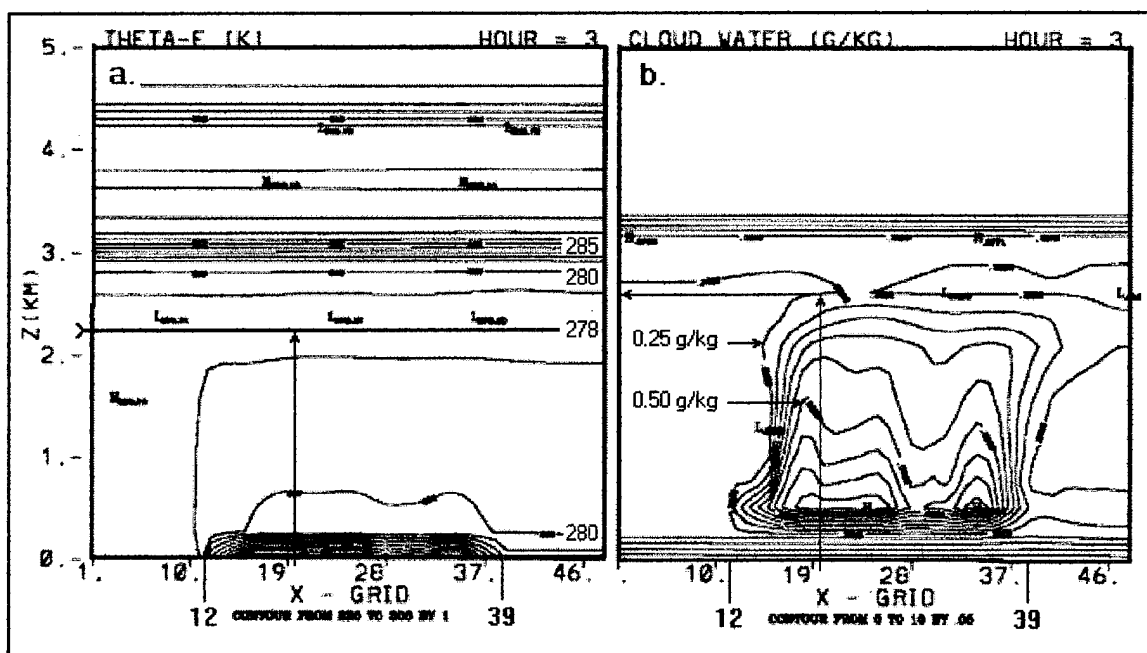


Fig. 43. Three hour forecast for values over Lake Ontario 12 January 1990. The vertical line at grid point 21 marks the position of an air column that left the shoreline three hours previously. The predicted cloud top exceeds the isentropic minima, suggesting overshooting and entrainment above the 278 K level.

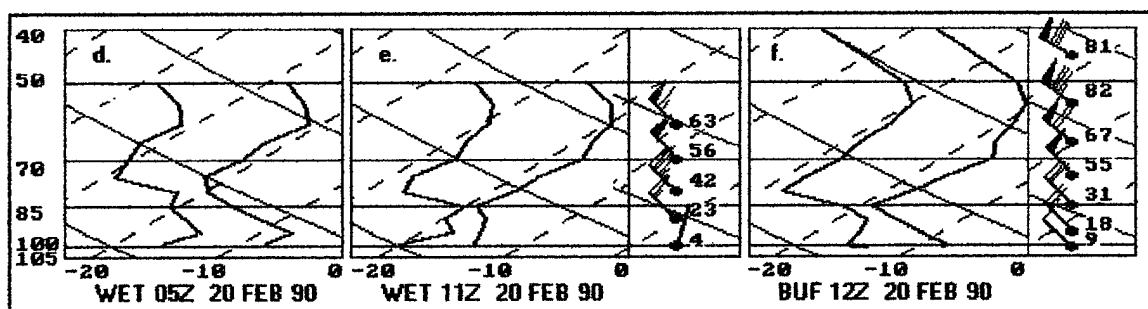


Fig. 44. Observed soundings for 20 February 1990.

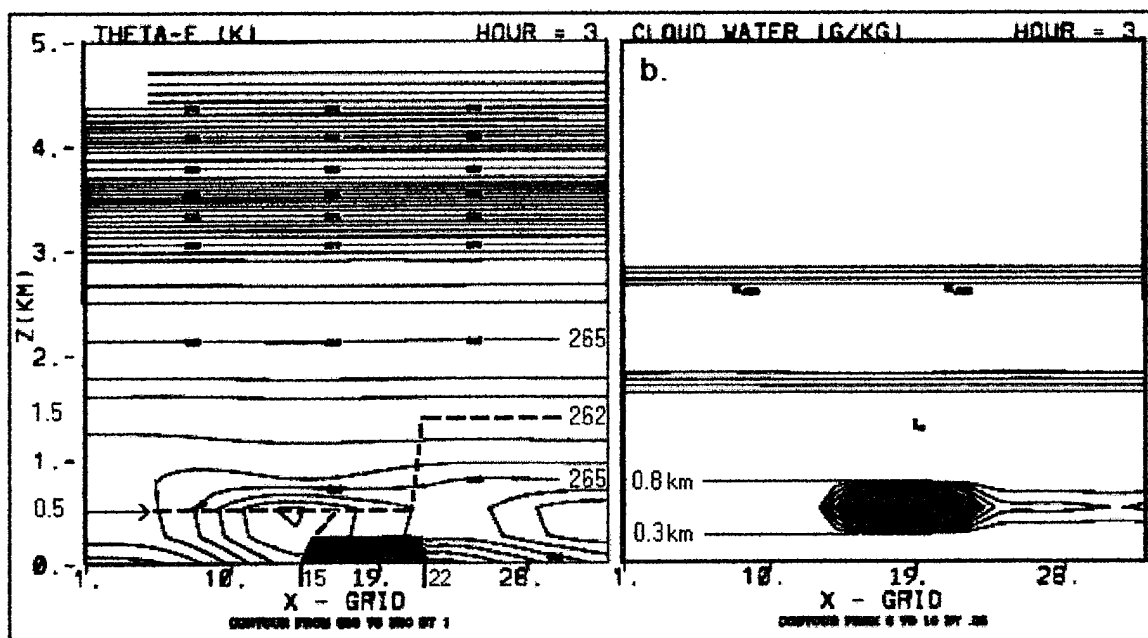


Fig. 45. Three hour forecast for values over Lake Ontario 20 February 1990. The lake extends from grid point 15 through 22.

## 6. SUMMARY AND CONCLUSIONS

### 6.1 SUMMARY

Previous studies define lake-effect storms as autumn and winter mesoscale phenomena that occur leeward of the Great Lakes following the passage of polar or arctic air masses over the much warmer lakes. The cold air masses are destabilized by lake-to-air sensible and latent heat fluxes, resulting in a surface superadiabatic layer and a well-mixed CBL below a capping subsidence inversion. Lake-effect clouds and storms are expected when the temperature lapse between the lake surface and the 850 mb level is equal to or greater than 13 °C, roughly a dry adiabatic lapse rate. Storm soundings show a correlation between lake-effect intensity and CBL depth. Weak cases were limited by a low capping inversion, while strong cases had CBL depths ranging from 2.3 to 3.1 km, suggesting that the CBL depth may be as important as the degree of instability in determining lake-effect snow intensity.

One of the challenges to forecasting lake-effect snow is the lack of accurate or timely upwind measurements. CIBLs are surface-forced mesoscale features within the planetary boundary layer that can vary in depth or orientation. Such boundary layer structures are not adequately sampled in the Great Lakes region due to the coarse spatial and temporal resolution of the upper air network, and the placement of sounding sites with respect to land and lake surfaces. The LOWS project applied upwind and downwind soundings and a mesoscale array of advanced remote sensors to monitor lake-effect snowstorms and their precursors over and downwind of Lake Ontario.

I have written a computer program using several empirical equations to analyze soundings and estimate over-lake values such as air temperature, dewpoint and wind speed, CIBL depths, and the LCL heights over Lake Ontario during the unstable season.

An hourly temporal resolution is possible, and would provide more detail than the synoptic soundings taken every 12 hours.

In this study, upwind soundings were analyzed to determine individual layer stabilities for input to equation (2). Soundings sharing common origins were selected to reduce the impact of differences caused by upwind land or lake surfaces. Some Egbert soundings (not presented in this study) had deeper mixed-layers than soundings downwind of Lake Ontario. It is possible that CIBLs were sampled downwind of either Lake Huron or Georgian Bay at Egbert, but this pre-conditioned air was not observed at all sounding sites downwind of Lake Ontario.

The predicted over-water windspeeds are used to determine shoreline windshifts, and over-water fetch and drag coefficients, while over-water temperatures and dewpoints are used to predict LCL heights. The program uses upwind soundings and surface weather observations, and the lake surface temperature as input, and can be quickly and easily executed using different weather station observations, or a single station with observed or forecast temperatures and winds. The program may be used in this manner to provide an hourly temporal resolution.

The over-lake surface layer values were compared to observations along the southern shore of Lake Ontario, and estimated CIBL depths and LCL heights were compared to downwind mixed-layers and cloud bases for both long-fetch and a short-fetch cases. CIBLs and LCLs were also calculated using variations in observed input values such as colder air, higher dewpoints, different wind directions and speeds, varying stable layer depths, and combinations of these factors.

These results were also compared to the output from a 2-dimensional numerical mesoscale model. The empirical program and the numerical model output both compared well with downwind shoreline sounding measurements, but differed in some over-water

details. While there was no research aircraft available to provide the true over-water details, the numerical model results are expected to be more accurate, mainly because the consequence of released latent heat in the cloud layer explicitly affects the CIBL depth.

## 6.2 CONCLUSIONS

- The impact of the upwind sounding structure on CIBL growth was evident, where stable layers hindered CIBL growth, inversions limited convection or neutral layers were quickly invaded.
- Varying surface observations produce varying CIBL depths, affecting the over-water fetch, and lake-surface to air instability.
- The upwind moisture content strongly affects over-lake cloud formation, with extremely dry air masses requiring more time to become saturated.
- Mixed-layer depth is underpredicted when deep clouds were present, since TIBL equations do not apply latent heat of condensation to the CIBL growth.

## 6.3 FUTURE RESEARCH

Future research would involve the development of a cloud-filled CIBL equation for cases in which the predicted LCL is lower than the CIBL. The latent heat of condensation would increase the depth of the convectively mixed-layer more than sensible heating alone would accomplish.

Upwind soundings could be provided by RASS units if they could be adjusted for service in arctic air masses and made to satisfy Canadian radio frequency restrictions. Hourly model sounding forecasts have been made available to the Buffalo forecast office for use in mesoscale model evaluations (Niziol et al. 1995), and could be used in lieu of observed profiles.

## REFERENCES

- Agee, E. M., and S. R. Gilbert, 1989: An aircraft investigation of mesoscale convection over Lake Michigan during 10 January 1984 cold air outbreak. *J. Atmos. Sci.*, **46**, 1877-1897.
- Ballentine, R. J., 1982: Numerical simulation of lake-breeze induced snowbands along the western shore of Lake Michigan. *Mon. Wea. Rev.*, **110**, 1544-1553.
- Braham, R. R., Jr., 1983: The Midwest snow storm of 8-11 December 1977. *Mon. Wea. Rev.*, **111**, 253-272.
- Businger, J. A., J. C. Wyngaard, Y. Izumi and E. F. Bradley, 1971: Flux-profile relationships in the atmospheric surface layer. *J. Atmos. Sci.*, **28**, 181-189.
- Byrd, G. P., R. A. Anstett, J. E. Heim, and D. M. Usinski, 1991: Mobile sounding observations of lake-effect snowbands in western and central New York. *Mon. Wea. Rev.*, **119**, 2323-2332.
- Chang, S. S., and R. R. Braham, Jr., 1991: Observational study of a convective internal boundary layer over Lake Michigan. *J. Atmos. Sci.*, **48**, 2265-2279.
- Dewey, K. F., 1975: The Prediction of Lake Huron lake-effect snowfall systems. *J. Appl. Meteor.*, **14**, 3-7.
- \_\_\_\_\_, 1979a: Lake Erie induced mesosystems - An operational forecast model. *Mon. Wea. Rev.*, **107**, 421-425.
- \_\_\_\_\_, 1979b: An objective forecast method for Lake Ontario induced snowfall systems. *J. Appl. Meteor.*, **18**, 787-793.
- Duffield, G. F., and G. D. Nastrom, 1983: *Equations and algorithms for meteorological applications in Air Weather Service*. Air Weather Service, Scott Air Force Base, Illinois. 58 pp.
- Eichenlaub, V. L., 1979: *Weather and climate of the Great Lakes region*. Univ. of Notre Dame Press, Notre Dame, Indiana. 335 pp.



- Gamo, M., S. Yamamoto, O. Yokoyama, and H. Yashikado, 1983: Structure of the free convective internal boundary layer above the coastal area. *J. Meteorol. Soc. Japan*, **61**, 110-124.
- Hjelmfelt, M. R., and R. R. Braham, Jr., 1983: Numerical simulation of the airflow over Lake Michigan for a major lake-effect snow event. *Mon. Wea. Rev.*, **111**, 205-219.
- \_\_\_\_\_, 1990: Numerical study of the influence of environmental conditions on lake-effect snowstorms over Lake Michigan. *Mon. Wea. Rev.*, **118**, 138-150.
- \_\_\_\_\_, 1992: Orographic effects in simulated lake-effect snowstorms over Lake Michigan. *Mon. Wea. Rev.*, **120**, 373-377.
- Holland, J. Z., W. Chen, J. A. Almazan, and F. C. Elder, 1981: Atmospheric Boundary Layer. *IFYGL - The International Field Year for the Great Lakes*. Aubert, E. J., T. L. Richards, Eds., NOAA, Great Lakes Environmental Research Laboratory, Ann Arbor, Michigan.
- Holroyd, E. W., III, 1971: Lake-effect cloud bands as seen from weather satellites. *J. Atmos. Sci.*, **28**, 1165-1170.
- Hsu, S. A., 1986: Correction of land-based wind data for offshore applications: A further evaluation. *J. Phys. Oceanogr.*, **16**, 390-394.
- \_\_\_\_\_, 1988: *Coastal meteorology*. Academic Press, San Diego, California. 260 pp.
- Huang, C. Y., 1990: A mesoscale planetary boundary layer numerical model for simulations of topographically induced circulations. Ph.D Dissertation, North Carolina State University, 253pp.
- \_\_\_\_\_, and S. Raman, 1991: Numerical simulation of January 28 cold air outbreak during GALE, Part I: The model and sensitivity tests of turbulence closures. *Boundary-Layer Meteorol.* **55**, 381-407.
- Lavoie, R. L., 1972: A mesoscale numerical model of lake-effect storms. *J. Atmos. Sci.*, **29**, 1025-1040.
- Moore, P. K., and R. E. Orville, 1990: Lightning characteristics in lake-effect storms. *Mon. Wea. Rev.*, **118**, 1767-1782.

- Niziol, T. A., 1986: Operational forecasting of lake-effect snowfall in western and central New York. *11th Conference on Weather Forecasting and Analysis*, Kansas City, Missouri, Amer. Meteor. Soc., 200-205.
- \_\_\_\_\_, 1987: Operational forecasting of lake-effect snowfall in western and central New York. *Wea. Forecasting*, **2**, 310-321.
- \_\_\_\_\_, W. R. Snyder, and J. S. Waldstreicher, 1995: Winter weather forecasting throughout the eastern United States. Part IV: Lake effect snow. *Wea. Forecasting*, **10**, 61-77.
- Passarelli, R. E., Jr, and R. R. Braham Jr., 1981: The role of the winter land breeze in the formation of Great Lake snow storms. *Bull. Amer. Meteor. Soc.*, **62**, 482-491.
- Peace, R. L., Jr., and R. B. Sykes, Jr., 1966: Mesoscale study of a study of a lake effect snow storm. *Mon. Wea. Rev.*, **94**, 495-507.
- Peters, L. K., and G. R. Carmichael, 1976: On the criteria for the occurrence of fumigation inland from a large lake - Authors Reply. *Atmos. Env.*, **12**, 173.
- Phillips, D. W., 1972: Modification of surface air over Lake Ontario in winter. *Mon. Wea. Rev.*, **100**, 662-670.
- \_\_\_\_\_, and J. A. Alamazan, 1981: Meteorological Analysis. *IFYGL - The International Field Year for the Great Lakes*. Aubert, E. J., T. L. Richards, Eds., NOAA, Great Lakes Environmental Research Laboratory, Ann Arbor, Michigan.
- Reinking, R. F., R. A. Kropfli, B. E. Martner, B. W. Orr, J. B. Snider, T. Uttal, R. J. Zamora, R. Caiazza, R. A. Maraio, R. S. Penc, A. J. Koscielny, G. P. Byrd, R. J. Ballentine, A. Stamm, R. B. Sykes, T. A. Niziol, C. Bedford, P. I. Joe, and A. Eschner, 1991: *Lake Ontario winter storms project final technical report*. Kaman Sciences, Colorado Springs, CO, 210 pp.
- Resio, P. T., and C. L. Vincent, 1977: Estimation of winds over the Great Lakes. *J. Waterways Harbors Coastal Div.*, ASCE, **102**, 265-283.
- Rothrock, H. J., 1969: An aid to forecasting significant lake snows. Tech. Memo, WBTM CR-30, National Weather Service, Central Region, Kansas City, 12 pp.
- Stull, R. B., 1988: *An introduction to boundary layer meteorology*. Kluwer Academic Publishers, Dordrecht, Netherlands. 667 pp.

- Stunder, M. and S. Sethuraman, 1985: A comparative evaluation of the coastal internal boundary-layer height equations. *Boundary-Layer Meteorol.*, **32**, 177-204.
- Schwab, D. J., 1978: Simulation and forecasting of Lake Erie storm surges. *Mon. Wea. Rev.*, **106**, 1476-1487.
- Venkatram, A., 1977: A model of internal boundary-layer development. *Boundary-Layer Meteorol.*, **11**, 419-437.
- \_\_\_\_\_, 1986: An examination of methods to estimate the height of the coastal internal boundary layer. *Boundary-Layer Meteorol.*, **36**, 149-156.
- Wallace, J. M., and P. V. Hobbs, 1977: *Atmospheric Science, an introductory survey*. Academic Press, Inc., Orlando, Florida. 467 pp.
- Weisman, B., 1976: On the criteria for the occurrence of fumigation inland from a large lake. *Atmos. Env.*, **12**, 172-173.

## 8. APPENDIX

```

1  CLS      'Algorithm to calculate CIBL depths using hourly observations
2  PRINT "A program to find over-lake CIBL depths using hourly sfc obs."
3  PRINT : PRINT "By Richard A. Anstett"      'File "CIBL0330.BAS
4  REM Using Venkatram's equation

30 LET F = .2          'Entrainment fraction
31 LET Cp = 1004.67     'Specific heat, const press, dry air
32 LET g = 9.81         'Accel due to gravity
33 LET L = 2500000      'Latent heat of condensation
34 LET Rd = 287.04      'Gas const, dry air
35 LET rho = 1.2        'Air density near surface
36 LET Time = 300       'Time step, seconds per five minutes
37 LET Totaldx = 0
38 REM Totaldx, the sum of Time fetches, initially zero at shoreline

39 LET x = 0           'flexible shoreline fetch, defined when new layer is
40                     'invaded, and a new lapse rate is worked against.
43 LET Zio = 0         'Pre-existing dry adiabatic (near-neutral) depth

100 REM -----
105 PRINT : INPUT "Enter mean Lake Temp, Deg C (ex: 2)"; Tw
110 PRINT : PRINT "Using a surface observation: 25 BKN 7 M/-10/-15/3220/005"
115 PRINT "Enter surface data: -10,-15,32,20,005"
120 INPUT Tal, Tdi, ddl, ffl, alt

122 LET stb = Tal - Tw   'Air-Lake delta T
124 LET ffms = ffl * .5144 'Convert Knots to m/s

126 REM Find the shoreline wind shift, Ddd

128 LET Ddd = (12.5 - 1.5 * stb) - (.38 - .03 * stb) * ffms
130 LET Ddd = Ddd / 10
134 LET dd = ddl + Ddd
136 IF dd < 36 THEN 140
138 LET dd = dd - 36

140 REM Fetch is determined by the wind direction over the Lake

145 IF dd >= 22.5 AND dd < 23.5 THEN fetch = 110000 ELSE 150
146 GOTO 250
150 IF dd >= 23.5 AND dd < 24.5 THEN fetch = 150000 ELSE 155
151 GOTO 250
155 IF dd >= 24.5 AND dd < 25.5 THEN fetch = 190000 ELSE 160
156 GOTO 250
160 IF dd >= 25.5 AND dd < 26.5 THEN fetch = 240000 ELSE 165
161 GOTO 250
165 IF dd >= 26.5 AND dd < 27.5 THEN fetch = 225000 ELSE 170
166 GOTO 250
170 IF dd >= 27.5 AND dd < 28.5 THEN fetch = 180000 ELSE 175

```

```

171 GOTO 250
175 IF dd >= 28.5 AND dd < 29.5 THEN fetch = 140000 ELSE 180
176 GOTO 250
180 IF dd >= 29.5 AND dd < 30.5 THEN fetch = 130000 ELSE 185
181 GOTO 250
185 IF dd >= 30.5 AND dd < 31.5 THEN fetch = 120000 ELSE 190
186 GOTO 250
190 IF dd >= 31.5 AND dd < 32.5 THEN fetch = 115000 ELSE 195
191 GOTO 250
195 IF dd >= 32.5 AND dd < 33.5 THEN fetch = 110000 ELSE 200
196 GOTO 250
200 IF dd >= 33.5 AND dd < 34.5 THEN fetch = 100000 ELSE 205
201 GOTO 250
205 IF dd >= 34.5 AND dd < 35.5 THEN fetch = 92500 ELSE 210
206 GOTO 250
210 IF dd >= 35.5 AND dd = 36 THEN fetch = 85000 ELSE 215
211 GOTO 250
215 IF dd >= .1 AND dd < .5 THEN fetch = 85000 ELSE 220
216 GOTO 250
220 IF dd >= .5 AND dd < 1.5 THEN fetch = 92500 ELSE 225
221 GOTO 250
225 IF dd >= 1.5 AND dd < 2.5 THEN fetch = 100000 ELSE 230
226 GOTO 250
230 IF dd >= 2.5 AND dd < 3.5 THEN fetch = 110000 ELSE 235
231 GOTO 250
235 IF dd >= 3.5 AND dd < 4.5 THEN fetch = 115000 ELSE 240
236 GOTO 250
240 IF dd >= 4.5 THEN fetch = 120000

250 PRINT : INPUT "Ready to Proceed? (y/n)"; A$
255 IF A$ = "n" THEN 1999
260 IF A$ = "N" THEN 1999
265 CLS
270 PRINT : INPUT "Use last sounding data file? (y/n)"; B$
275 IF B$ = "y" THEN 400
280 IF B$ = "Y" THEN 400

300 REM -----
310 PRINT "Enter sounding to 500 mb (from TTAA/BB): PPP, +/-TT.T, DD"
315 LET Lvl$ = 0
320 LET AglHgt = 0
325 OPEN "sounding.dat" FOR OUTPUT AS #1

330 PRINT "Enter press (PPP) to 500 mb, temp (+/-TT.T) dewpt deprssn (DD)"
335 PRINT "seperated by commas, ex: 850,-16.3,65"
340 INPUT Pmb, T, dd
345 PRINT #1, Pmb; ", "; T; ", "; dd

350 LET Lvl$ = Lvl$ + 1          'Count the levels
355 IF Pmb <= 500 THEN 370      'At 500 mb, CLOSE file 1
360 GOTO 340

370 CLOSE 1                    'CLOSE output file 1

```

```

380 PRINT : PRINT : INPUT "Ready to Proceed? (y/n)"; D$
385 IF D$ = "n" THEN 1999

400 REM -----
405 REM Identify distinct layers and layer Lapse Rates (LR)
410 LET CountLR = 1

420 REM Lapse rate layer analysis
425 OPEN "sounding.dat" FOR INPUT AS #1 'Get input from file 1
430 OPEN "layers.dat" FOR OUTPUT AS #2 'Place output in file 2
435 PRINT : PRINT "Lower T Upper T LyrThk PmbL PmbU"

440 INPUT #1, PmbL, TL, TddL 'Read data for lower level
445 INPUT #1, PmbU, TU, TddU 'Read data for upper level

460 LET PpasL = PmbL * 100 'Convert lower lvl press, mb - pascals
465 LET PpasU = PmbU * 100 'Convert upper lvl prs, mb to pascals

470 LET TkL = TL + 273.16 'Convert lower level Temp C to K
475 LET TkU = TU + 273.16 'Convert higher level Temp C to K

480 IF TddL > 55 THEN 490 'Lower level dewpoint depressions
485 LET TdL = TL - TddL / 10 '45 = 4.5
490 LET TdL = TL - (TddL - 50) / 10 '65 = 15

500 IF TddU > 55 THEN 510 'Upper level dewpoint depressions
505 LET TdU = TU - TddU / 10 '45 = 4.5
510 LET TdU = TU - (TddU - 50) / 10 '65 = 15

520 REM Lower and Upper level potential temperatures
525 ThetaL = TkL * (1000 / PmbL) ^ .286
530 ThetaU = TkU * (1000 / PmbU) ^ .286

540 REM Lower and Higher level Vapor pressures in Millibars
545 LET eL = 6.11 * 10 ^ (7.5 * TdL / (237.3 + TdL))
550 LET eU = 6.11 * 10 ^ (7.5 * TdU / (237.3 + TdU))

560 REM TkvL/U: Lower and Upper level Virtual Temps
565 LET TkvL = TkL / (1 - (eL / PmbL) * (1 - .622))
570 LET TkvU = TkU / (1 - (eU / PmbU) * (1 - .622))
575 LET Tkvm = (TkvL + TkvU) / 2 'Mean Virtual Temp

580 REM Layer Thickness
585 LET LyrThk = (Rd * Tkvm / g) * LOG(PmbL / PmbU)

590 LET L$ = "###.# ###.# ##### #####"
600 LET AglHgt = AglHgt + LyrThk 'Top of current layer, meters AGL
605 PRINT USING L$; TL; TU; LyrThk; PmbL; PmbU

610 LET LR = (TU - TL) / LyrThk 'Layer Temp Lapse Rate, deg C per m
615 LET PTLR = (ThetaU - ThetaL) / LyrThk 'Layer Pot Temp LR, deg K per meter

```

```

620 PRINT #2, CountLR; ", "; AglHgt; ", "; LyrThk; ", "; LR; ", "; PTLR
625 REM
630 REM
635 IF EOF(1) THEN 670          'CLOSE files IF at End Of File #1

640 IF CountLR = LvlS THEN 670  'Cease and desist
645 LET PmbL = PmbU            'step up lower level prior to
650 LET TL = TU                'reading next higher level

660 LET CountLR = CountLR + 1
665 GOTO 445
670 CLOSE 1                    'CLOSE files 1 and 2
675 CLOSE 2

700 REM -----
701 REM Observations and PBL calculations

705 PRINT : PRINT : INPUT "Ready to Proceed? (y/n)"; E$
710 IF E$ = "n" THEN 1999
715 OPEN "sfcllys.dat" FOR OUTPUT AS #3      'Prepare to save calculations
720 OPEN "ciblcld.dat" FOR OUTPUT AS #4

725 LET countZi = 1
740 OPEN "layers.dat" FOR INPUT AS #2        'Open file
745 INPUT #2, CountLR, AglHgt, LyrThk, LR, PTLR 'Read the data
750 CLS

755 IF alt < 500 THEN 770          'Alstg >= 30.00 inches, jump to 1085

760 LET alt = (alt + 2000) / 100  'Alstg < 30.00 inches
765 GOTO 775                      'jump to converting mb to pascals

770 LET alt = (alt + 3000) / 100  'Alstg const, assume flow along isobar

775 LET Pmb = (alt * 33.865) - 9.3 'inches mercury to mbs and pascals
780 LET Ppas = Pmb * 100          'Lake is 75 m MSL, subtract 9.3 mb
782                             'using 1 mb = 8 meters.

785 REM Calcs for over water T, Td, ff      'stb from line 124

790 IF stb < -10.4 THEN 900        'Very unstable, skip to 900
795 IF stb < -3.4 THEN 850        'Stable lake-land, GOTO 850

800 REM Neutral (-3.4 to 3.4 deg C)
805 LET Taw = .29 + .47 * Tal + .52 * Tw
815 LET ffw = 3.55 + .92 * ffl - .28 * stb + 1.29 * LOG(Time) / 2.3026
820 LET spdmps = ffw * .5144
825 LET spdkmh = ffw * .5144 * 3.6
830 LET dx = spdmps * 300          'fetch for a 5 min wind spd in meters
833 LET Totaldx = Totaldx + dx    'How far the air has moved over lake
834 LET x = x + dx
835 LET Tdw = -.35 + .72 * Tdi + .31 * Tw
840 GOTO 940

```

```

850 REM Unstable (-3.5 to -10.4 deg C)
855 LET Taw = -4.78 + .67 * Tal + .42 * Tw + 1.12 * LOG(Time) / 2.3026
860 LET ffw = -2.5 + 1.01 * ffl + 1.33 * LOG(Time) / 2.3026
865 LET spdmps = ffw * .5144
870 LET spdkmh = ffw * .5144 * 3.6
875 LET dx = spdmps * 300 'wind spd for a 5 min fetch
878 LET Totaldx = Totaldx + dx 'How far the air has moved over lake
879 LET x = x + dx
880 LET Tdw = .03 + .94 * Tdi + .11 * Tw + .02 * Totaldx / 1000 * .54
885 GOTO 940 'convert dx from m to nmi

900 REM Very unstable (stb < -10.4 deg C), values at approx 2.5 meters
905 LET Taw = -9.77 + .6 * Tal + .54 * Tw + 2.8 * LOG(Time) / 2.3026
910 LET ffw = -2.79 + 1.05 * ffl + 1.46 * LOG(Time) / 2.3026
915 LET spdmps = ffw * .5144
920 LET spdkmh = ffw * .5144 * 3.6
925 LET dx = spdmps * 300 'wind spd for a 5 min fetch
928 LET Totaldx = Totaldx + dx 'How far the air has moved over lake
929 LET x = x + dx
930 LET Tdw = -5.64 + .56 * Tdi + .46 * Tw + .05 * Totaldx / 1000 * .54
931 'convert dx from m to nmi

940 IF Taw > Tw THEN LET Taw = Tw
950 LET U = spdmps

1000 REM Calculate vapor pressures, units in millibars
1005 LET ew = 6.11 * 10 ^ (7.5 * Tw / (237.3 + Tw)) 'at lake sfc in mbs
1010 LET eaw = 6.11 * 10 ^ (7.5 * Tdw / (237.3 + Tdw)) 'overwater air in mbs

1015 REM Calc Absolute Humidity at lake surface and at 2.5 m
1020 LET qw = .622 * ew / Pmb
1025 LET qaw = .622 * eaw / Pmb

1030 REM Calc sensible (hs) and latent (hq) heat fluxes from lake to air
1031 LET Cd = (.75 + .067 * U) / 1000 'Stull table 7-3, pg 267
1035 LET hs = rho * Cd * Cp * U * (Tw - Taw)
1040 LET hq = rho * Cd * L * U * (qw - qaw) 'Ch = Cd Stull 7.4.1f, pg 263
1041 LET P$ = "###.### ##.### ##.### ##.### ###.## ###.##"
1042 PRINT "e-lake e-10m q-lake q-10m hs hq"
1043 PRINT USING P$; ew; eaw; qw; qaw; hs; hq
1044 PRINT : PRINT : INPUT "Ready to Proceed? (y/n)"; J$
1045 IF J$ = "n" THEN 1999
1046 IF J$ = "N" THEN 1999

1047 LET S$ = "###.# #.### ##.## ###.# ###.## ###.## #####"
1048 PRINT : PRINT " U Cd Taw Tdw hs hq dx"
1049 PRINT USING S$; U; Cd; Taw; Tdw; hs; hq; dx
1050 LET T$ = "###.# ### ##.## ###.# ##### ####### #######"
1051 PRINT : PRINT " ffl dir alt Pmb Ppas Step Count fetch"
1052 PRINT USING T$; ffl; dd; alt; Pmb; Ppas; countZi; fetch
1053 PRINT : PRINT : INPUT "Ready to Proceed? (y/n)"; g$

```



```

1054 IF g$ = "n" THEN 1999
1055 IF g$ = "N" THEN 1999

1100 REM -----
1105 REM cloud calculations

1110 REM determine mixing ratio (r) at 10m
1115 LET r = .622 * eaw / (Pmb - eaw)      'mixing ratio in millibars

1120 REM convert Taw to degrees Kelvin, find T P and Z at LCL
1125 LET Tkaw = Taw + 273.16              'overwater air temp, deg K
1130 REM LET Tlcl = (2840 / (3.5 * LOG(Tkaw) - LOG(Pmb * r / .622 + r) - 7.108)) + 55
1135 LET Tlcl = Tdw - (.212 + .001571 * Tdw - .000436 * Taw) * (Taw - Tdw) + 273.16
1140 LET Plcl = Pmb * (Tlcl / Tkaw) ^ 3.5  'NOTE: In BASIC, LOG is ln
1145 LET Twlm = (Tkaw + Tlcl) / 2          'Mean T from 10m to LCL
1150 LET Zlcl = (Rd * Twlm / g) * LOG(Pmb / Plcl) 'NOTE: In BASIC, LOG is ln
1151 LET K$ = "###.# ###.# ###.# ###.# ###.#"
1152 PRINT " Taw Tkaw Tlcl Plcl Zlcl x-fetch"
1153 PRINT USING K$; Taw; Tkaw; Tlcl; Plcl; Zlcl; x

1200 REM -----
1210 REM Venkatram's eqtn

1220 IF PTLR < 0 THEN LET PTLR = .0005
1225 IF PTLR > .002 THEN 1250
1230 LET Zio = AglHgt
1235 IF EOF(2) THEN 1250
1240 INPUT #2, CountLR, AglHgt, LyrThk, LR, PTLR
1245 GOTO 1220

1250 REM TIBL equations assume a dry adiabatic LR (.0098 deg/m) in the CIBL
1255 LET Zid = Zio + (Cd * 2 * ABS(Tw - Tal) * x / PTLR * (1 - 2 * F)) ^ .5
1270 LET Tzid = (Taw - Zid * .0098)      'Temp at Zid (m * deg/m = deg)
1275 LET Tkzid = Tzid + 273.16
1280 LET Pzid = Pmb * (Tkzid / Tkaw) ^ 3.5 'Pressure at Zid

1290 IF Zid < Zlcl THEN 1480      'Conden pt abv mixing hgt, dry CIBL

1300 LET Zi = Zid

1500 REM -----

1510 REM Write data to file 3 and 4

1515 LET W$ = "###.#####.###.# ###.# ###.# ###.#####.#####.###.# ###.#"
1520 PRINT #3, USING W$; countZi; Totaldx; U; Taw; Tdw; qw; qaw; hs; hq

1615 LET x$ = "###.#####.#####.###.# #####.###.# #####.#####"
1620 PRINT #4, USING x$; countZi; Totaldx; Zid; Tkzid; Pzid; Tlcl; Plcl; Zlcl

1621 LET Y$ = "#####.#####.#####.#####.#####.#####."
1622 PRINT " Zid AglHgt LR PTLR Totaldx"
1623 PRINT USING Y$; Zi; AglHgt; LR; PTLR; Totaldx

```

```
1630 LET countZi = countZi + 1
1635 IF Totaldx >= fetch THEN 1992 'Reached the end of the lake, stop
1640 LET Time = Time + 300

1645 IF Zi < AglHgt THEN 1690      'If Zi is less THEN current lyr top
1650 LET Zio = AglHgt              'Now we work on next higher layer
1655 LET x = 0
1680 IF EOF(2) THEN 1690          'skip reading IF at End Of File #2
1685 INPUT #2, CountLR, AglHgt, LyrThk, LR, PTLR 'If we need higher lyr data

1690 PRINT : PRINT : INPUT "Ready to Proceed? (y/n)"; N$
1695 IF N$ = "n" THEN 1992
1700 IF N$ = "N" THEN 1992

1710 GOTO 790                    'Loop for next fetch step

1992 CLOSE 2                    'close files 2, 3, 4
1994 CLOSE 3
1996 CLOSE 4

1999 END
```